NUREG/CR-2331
BNL-NUREG-51454
VOL. 3, NO. 4

SAFETY RESEARCH PROGRAMS SPONSORED BY OFFICE OF NUCLEAR REGULATORY RESEARCH

QUARTERLY PROGRESS REPORT
OCTOBER 1 — DECEMBER 31, 1983

Date Published — May 1984

DEPARTMENT OF NUCLEAR ENERGY, BROOKHAVEN NATIONAL LABORATORY
UPTON, NEW YORK 11973

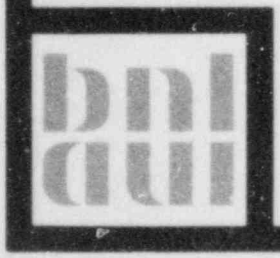

Prepared for the U.S. Nuclear Regulatory Commission
Office of Nuclear Regulatory Research
Contract No. DE-AC02-76CH00016

NUREG/CR-2331
BNL-NUREG-51454
VOL. 3, NO. 4
AN, R-1,4,5,7,8, RD

SAFETY RESEARCH PROGRAMS SPONSORED BY OFFICE OF NUCLEAR REGULATORY RESEARCH

QUARTERLY PROGRESS REPORT
OCTOBER 1 — DECEMBER 31, 1983

Herbert J.C. Kouts, Department Chairman
Walter Y. Kato, Deputy Chairman

Principal Investigators:

R.A. Bari	W.T. Pratt
R.J. Cerbone	M. Reich
T. Ginsberg	P. Saha
G.A. Greene	C. Sastre
J.G. Guppy	J.H. Taylor
R.E. Hall	J.R. Weeks
W.J. Luckas, Jr.	W. Wulff
J.N. O'Brien	D. van Rooyen

Compiled by: Allen J. Weiss
Manuscript Completed March 1984

DEPARTMENT OF NUCLEAR ENERGY
BROOKHAVEN NATIONAL LABORATORY, ASSOCIATED UNIVERSITIES, INC.
UPTON, NEW YORK 11973

Prepared for the
OFFICE OF NUCLEAR REGULATORY RESEARCH
U.S. NUCLEAR REGULATORY COMMISSION
CONTRACT NO. DE-AC02-76CH00016
FIN NOS. A-3011,-3014,-3015,-3016,-3024,-3041,-3208,-3215,-3219,-3225,
-3226,-3227,-3257,-3260,-3266,-3268,-3270,-3271

Available from
GPO Sales Program
Division of Technical Information and Document Control
U.S. Nuclear Regulatory Commission
Washington, D.C. 20555
and
National Technical Information Service
Springfield, Virginia 22161

FOREWORD

The Advanced and Water Reactor Safety Research Programs Quarterly Progress Reports have been combined and are included in this report entitled, "Safety Research Programs Sponsored by the Office of Nuclear Regulatory Research - Quarterly Progress Report." This progress report will describe current activities and technical progress in the programs at Brookhaven National Laboratory sponsored by the Division of Accident Evaluation, Division of Engineering Technology, and Division of Facility Operations of the U. S. Nuclear Regulatory Commission, Office of Nuclear Regulatory Research.

The projects reported are the following: High Temperature Reactor Research, SSC Development, Validation and Application, CRBR Balance of Plant Modeling, Thermal-Hydraulic Reactor Safety Experiments, Development of Plant Analyzer, Code Assessment and Application (Transient and LOCA Analyses), Thermal Reactor Code Development (RAMONA-3B), Calculational Quality Assurance in Support of PTS; Stress Corrosion Cracking of PWR Steam Generator Tubing, Bolting Failure Analysis, Probability Based Load Combinations for Design of Category I Structures, Mechanical Piping Benchmark Problems, Identification of Age-Related Failure Modes; Analysis of Human Error Data for Nuclear Power Plant Safety-Related Events, Human Factors in Nuclear Power Plant Safeguards, Emergency Action Levels, and Protective Action Decision Making. The previous reports have covered the period October 1, 1976 through September 30, 1983.

TABLE OF CONTENTS

TABLE OF CONTENTS (Cont'd.)

TABLE OF CONTENTS (Cont'd.)

FIGURES

FIGURES (Cont'd.)

FIGURES (Cont'd.)

TABLES

I. DIVISION OF ACCIDENT EVALUATION

SUMMARY

High Temperature Reactor Research

At the end of this quarter, the accumulated oxidation time for the Stackpole 2020 medium sized samples (3 inches ϕ x 6 inches long) was 4,812 hours (~200 days). These samples will be strength tested after one year's accumulated oxidation time.

The effects of He flow rate, experiment duration time, and temperature gradient on the amount of aerosol formation were studied with silver at 1500°C. It seems that the aerosol formation may not be affected much by the flow rate of the coolant gas. However, it appears that the reactor column temperature affects the amount of aerosol formation rather significantly even when the temperature variation is not large (< 11°C).

An experimental setup to study the integrated fission product transport under a simulated accident condition has been completed. Mock-up fuel blocks with simulated fission products are to be taken to high temperatures up to 3000°C. We have completed two preliminary runs filling the fuel channels with Mo_2C. In both runs, the chimney that was connected to the cooling channel at the center of the H451 susceptor was completely blocked. The experimental setup is under modification to get rid of the possible cause for this, and blocking mechanism is under investigation.

Our assessment of containment atmosphere responses with burning during severe accidents under conditions more remote than those considered in previous analyses was completed, showing essentially that the previous analyses, and in particular the siting study, were conservative.

Improvements in the THATCH code treatment of the thermal barrier were made, affecting primarily long term runs without LCS, i.e., with PCRV concrete degradation.

Results of the idealized analysis of vapor migration in concrete were documented. Application to conditions during PCRV concrete degradation is currently in progress.

SSC Development, Validation and Application

The Super System Code (SSC) Development, Validation and Application Program encompasses a series of three computer codes: (1) SSC-L for system transients in loop-type LMFBRs, (2) SSC-P for system transients in pool-type LMFBRs, and (3) SSC-S for long term shutdown transients. In addition to these code development and application efforts, validation of these codes is an ongoing task.

Under SSC-L activities, the previously developed, two-dimensional, transient model to account for intra-assembly heat and flow redistribution effects was tested. Initial validation studies to test the model against experimental data were accomplished and a report was written describing the modeling and preliminary results. The next step is to carry this work forward and include it in an improved representation of inter-assembly heat transfer effects under low flow conditions. This inter-assembly work is currently being concentrated on modeling needs for the interstitial sodium and duct wall temperatures. In a joint effort with the GRS/FRG, a study is being conducted to assess any potential safety implications of using flow control devices in the sodium loops. Such devices are typically used in German designs. Under the area of user support, work is continuing to provide the specific modeling needs of several special control system-related features of the SNR-300 design.

Efforts on the SSC-P code continued in order to make it compatible with the base program library and be able to take advantage of many improvements accomplished under SSC-L development. Additionally, changes necessary to provide an improved model of the EBR-II primary loop representation were defined. These include changes to account for hydraulic-related features as well as thermal features, such as heat transfer to the cold pool from the hot leg "Z" pipe.

Work on SSC-S remains focused on the improved upper plenum modeling. The stand-alone code was tested using a 15 x 13 variable mesh spacing for a simulation of the FFTF upper plenum, using boundary conditions typical of a coastdown to natural convection event.

Having accomplished the comparisons of SSC results to the long term experimental data from the FFTF tests, validation studies with the FFTF data have been completed. A report discussing the long term results and comparisons is being written.

CRBR Balance of Plant Modeling

The Balance of Plant (BOP) Modeling Program deals with the development of safety analysis tools for system simulation of nuclear power plants. It provides for the development and validation of models to represent and link together BOP components (e.g., steam generator components, feedwater heaters, turbine/generator, condensers) that are generic to all types of nuclear power plants. This system transient analysis package is designated MINET to reflect the generality of the models and methods, which are based on a momentum integral network method. The code is to be fast-running and capable of operating as a self-standing code or to be easily interfaced to other system codes.

The turbine stage model that was recently incorporated into the MINET code is functioning properly. Due to convergence difficulties for modules with very large pressure gradients, the steady-state network pressure and flow solver was modified. The modeling of Version 1 of MINET is completed. One of the major features to be included into Version 2 will be a generic control system representation.

Testing of Version 1 continues in the following areas, where improvements or new features have been added: Thom two-phase friction multiplier; improved iterative scheme for steady-state heat exchanger calculations; critical flow modeling changes; and revisions to the global steady-state solver, particularly for underconstrained problems.

Work is progressing on interfacing MINET with RAMONA-3B, for BWR plant transient analysis, in support of the SASA Program. The MINET code will provide improved feedwater/ECCS flow and temperature boundary conditions to the RAMONA code. Both codes have numerous options available for specifying a variety of boundary conditions via input tabular data. We are currently planning to link the codes together using these tabular input points. Thus, even though the codes will be coupled and advancing in time together, they will be essentially unaware of each other.

Thermal Hydraulic Reactor Safety Experiments

The ex-vessel debris bed quench front propagation data are presented in dimensionless form and are compared with the model prediction. The results suggest that for the 6- and 12-mm particle beds, water initially penetrates more rapidly than the theory predicts. The 12-mm particle beds show us downward frontal propagation.

In-vessel bottom-quench experimental data are presented for the average bed heat flux as a function of initial bed temperature. The agreement with the model prediction is reasonable, considering the data scatter.

An experimental apparatus was constructed to study liquid-liquid film boiling with transverse non-condensable gas bubbling which simulates gas release from concrete during core-concrete interactions. Data are presented for pools of molten lead and molten Wood's metal using Freon-11 as the boiling coolant. The measured boiling heat flux for gas superficial velocities in the range 0.6 - 1.0 cm/s are up to a factor of three higher than the heat fluxes predicted by the Berenson film boiling model.

Development of Plant Analyzer

The LWR Plant Analyzer Program is being conducted to develop an engineering plant analyzer capable of performing accurate, real-time and faster than real-time simulations of plant transients and small-break loss of coolant accidents (SBLOCAs) in LWR power plants. The first program phase was carried out earlier to establish the feasibility of achieving faster than real-time simulations and faster than mainframe, general-purpose computer (CDC-7600) simulations through the use of modern, interactive, high-speed, special-purpose minicomputers, which are specifically designed for interactive time-critical systems simulations. It has been successfully demonstrated that special-purpose minicomputers can compete with, and outperform, mainframe

computers in reactor simulations. The current program phase is being carried out to provide a complete BWR simulating capability, including on-line, multi-color graphics display of safety-related parameters.

The Plant Analyzer Program is directed primarily toward reactor safety analyses, but its results are also useful for on-line plant monitoring and accident diagnosis, for accident mitigation, further for developing operator training programs and for assessing and improving existing and future training simulators. Major assets of the simulator under development are its extremely low cost, unsurpassed convenience of operation and high speed of simulation. Major achievements of the program are summarized below.

Existing simulator capabilities and limitations regarding their representation of the Nuclear Steam Supply System have been assessed previously. Simulators reviewed at the time have been found to be limited to steady-state simulations and to restricted quasi-steady transients within the range of normal operating conditions.

A special-purpose, high-speed peripheral processor had been selected earlier, which is specifically designed for efficient systems simulations at real-time or faster computing speeds. The processor is the AD10 from Applied Dynamics International (ADI) of Ann Arbor, Michigan. A PDP-11/34 minicomputer serves as the host computer to program and control the AD10 peripheral processor. Both the host computer and the peripheral processor have been operating at BNL since March 15, 1982.

An existing model for nonequilibrium, nonhomogeneous two-phase flow in a specific BWR hydraulics system has been implemented on the AD10 processor for the purpose of comparing the computing speed and accuracy of the AD10, as it executes the code called HIPA-PB2 for High-Speed Interactive Plant Analysis of the Peach Bottom-2 BWR power plant. The implementation of HIPA-PB2 has been carried out in the high-level language MPS-10 of the AD10.

It has been demonstrated during the last quarter of 1982 that the AD10 special-purpose peripheral processor can produce accurate simulations of BWR design base transients at computing speeds ten times faster than real-time and 110 times faster than the CDC-7600 mainframe computer carrying out the same simulation.

After the successful completion of the feasibility demonstration, work has continued to expand the hydraulics simulation used for that demonstration to produce the capability of simulating the entire nuclear steam supply system as well as the flow of the working medium through turbines, condensers and feedwater trains.

Models have been developed and implemented for point neutron kinetics with five feedback mechanisms and seven scram trip initiations, for thermal conduction in fuel elements, for steam line dynamics capable of simulating acoustical effects from sudden valve actions, for turbines, condensers, feedwater preheaters and feedwater pumps, and for emergency coolant injection systems.

The software systems of both the PDP-11/34 host computer and the AD10 special-purpose peripheral processor have been upgraded to achieve greater computing speed and a larger number of analog input/output channels. Two AD10s are coupled via a direct bus-to-bus interface to compute in parallel.

During the last reporting period, models had been developed, scaled and implemented for the feedwater controller, the pressure regulator and the recirculation flow controller. Twenty-eight parameters for initiating control systems and valve failures and for selecting set points can now be changed on-line from a 32-channel control panel. Sixteen dedicated analog output lines are provided for the simultaneous display of 15 selected parameters. All input-output channels are addressed approximately 200 times per second.

During the current reporting period, all program modules have been combined into the HIPA-PB2 code. The entire BWR power plant simulation, including the nuclear steam supply system, the steam line with all valves, the turbines, condensers, feedwater preheater and pumps and the control systems, have been executed for the first time. Fifteen selected parameters can be stored simultaneously in the IBM Personal Computer and then displayed in labelled diagrams. A silent movie has been produced to show how the plant analyzer is operated and how it responds to on-line analog signals.

Work has been started on developmental assessment and on expanding the plant analyzer capabilities to other plants.

The interest in the Plant Analyzer Development Program continues to be high, both in domestic and foreign institutions. Nine presentations were given with demonstrations to foreign visitors, and two invited papers have been submitted for presentation and publication during the current reporting period.

Code Assessment and Application (Transient and LOCA Analyses)

Two major code application tasks, namely, the RESAR-3S large break LOCA study and the typical BWR/4 MSIV closure ATWS analysis, that were initiated in FY 1983, are in the final stages of completion. Also, the code assessment activity is about to resume after the implementation of the TRAC-BD1/MOD1 code on the BNL computer.

Two large break LOCA calculations have been performed for a Westinghouse four-loop RESAR-3S plant using the TRAC-PD2/MOD1 code. One of the calculations used the best-estimate initial and boundary conditions, whereas the other one used the evaluation or licensing type conditions. The physical or thermohydraulic models for both calculations were, of course, best-estimate. A comparison of these calculations with the Westinghouse licensing or Appendix K calculation indicates that there is an overall safety margin of approximately 1200°F, of which approximately 700°F is due to the conservative or licensing type physical models, and approximately 500°F is due to the licensing type initial and boundary condition.

A typical BWR/4 MSIV closure ATWS analysis has been performed using the RAMONA-3B (with three-dimensional neutron kinetics) and TRAC-BD1 (with point kinetics) codes. The RAMONA-3B calculation has been carried out up to 560 seconds, whereas the TRAC-BD1 calculation has been performed until the reactor power reached approximately 2% of the steady state value at approximately 1100 seconds. The suppression pool water temperature at this time has been calculated to be approximately 170°F. Another TRAC-BD1 calculation with the RAMONA-3B calculated core power was performed for the first 150 seconds for the specific comparison of the thermohydraulic responses of both TRAC-BD1 and RAMONA-3B codes. Based on these results and computer running times, it is recommended that the RAMONA-3B code be extensively used for the analysis of ATWS type events in BWRs.

Thermal Reactor Code Development (RAMONA-3B)

Extended support has been provided to the Code Assessment and Application program for a typical BWR/4 MSIV closure ATWS analysis using RAMONA-3B. In the course of this activity, several coding errors in the hydraulics part of the code have been corrected, and the calculation has been run up to 560 seconds of the transient.

Several corrections and/or improvements have also been made in the neutronics part of the code. The reactivity edits developed by Scandpower have been implemented at BNL. Work has also been initiated to verify the Scandpower procedure of collapsing three-dimensional cross sections to one-dimensional data.

Calculational Quality Assurance in Support of PTS

The review of TRAC input decks and steady state results for the Calvert Cliffs plant has been completed and documented in a BNL memorandum. A quick review of all the Calvert Cliffs transient results has also been completed and is being documented.

Review of the RELAP5 input decks for the H. B. Robinson plant has begun. A simple procedure for quantitative review and extrapolation of TRAC and/or RELAP5 results has also been developed based on overall mass and energy balances.

Finally, the latest version of the TRAC-PWR code, namely, the TRAC-PF1/MOD1 code, has been successfully implemented on the BNL computer and is available for code assessment and application.

1. High Temperature Reactor Research

1.1 Graphite and Ceramics (B. S. Lee, J. H. Heiser, III, and D. R. Wales)

1.1.1 Long Term Oxidation Experiments

At the end of this quarter, the accumulated oxidation time for the Stackpole 2020 medium sized samples (3 inches ϕ x 6 inches long) was 4812 hours (~200 days). These samples will be strength tested after one-year's accumulated oxidation time.

The data acquisition system for Helium Impurities Loop No. 1 has been improved. Now all the data for CO, CO_2, CH_4, H_2O, H_2 and time are collected by two Tektronix 4923 tape recorders, and are processed by a Tektronix 4051 computer. Equipment is on order which will permit all the data to be collected by one tape recorder.

1.2 Fission Product Migration (B. S. Lee, J. H. Heiser, III, C. C. Finfrock and C. Sastre)

1.2.1 Fission Product Migration By an Aerosol Formation

As described in the last progress report, we have built a system that can heat a small graphite susceptor enclosed in a water cooled quartz reactor tube up to 2100°C. This system was improved by the addition of an automatic temperature controller. Now, the specimen temperature can be kept constant within a couple of degrees at ~1500°C. The completed system with a Faraday cage is shown in Figure 1.2.1

During this quarter, the effects of He flow rate, experiment duration time and temperature gradient on the amount of aerosol formation were studied.

1.2.1.1 The Effect of He Flow Rate on the Aerosol Formation

Fission product aerosol formation/transportation was studied with silver varying the flow rate of the coolant, He + 1% H_2O. Eleven experimental runs of 30-minute duration each were carried out with flow rates varying from 100 to 1000 cc/min, and the results are shown in Figure 1.2.2.

The amount of the silver collected by a filter seems proportional to the flow rate of the coolant. This indicates that the aerosol formation may not be affected much by the flow rate of the coolant gas, because the aerosol collected by a filter divided by the total volume of coolant passing through the system is about the same for different flow rates.

Similar experiments are planned for other fission products.

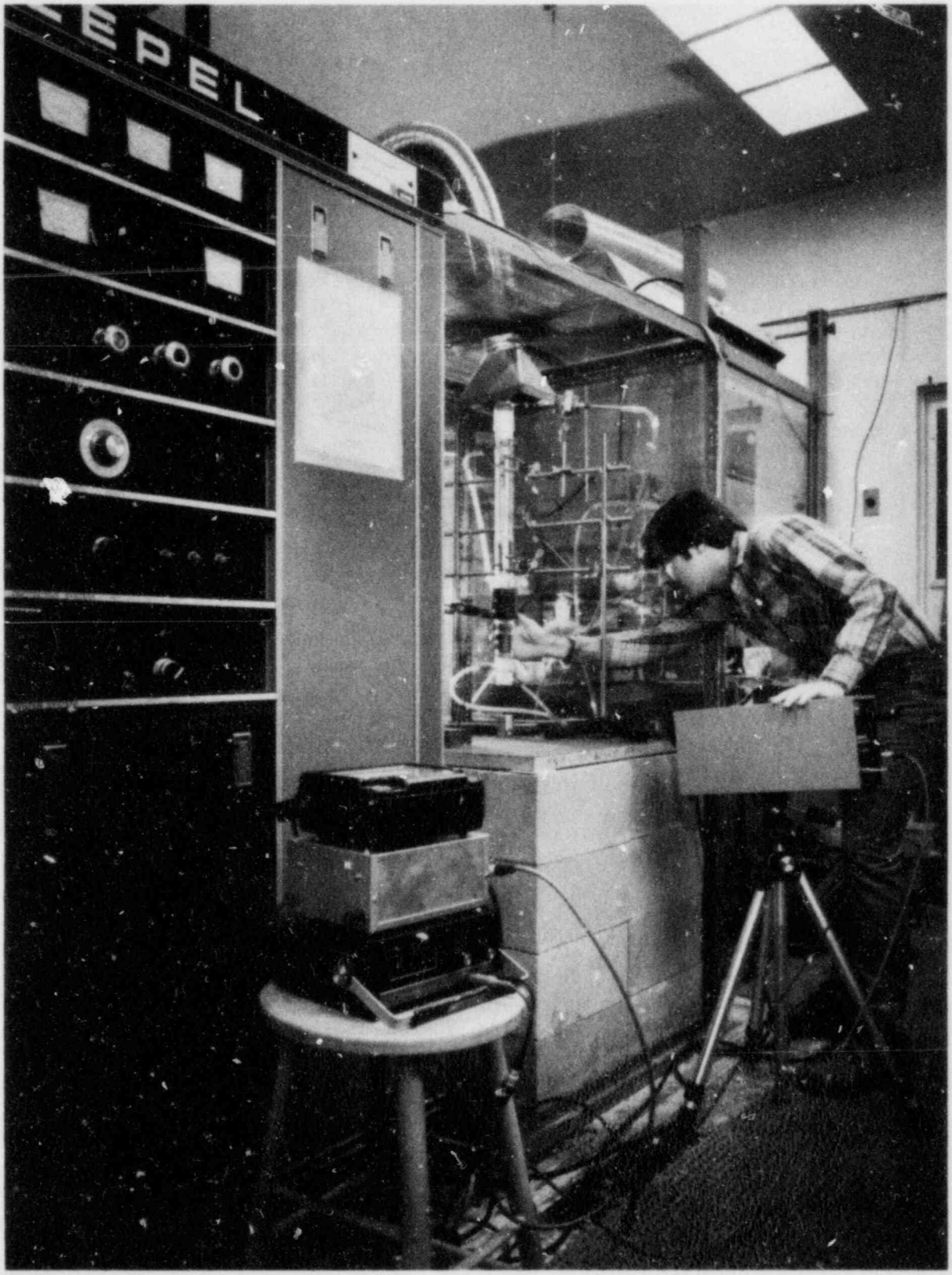

Figure 1.2.1 The induction furnace and the experimental set-up for aerosol formation study.

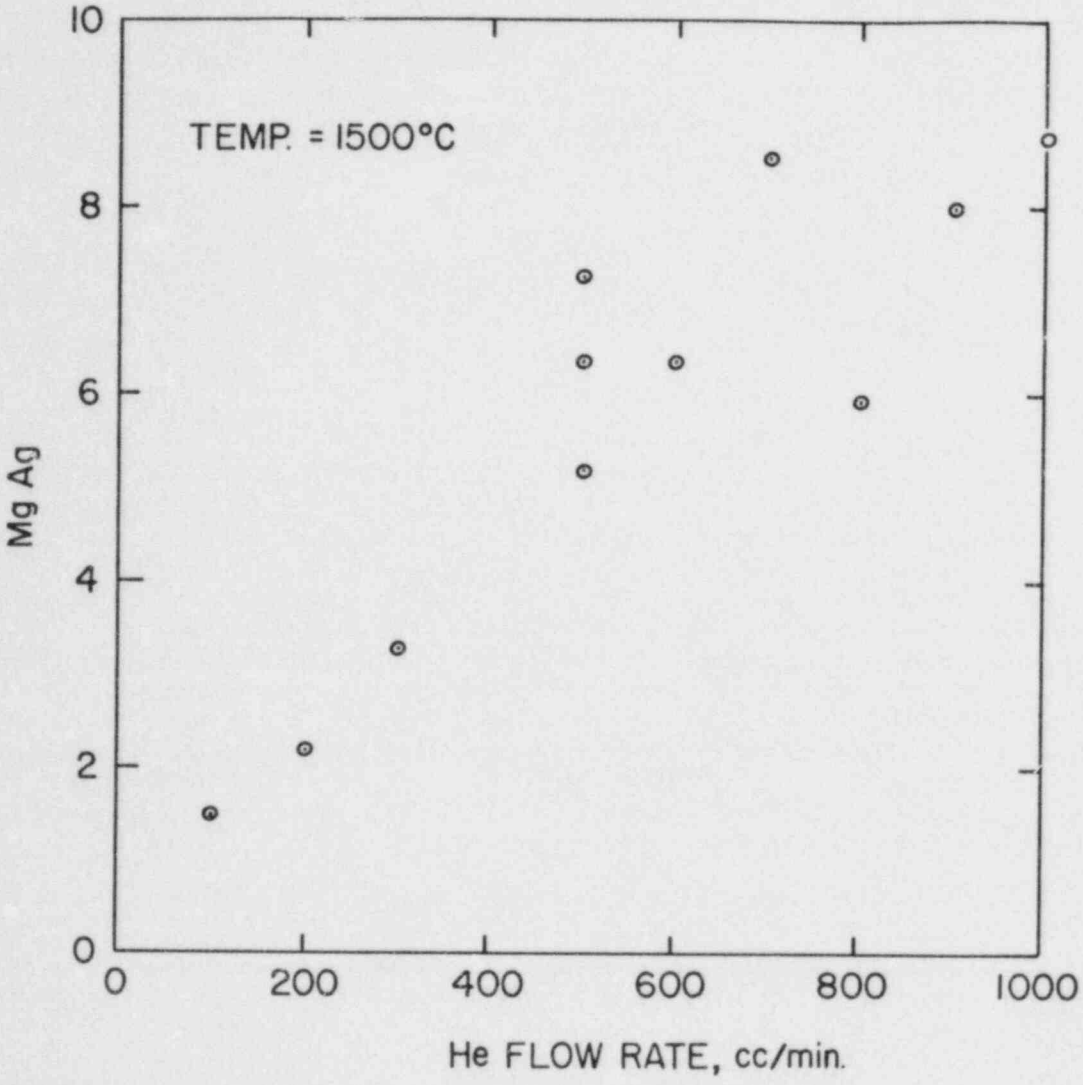

Figure 1.2.2 Silver aerosol collected by a filter as a function of He flow rate.

1.2.1.2 The Effect of Experiment Duration Time on the Aerosol Formation

To select the optimum experiment duration time, the amount of aerosol forming was measured as a function of duration time with a flow rate of 500 cc/min. As shown in Figure 1.2.3, the amount of aerosol collected is proportional to the duration time, and it was decided that the experiment duration time will be 2 hours for future runs.

1.2.1.3 The Effect of Temperature Gradient On the Aerosol Formation

In the classical nucleation theory, (Hirth and Pound, 1963) the homogeneous nucleation rate from vapor phase is

$$J = J_o \exp \frac{16\pi\sigma^3}{3kT\left(\frac{kT}{\Omega} \ln \frac{P}{P_e}\right)^2} , \qquad (1.2.1)$$

where Ω = molecular volume
σ = specific interfacial free energy
P = vapor pressure
P_e = equilibrium vapor pressure

Because the supersaturation ($\frac{P}{P_e}$) enters into the exponential term of Equation 1.2.1, the rate of nucleation is sensitive to the degree of supersaturation (Kingery, 1960). Thus, the temperature of the reactor tube column temperature was varied to study the effect of the temperature gradient in the tube on the amount of aerosol formed. The easiest way to vary the column temperature is varying the flow rate of the cooling water. Only the temperature at the top of the tube was measured, and the temperature difference between the slowest and the highest flow rate was about 11°C. Figure 1.2.4 shows the amounts of silver collected by filters vs. H_2O flow rate in the cooling jacket. The experiments were conducted at 1500°C for 2 hrs each with He flow rate of 500 cc/min. It appears that the reactor column temperature affects the amount of aerosol formation rather significantly even though the temperature variation was not large (<11°C). This study will continue in a more systematical way in the future.

1.2.2 Intregated Fission Product Transport Experiments

An experimental set-up to study the integrated fission product transport under a simulated accident condition has been completed. Mock-up fuel blocks with simulated fission products are to be taken to high temperatures up to 3000°C. We have completed two preliminary runs filling the fuel channels (12.7 mm ϕ) with Mo_2C. Helium is flowing through a cooling channel (14.3 mm) at the center of a susceptor (82.5 mm ϕ x 152.4 mm long). The first run was for 30 minutes at ~3000°C. After the run, the filter did not show any aerosols. It was found that the chimney was completely blocked at the interface between the cooling channel and the chimney as shown in Figure 1.2.5 and 1.2.6. It was believed that the filter may have given too much resistance to the He flow, and the He inside the chimney was stagnant.

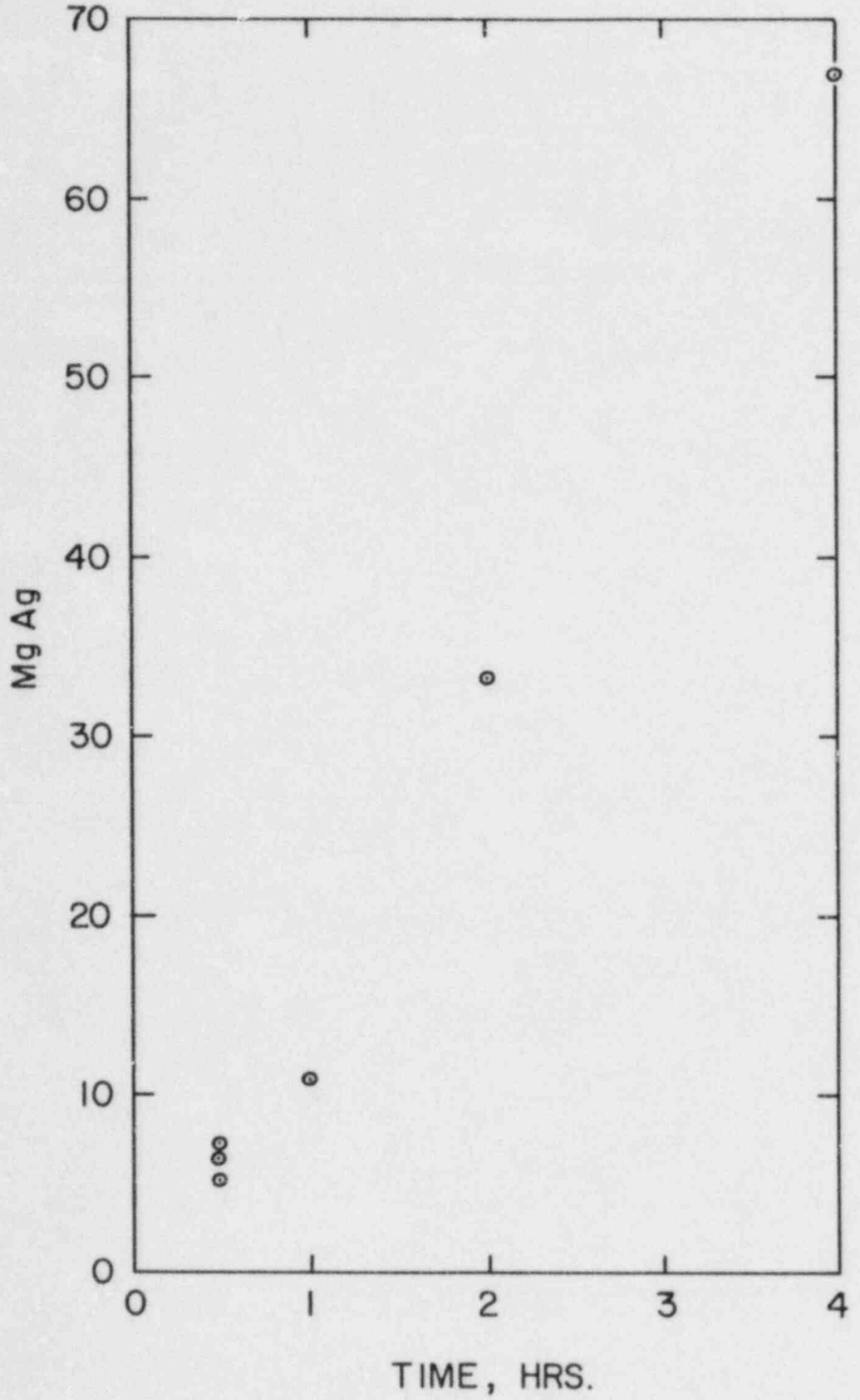

Figure 1.2.3 Silver aerosol collected by a filter as a function of time.

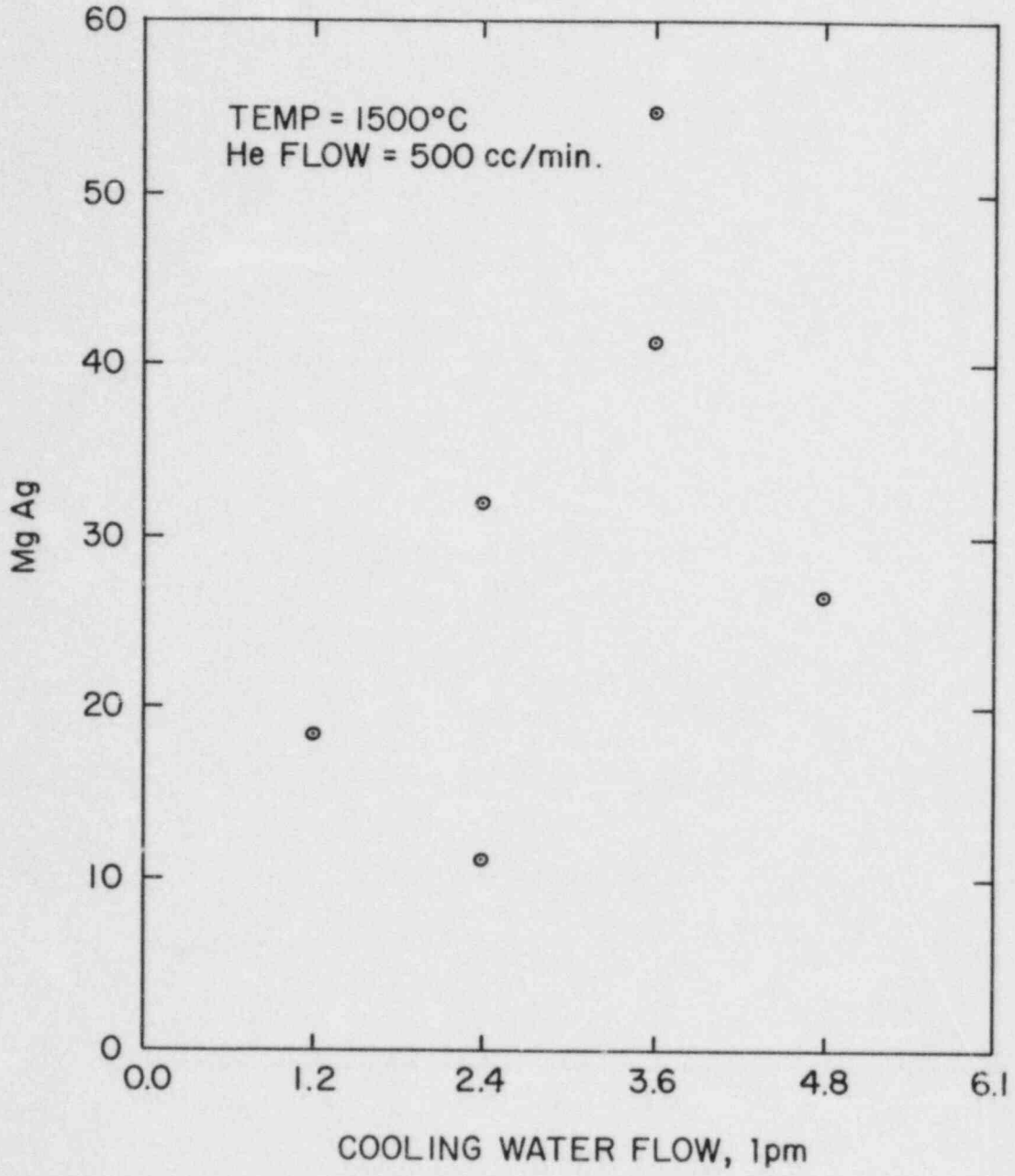

Figure 1.2.4 The effect of temperature gradient on the aerosol formation.

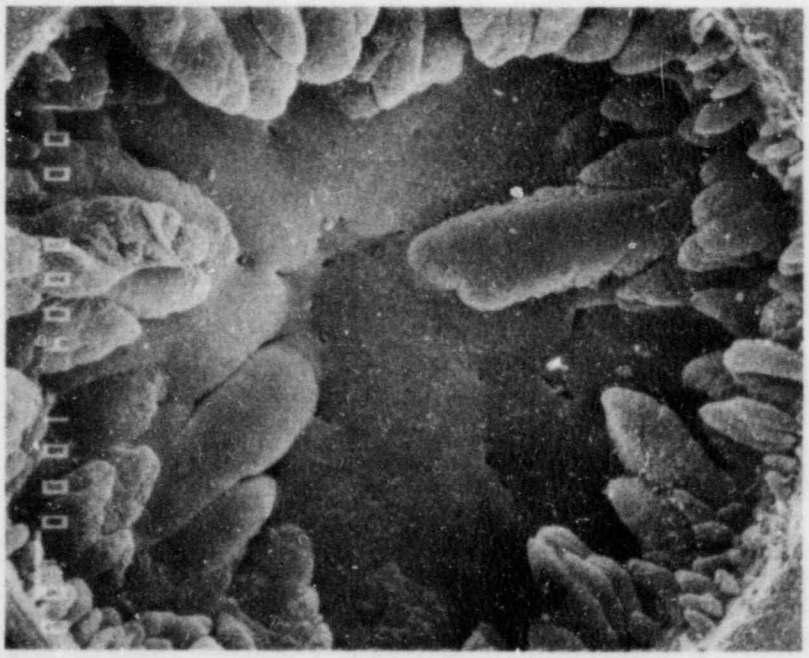

Figure 1.2.5 Blocked portion of the chimney that was connected to a H451 susceptor heated at 3000°C for 1/2 hour. Mag. 10X.

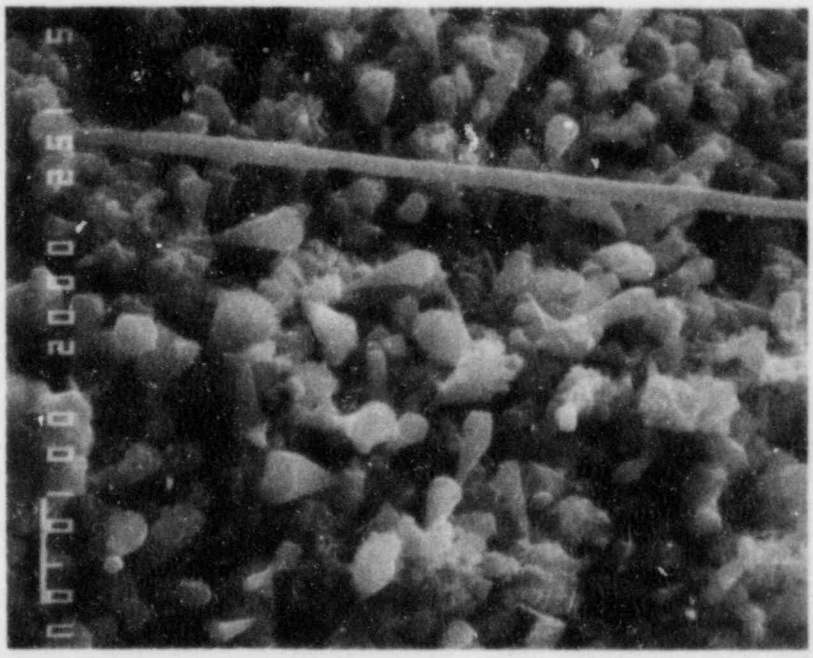

Figure 1.2.6 Condensed graphite particles on the surface of the blocked portion of the chimney. Mag. 1500X.

In the second run, He gas was pulled by a mechanical vacuum pump that was connected after a filter. However, the chimney was blocked again. There is a possibility that we are pulling too much so that air enters the system to oxidize the graphite. We are modifying the system to get rid of this possibility, and the blocking mechanism is under investigation.

1.2.3 Fission Product Migration in H451 Graphite

The experimental part of fission product migration study in H451 graphite were completed last quarter and are summarized in Table 1.2.1. As shown in this table, we have conducted many experiments, and, as a result, have accumulated large amounts of diffusion data. We are in the process of summarizing all the information we have.

To get more information on the physical condition at the interface between graphite and the molten pool of fission products, Mo_2C was filled in a cavity in a H451 graphite block and heated at ~3000°C for 1/2 hour (the same graphite block described in Section 1.2.2), and the cross section vertical to the graphite/fission product interface was examined with a scanning electron microscope and x-ray mapping method. This information is needed to explain the ''virtual source'' observed in the experimental results (Uneberg et al, 1980).

Figure 1.2.7 a) shows the cross section of the cavity that was filled with Mo_2C. As can be seen in this picture, graphite dissolved into the molten pool of Mo_2C, and changed the composition of the molten carbide probably to MoC. Upon cooling, graphite reprecipitated as black bars in this picture. Figure 7 b) is a molybdenum x-ray map of the same area, and shows an abrupt change in Mo concentration at the (Mo_2C + C)/graphite interface. This could possibly explain the very low ''virtual source'' mentioned earlier. Analysis of the diffusion data will continue.

Table 1.2.1

Summary of the Fission Product Migration in H451 Graphite Experiments

Diffusant	Temperature (°C)	Duration (hrs)	Remark*
Mo_2C	2250	0.67	61978
	2400	4	62178
	2800	1	11080
	2850	4	41579
	2900	1	32679
	2950	2	42380
		8	42078
	3000	4	41778
	3100	0.55	11680
	3200	1	4479
	3300	0.73	32380
UC_2/ThC_2 (1:1 mole ratio)	2700	1.67	120181
	2800	1.67	111081
	2900	1	42881
		1.67	82581
	3000	1	110680
		1	51181
		2	91581
UC_2	2900	1.75	110281
ThC_2	2900	1.75	102681
Y-Yb-Mo-Rh-La -Nb-Zr mixtures (eqi-molar mixture)	2500	2	51883
	2800	2	52783
	2900	2	5483
	3000	2	41583
	3200	0.083	20283
		0.5	32383
YC_2	2900	2	12883

* experiment identification number.

(a)

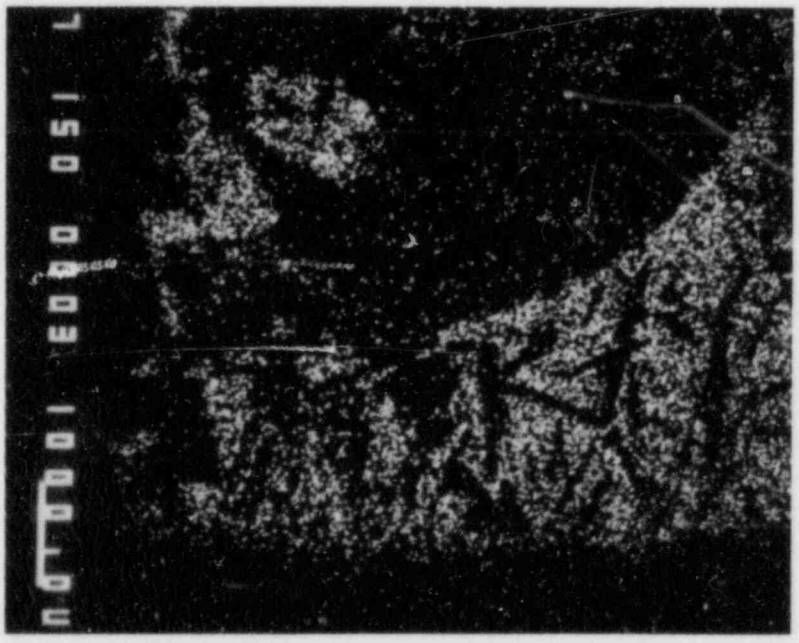

(b)

Figure 1.2.7 a) Cross section of the cavity that was filled with Mo_2C and heated at 3100°C for 1/2 hour. Mag. 15X.
b) x-ray map for Mo of the same area as a.

1.3 Analytical

1.3.1 HTGR Code Library (J. Colman)

Table 1.3.1

HTGR Code Library - Alphabetic Code Order

Program	Origin/ Code Date	BNL Status	Function
BLAST	ORNL/ACC 8/76 (BNL 1/80)	OP	A dynamic simulation of the HTGR reheater-steam generator module.
BLOOST/ BLOOST-7	GA/SAI 1/70	OP	Performs zero-dimensional reactor kinetics calculations.
CHAP-1 (Jan. 1978)	LASL 2/77	OP	Simulates the overall HTGR plant with both steady state and transient solution capabilities.
CIRC (JETS)	BNL 4/78	OP	Calculates fluid dynamics in an HTGR containment vessel following a depressurization accident.
CNTB-7	GA 7/79	OP	Analysis of Partially mixed containment atmospheres during depressurization events.

ACC = Argonne Code Center.
BAW = Babcock and Wilcox.
BNL = Brookhaven Nat. Lab.
BPNW = Battelle Pacific N.W.
GA = General Atomic.
LASL = Los Alamos Scientific Lab.
NOP = Non-Operational.
OP = Operational
ORNL = Oak Ridge National Lab.
P = Proprietary.
SAI = Science Applications, Inc.

Program	Origin/ Code Date	BNL Status	Function
CONTEMP-G (CONTEMPT-G)	GA-BAW 2/74	OP (P)	Simulates temperature-pressure response of an HTGR containment atmosphere to postulated coolant circuit depressurization.
CORCON	GA 7/74	OP (P)	Computes the temperature history and fission product redistribution following a loss of all convective cooling of the core.
CORTAP	ORNL ACC 1/77 (BNL 1/80)	OP	A coupled neutron kinetics - heat transfer program for the dynamics simulation of the HTGR core.
DECAYREM	ORNL 5/74	OP	RSIC Data Library Collection.
DIFFTA	BNL 11/75	OP	Finite element method code for Steady State Heat Conduction, Fission Product Migration and Neutron Diffusion Calculations.
ENDFB and Satellite Codes	BNL	OP	Evaluated Nuclear Data File/B and file manipulation codes.
EVAP	BNL 5/78	OP	A model for the Migration of Fission Products along the coolant channels of an HTGR following a hypothetical accident of complete loss of cooling.
EXREM	ORNL 2/75	OP	Calculates external radiation doses.
FENG	LASL 2/77	OP	One of three codes which create or add to the reactions data library for QUIL and QUIC codes. Reactions added are of type Free Energy.
FEVER-7	GA	OP	Performs one-dimensional, diffusion theory, burnup and reload calculations.

Program	Origin/ Code Date	BNL Status	Function
FLAC	GA	OP	Calculates steady state flow distributions in arbitrary networks with heat addition.
FPPROD	BNL 3/78	OP	Performs simplified fission product production analysis.
FYSMOD	LASL 9/76	NOP	Calculates the two-dimensional solution of HTGR core blocks subjected to external motion.
GAKIT	GA 9/68	OP	Performs one-dimensional multigroup kinetics calculations with temperature feedback.
GAMBLE	GA	OP	A program for the solution of the multigroup neutron-diffusion equations in two dimensions, with arbitrary group scattering.
GGC4	GA/ACC	OP	Prepares broad thermal cross sections from the tape produced by WTFG and MAKE.
GOPTWO/ GOP-3	BPNW 6/75 BPNW 10/76	OP NOP	Graphite Oxidation Program. Analyzes the steady state graphite burnoff and the primary circuit levels of impurities.
HAZARD	BNL 3/77	OP	Analyzes gas layering and flammability in an HTGR containment vessel following a depressurization accident.
H-CON1	BNL 5/76	OP	Calculates one-dimensional heat conduction for an HTGR fuel pin by finite difference method.
HYDRA-1	BNL 5/76	OP	A program for calculating changes in enthalpy single phase liquid due to external heat source.
INREM	ORNL 2/75	OP	Calculates internal radiation doses.

Program	Origin/ Code Date	BNL Status	Function
INTERP	GA MICROX LIBRARY	OP	Prepares broad group cross sections from MICROX output data tapes.
JANAF	Dow Chemical Company 11/78	OP	JANAF Thermochemical Tables.
LARC-1	LASL 11/76	NOP	Calculates fission product release from BISO and TRISO fuel particles of an HTGR during the LOFC accident for single isotopes.
LARC-2	LASL	NOP	Similar to LARC-1; in addition, handles release from isotope chains.
LASAN-BNL LASAN-LASL	LASL/BNL 4/78	OP	A general systems analysis code consisting of a model independent systems analysis framework with steady state, transient and frequency response solution capabilities. There are two versions of the code available - the original LASL version and the converted BNL version.
LEAF	LASL 11/76	NOP	Calculates fission product release from a reactor containment building.
MAKE	SAI	OP	Prepares fine group fast cross section tape from GFE2 for spectrum codes.
NONSAP-C	LASL 10/78	NOP	Calculates static and dynamic response of three-dimensional reinforced concrete structures, in addition to creep behavior.
ORECA-1	ORNL-ACC 4/76	OP	Simulates the dynamics of HTGR cores for emergency cooling analyses. (Ft. St. Vrain)

Program	Origin/ Code Date	BNL Status	Function
ORIGEN	ORNL 4/75	OP	Solves the equation of radioactive growth and decay for large numbers of isotopes with arbitrary coupling.
ORTAP	ORNL-ACC 9/77	OP	A nuclear steam supply system simulation for the dynamic analysis of HTGR transients.
OXIDE-3	GA 1/74	OP (P)	Analyzes the transient response of the HTGR fuel and moderator to an oxidizing environment.
POKE	GA 7/70	OP (P)	Calculates steady state 1-D flow distributions and fuel and coolant temperatures in a gas cooled reactor.
PREPRO	GA	OP (P)	Prepares input data and source code revisions for RECA code.
PRINT	SAI	OP	Reads the fast cross section tape produced by MAKE.
QUIC	LASL 2/77	OP	Solves complex equilibrium distribution in chemical environments.
QUIL	LASL 2/77	OP	Solves complex equilibrium distribution in chemical environments.
RATE	LASL 7/78	OP	One of three codes which create or add to the reactions data library for QUIL and QUIC codes. Reactions added are of type Rate.
RATSAM-6	GA 5/77	OP	Analyses the transient behavior of the HTGR primary coolant system during accidents.
RECA	GA 8/70	NOP (P)	Calculates time dependent flow distributions and fuel and coolant temperatures in the primary system.
RICE	LASL 3/75	OP	Solves transient Navier-Stokes equations in chemically reactive flows.

Program	Origin/ Code Date	BNL Status	Function
SODEMME	BNL 8/77	OP	Calculates transient thermal hydraulic aspects of circulating gas systems
SOLGASMIX	ORNL 4/77	OP	Calculates equilibrium relationships in complex chemical systems.
SORS	GA 4/74	OP (P)	
SORSD	GA	OP (P)	Computes the release of volatile fission products from an HTGR core during thermal transients.
SORSG	GA	OP (P)	Computes the release of non-volatile gaseous fission products from an HTGR core during thermal transients.
SPRINT	GA/SAI	OP	Reads the thermal cross section tape produced by WIFG.
SURF	LASL 2/77	OP	One of three codes which create or add to the reactions data library for QUIL and QUIC codes. Reactions added are of type Surface.
SUVIUS	LASL	NOP	Solves the behavior of fission gases in the primary coolant of a gas-cooled reactor.
TAC2D	GA 9/69	OP	Performs two-dimensional, transient conduction analyses.
TAP	GA	OP (P)	Calculates the transient behavior of the integrated HTGR power plant.
TEMCO/TEMCO7	GA	OP	Computes reactor temperature coefficients from input cross section data.

Program	Origin/ Code Date	BNL Status	Function
THGRAF	BNL 11/77	OP	Calculates position and velocity of the thermo-chromatograph as a function of time for various models.
WTFG	GA	OP	Prepares fine group thermal cross section tape from GAND2 or FLANGE for spectrum codes.
1-DX		OP	Performs one-dimensional, diffusion theory, steady state calculations.

1.3.2 Containment Atmosphere Response (P. G. Kroeger)

An investigation of the containment atmosphere response under severe accident conditions, considering scenarios more remote than those of the recent source term study has been completed. The results confirm that the assumption of completely mixed atmospheres, as assumed in the source term study and in other preceding work, is conservative. Furthermore, it is shown that localized burning of pockets of combustibles requires the stipulation of further failures in an improbable way. Even then the resulting local pressure spikes which are close to the building failure pressure, since they are localized, do not appear to impose any dangerous stress levels on the CB structure. The report draft is currently being circulated for comment and will be released shortly.

1.3.3 Vapor Migration in Concrete (P. G. Kroeger and Y. Shiina)

The first idealized analysis of concrete migration in vapor has been documented in an informal report. Figure 1.3.1 shows typical concrete pressure and temperature distributions and liquid fractions resulting from an outer surface step change in temperature for the case of permeable outer surface (failed liner). Figure 1.3.2 shows corresponding results for the case of an impermeable outer surface (intact liner). The extension of this work to actual PCRV scenarios with varying surface tempertures is currently in progress.

1.3.4 Primary Loop Thermal Analysis under UCHA Conditions (P. G. Kroeger and J. Colman)

The additional capability to treat low thermal capacitances like the thermal barrier as quasi static layers has significantly improved the efficiency of the THATCH code for long term transients without LCS, and including the PCRV concrete. This modification also permits a simpler and more accurate analysis during the time of thermal barrier failure, and provides the option to partially retain thermal insulation at the side walls even after thermal barrier failure.

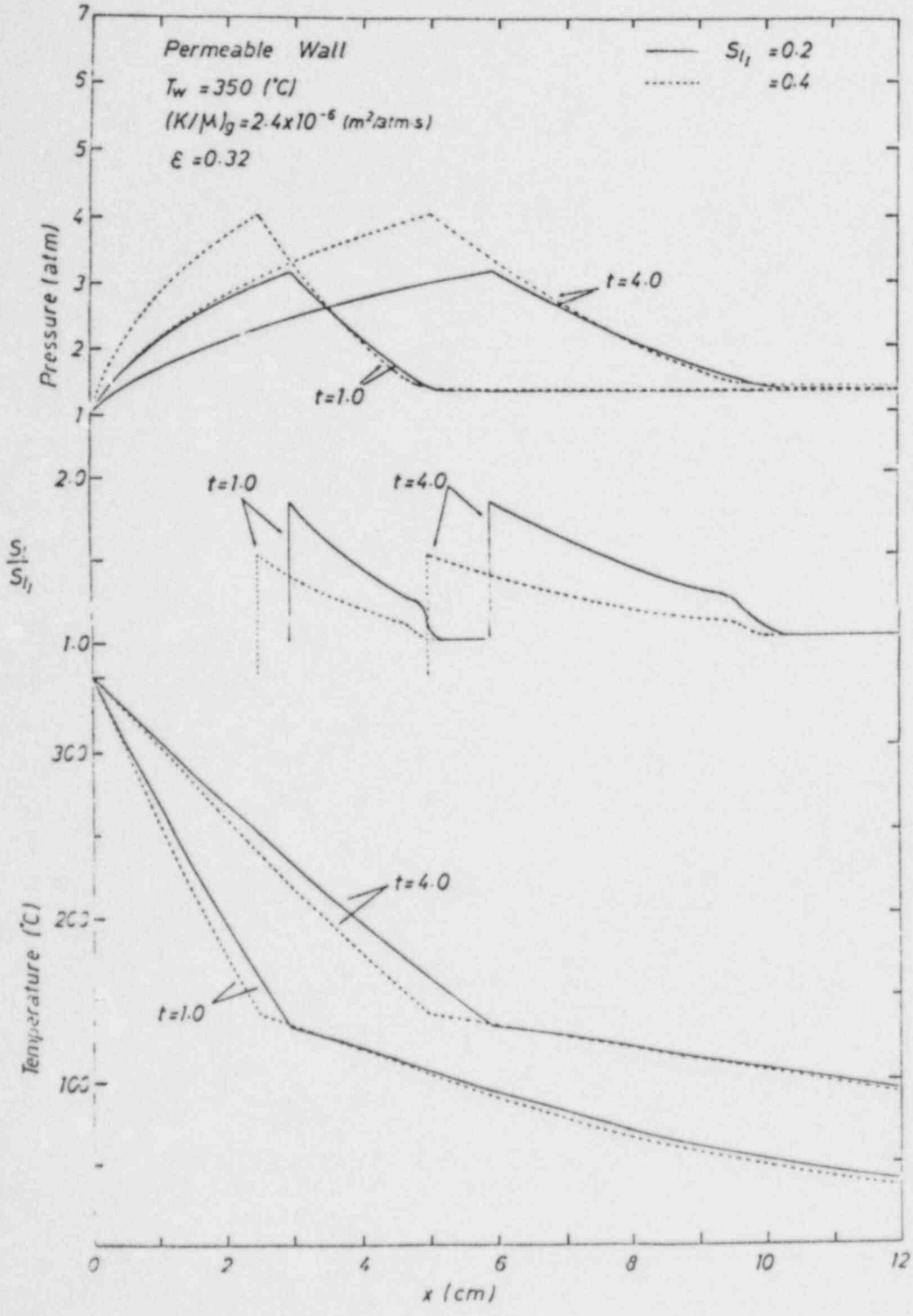

Figure 1.3.1 Typical temperature liquid and pressure distribution for case of permeable outer surface (Surface Temperature T_w=350°C; Permeability $(K/\mu)_g$=2.4x10^{-6} m^2/atms; Porosity ε=0.32, $S_{\ell i}$= initial liquid occupied void fraction; t=1 and 4 hrs.).

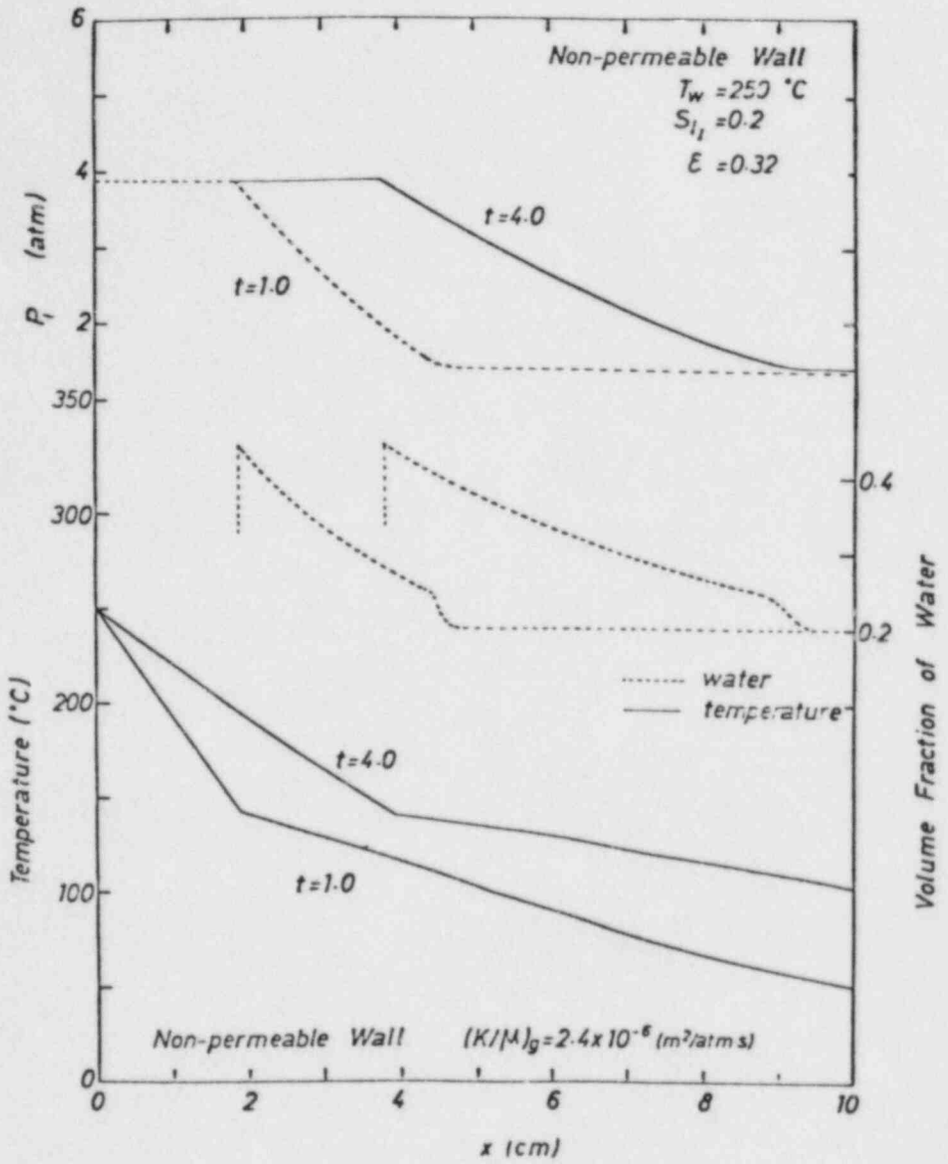

Figure 1.3.2 Typical temperature liquid and pressure distribution for case of impermeable outer surface (Surface Temperature T_w=250°C; Permeability $(K/\mu)g=2.4\times10^{-6}$ m²/atms; Porosity ε=0.32, $S_{\ell i}$= initial liquid occupied void fraction; t=1 and 4 hrs.)

REFERENCES

HIRTH, J. P. and POUND, G. M., Condensation and Evaporation, Pergamon Press, N.Y. 1963.

KINGERY, W. D., Introduction to Ceramics, p. 291, John Wiley and Sons, Inc. N.Y. 1967.

UNEBERG, G., SASTRE, C., and SCHWEITZER, D. G., Quarterly Progress Report January 1 - March 31, 1980, p. 76, BNL-NUREG-51217, 1980.

2. SSC Development, Validation and Application (J.G. Guppy)

The Super System Code (SSC) Development, Validation and Application Program deals with advanced thermohydraulic codes to simulate transients in LMFBRs. During this reporting period, work continued on three codes in the SSC series. These codes are: (1) SSC-L for simulating short-term transients in loop-type LMFBRs; (2) SSC-P which is analogous to SSC-L except that it is applicable to pool-type designs and (3) SSC-S for long-term (shutdown) transients occurring in either loop- or pool-type LMFBRs. In addition to these code development and application efforts, validation of these codes is an ongoing task. Reference is made to the previous quarterly progress report (Guppy, 1983a) for a summary of accomplishments prior to the start of the current period.

2.1 SSC-L Code (M. Khatib-Rahbar)

2.1.1 Steady State and Transient Modeling of Intra-Subassembly Heat Transfer and Flow Redistribution (M. Khatib-Rahbar, E.G. Cazzoli)

In Liquid Metal Fast Breeder Reactor (LMFBR) core designs, the fuel, blanket, control and shield assemblies are packed in a hexagonal configuration. The fuel and blanket assemblies consist of cylindrical fuel pins arranged in a closely packed triangular array separated by helical wire wraps. These wires also induce swirling flow which provides coolant mixing between subchannels.

During full power, steady state operation, the sodium flow Reynolds numbers range from 1.5×10^4 in the radial blanket to about 10^5 in the fuel assemblies. Following protected loss-of-flow transients, the flow regime changes from turbulent to transition and finally to laminar as the Reynolds numbers are reduced; subsequently leading to changes in the associated heat transfer modes from forced to mixed and eventually free convection (Khatib-Rahbar and Cady, 1981; Khatib-Rahbar and Cazzoli, 1983).

A number of detailed computer codes, generally written for applications to LMFBR design, are available (Khan, 1980). Due to the physical and numerical sophistication of these models, their application to long duration transient safety analysis problems is often constrained. Therefore, it is desirable to develop a numerically efficient model, supported by experimental data, capable of predicting heat transfer and flow regime behavior in LMFBR subassemblies under natural circulation conditions.

The present Two-Dimensional Intra-Subassembly Thermal-Hydraulics (TWIST) model is an extension to the simple porous body model proposed earlier (Khatib-Rahbar and Cazzoli, 1983). In this model, the presence of fuel rods is taken into account by inclusion of a volume porosity in the governing equations. The energy generation in the rods is modeled by a continuous volumetric heat source distribution. The energy transfer in the transverse direction is modeled by molecular conduction and an empirically determined effective eddy diffusivity (Khatib-Rahbar and Cazzoli, 1984).

The two-dimensional conservation equations are written (Khatib-Rahbar and Cazzoli, 1984) assuming; (1) Boussinesq approximation for incompressible fluids applies, (2) negligible axial conduction, (3) negligible viscous dissipation and (4) pressure is uniform at any axial level.

The solution for this two-dimensional parabolic flow is obtained by starting with known temperature and velocity distributions at an upstream station at a given time and marching in the streamwise direction. For every forward step, the temperature and velocity distribution in the cross-stream coordinate is calculated at one streamwise station. Thus, computationally, only a one-dimensional problem is solved (Khatib-Rahbar and Cazzoli, 1984; Patankar, 1980; Hornbeck, 1973). In implementing this method in the TWIST code, a fully implicit time differencing approach is utilized. This removes numerical instabilities and enhances computational efficiency.

The code requires as input: (1) the rod bundle geometry, (2) empirical data (friction factor, mixing parameters, etc.), (3) inlet velocity and temperature and (4) power distributions and decay characteristics. TWIST calculates; (1) steady-state (pre-transient) temperature and flow fields and (2) transient thermal-hydraulic conditions including the duct wall temperatures, the coolant temperatures and velocities, and the axial pressure distributions. The code also models the lower and upper fission gas plena, and allows variable time steps as governed by the user supplied accuracy criterion.

The TWIST code is being assessed using rod bundle experimental measurements typical of LMFBR conditions. Full-size, 61-pin radial blanket assembly heat transfer tests have been performed at Westinghouse (Engel, et al., 1980; Engel, et al. 1982) using electrically heated fuel rod simulators cooled by liquid sodium. These tests cover a wide range of flow and heat transfer regimes, namely, from fully turbulent to fully laminar flow, corresponding to forced, mixed, and free convection at both steady state (Engel, et al., 1980) and transient conditions (Engel, et al., 1982).

Figure 2.1 shows the calculated and measured steady-state transverse temperature distribution corresponding to a 2.8 to 1 power skew across the assembly, corresponding to high Reynolds number forced convection, and low Reynolds number natural convection conditions. It is seen that the calculated TWIST results are in good agreement with experimental measurements. The larger discrepancy in the low-power side of the bundle is influenced by the reduction in the flow area caused by fuel pin distortion and bowing as a result of large transverse power gradient. Similar observations have been made using COTEC, ENERGY, and COBRA-IV computer codes (Juneau and Khan, 1979). Figure 2.1 also demonstrates that improved mixing (higher ε_{∞}^{*}) leads to enhancement in energy redistribution across the assembly.

Figure 2.2 illustrates the results of a typical transient calculation for an undercooling experiment performed by (Engel, et al., 1982) which corresponds to a 1:0 maximum-to-minimum heat input gradient and gives rise to large temperature gradients between the heated and the unheated halves of the test section. Again, comparison of measured and calculated results illustrates

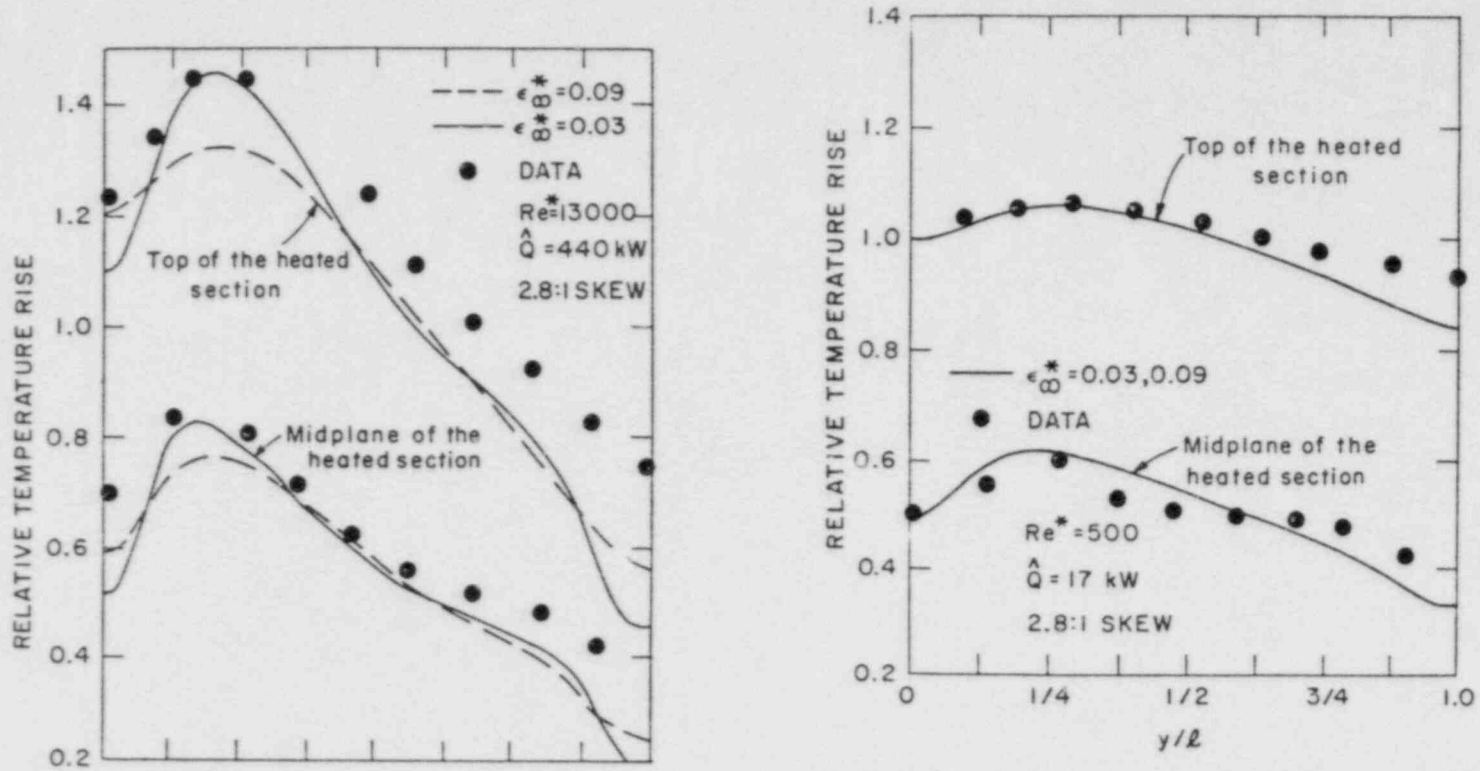

Fig. 2.1 Comparison of TWIST and Westinghouse Data for Steady-State Forced and Free Convection Conditions

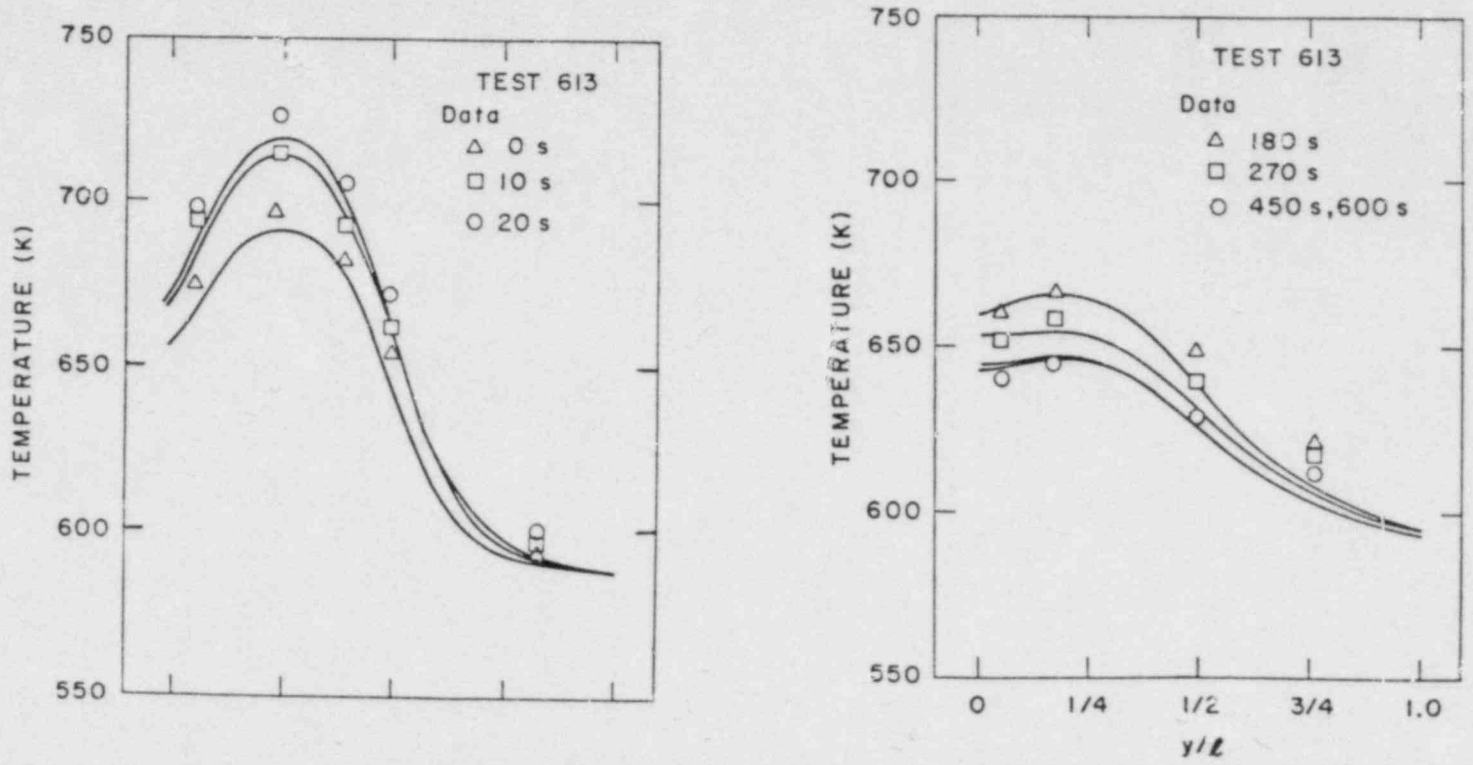

Fig. 2.2 Comparison of TWIST and Westinghouse Data for an Undercooling Transient

excellent agreements for steady-state and transient cross-assembly temperature profiles. It is seen that significant profile flattening takes place, reflecting the contribution of buoyancy-induced flow redistribution and transverse thermal conduction and mixing effects.

Due to the physical accuracy and numerical efficiency (5 to 10 times faster than real time) of TWIST, it provides an excellent tool for study of long duration natural circulation transients in LMFBR assemblies. The code can also be coupled with the SSC series of computer codes for best estimate evaluation of the maximum coolant temperatures within representative assemblies.

2.1.2 Safety Implications of Flow Control Valves (J.G. Guppy, U. Quast GRS/FRG)

In a joint effort with the GRS/FRG, SSC-L is being applied to investigate any potential detrimental effects on the primary loop flow rate and core flow rate and temperature responses, caused by operation of the post-scram flow control valves. These flow control valves are located in the cold legs and are regulated following scram to adjust the flow rates so as to maintain a fairly constant vessel outlet temperature and, thus, mitigate thermal shock effects.

The effect on the temperature response is shown in Figure 2.3. The results for two cases are presented; one in which the flow control valves (CV) operate, and one where they do not. In the "no CV" case, one can see that the core is overcooled due to the initial sharp decrease in the power-to-flow ratio following scram. After mixing with the upper plenum sodium, this temperature rampdown is transmitted to the loop piping and downstream components. With the control valves operating, the flow rates are controlled to maintain the core outlet temperature about a certain setpoint. As seen, some oscillation of the core temperature can result, but the temperature at the vessel outlet is essentially constant. Thus, the design goal of mitigating the thermal shock to the loop has been accomplished.

The corresponding response of the primary loop flow rates is shown in Figure 2.4. The results for three cases are presented here: 1) "no CV" following a normal scram, 2) "no CV" following a scram and loss of all pumping power (i.e., a natural circulation event) and 3) a case of normal scram with CV operating. The natural circulation event is included for comparison purposes to indicate that the use of flow control valves can potentially produce flow rates on a frequent basis that are even lower than those from this highly unlikely case. For the "CV operating" case, the flow rate will respond to the in and out movement of the valve gate.

For this study, the core was represented by five (5) channels: hot fuel, average fuel, hot blanket, average blanket and a non-nuclear channel to represent control and shield assemblies. Shown in Figure 2.5 is the response of the flow rate in the cold (non-nuclear) fifth channel. As seen, for the "CV operating" case, the flow rate in this channel may potentially reverse for a period of time. Physically, this is caused by buoyancy driven flow redistribution. Here, the hotter channels will divert flow to themselves from the

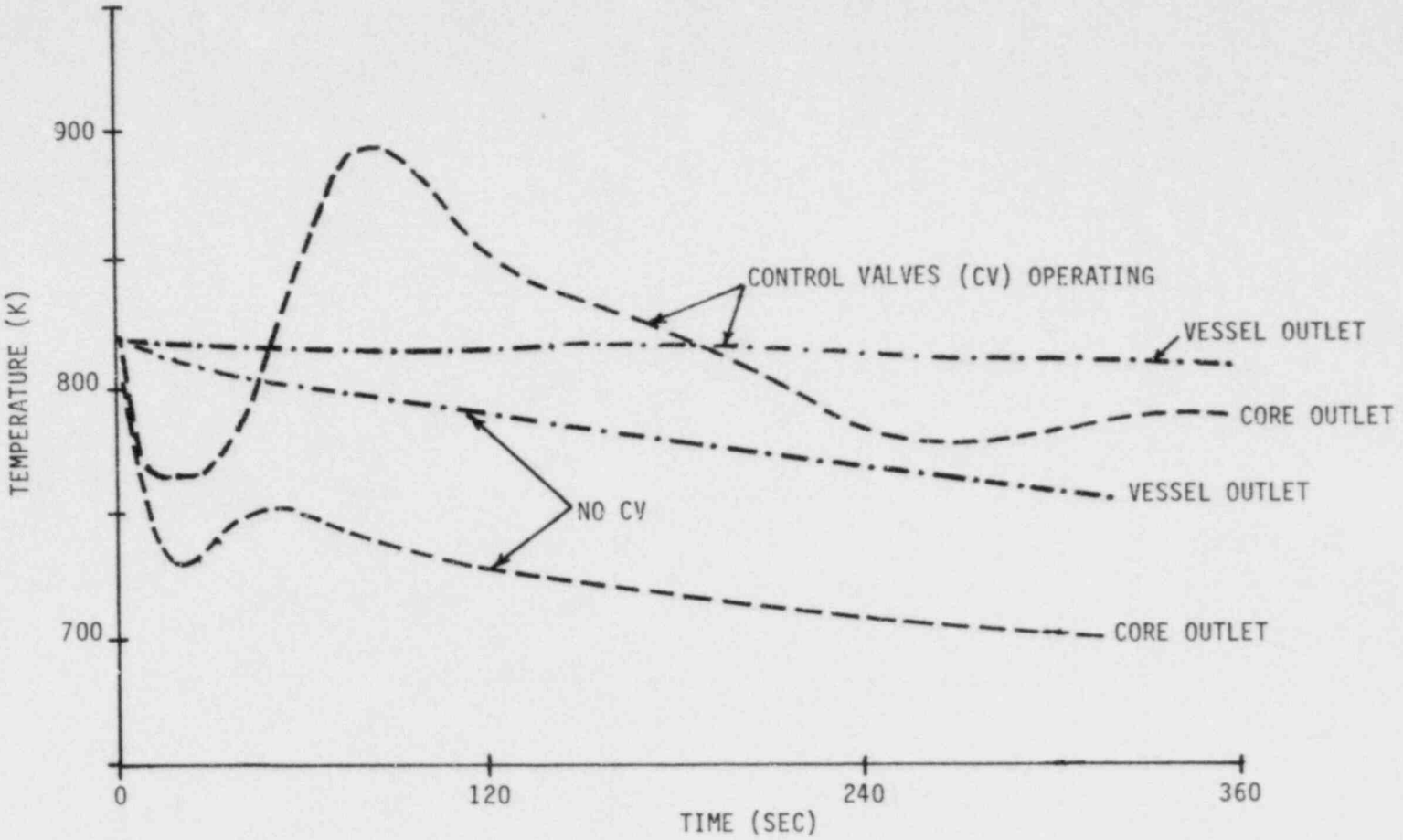

Fig. 2.3 Average Core and Vessel Outlet Temperatures

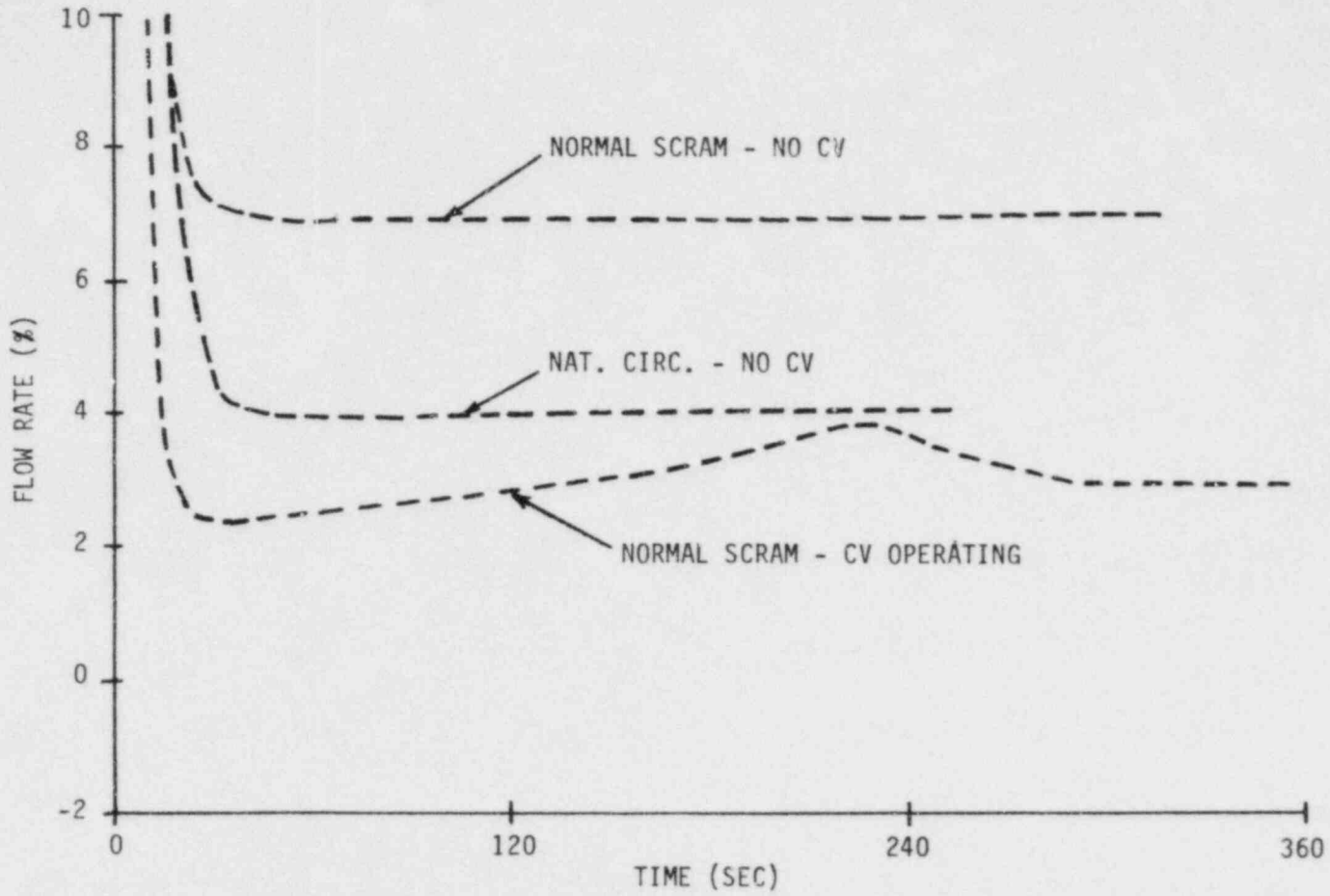

Fig. 2.4 Primary Loop Flow Rate

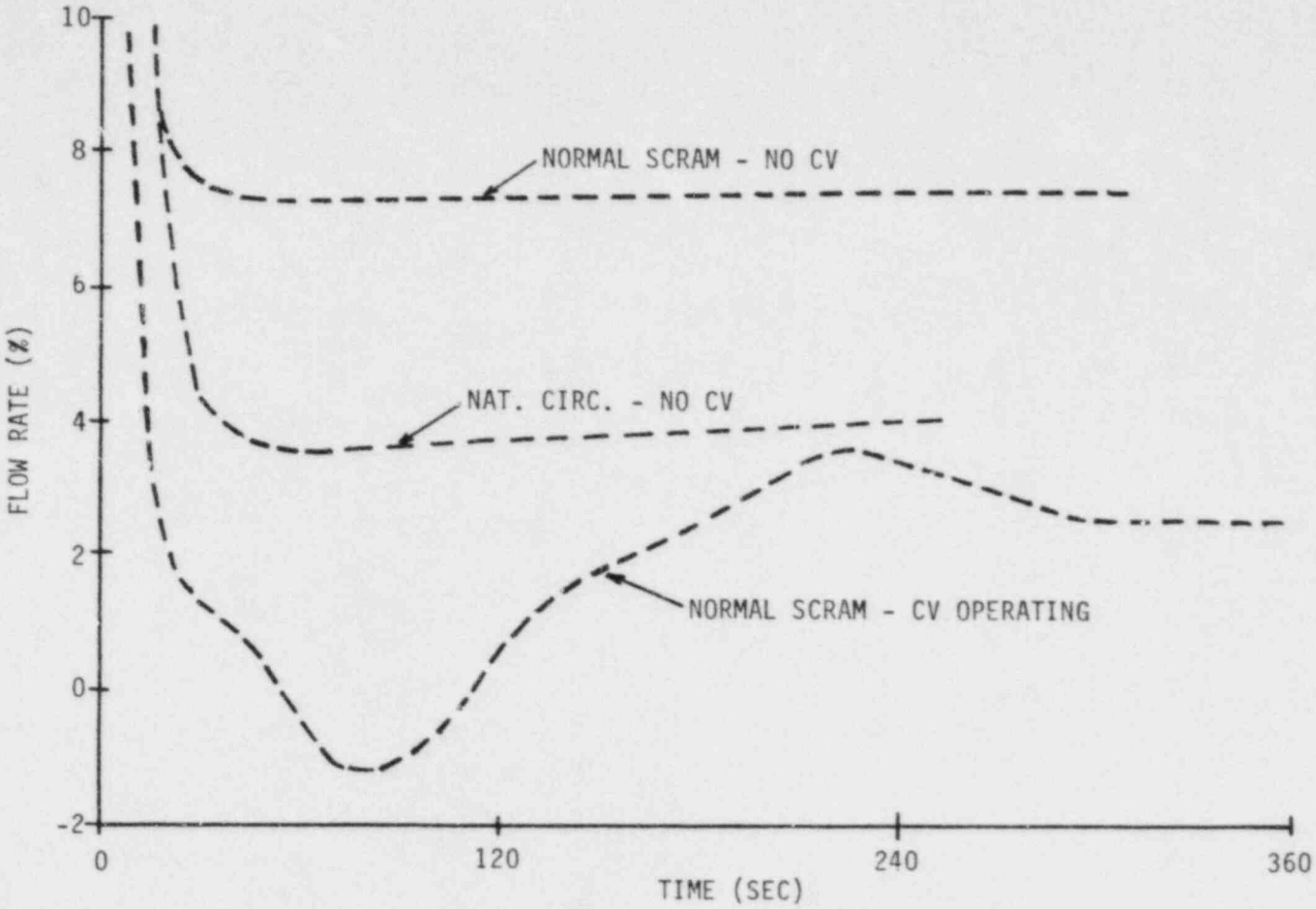

Fig. 2.5 Cold Channel Flow Rate

cooler ones. This effect will only be computed if the simulation includes an inter-assembly flow redistribution model, such as contained in SSC. If this flow reversal were to occur, it would have the potentially adverse effect of sweeping substantially hotter sodium from the upper plenum into the much cooler channel.

A second adverse effect which the flow control valves can potentially cause is illustrated in Figure 2.6. Plotted here are the responses of the hot fuel and blanket temperatures for two cases: with and without CV operating. As typified by these results, the heat producing assemblies have the potential of being subjected to substantially higher temperature fluctuations through the use of flow control valves. Study of these preliminary results is continuing.

2.1.3 Inter-Assembly Heat Transfer (W.C. Horak)

Development of an inter-assembly heat transfer model for inclusion in SSC has concentrated on two areas:

1) interstitial sodium

2) duct wall temperatures

Most inter-assembly heat transfer models consider the interstitial sodium to be stagnant, but certain experiments indicate interstitial coolant motion may provide an additional heat sink. Therefore, a parallel flow model for the interstitial coolant may need to be developed.

Various advanced nodal methods are being looked at to see if they are applicable to calculating duct wall temperatures. However, since earlier work has suggested that an in-line assembly model may be adequate for a system representation (as opposed to the more standard seven-assembly cluster used in detailed codes), extension of the present intra-assembly model appears to be the most promising approach.

2.1.4 User Support (J.G. Guppy, W.C. Horak, R.J. Kennett, U. Quast GRS/FRG)

A German engineer from the GRS visited BNL during this period to discuss SSC modifications and applications for analysis of the SNR-300 reactor system. Updates to a previous version of the SSC base program library had been developed to represent special design features of the SNR-300 which were not presently modeled. These included: 1) special control valves in the primary and secondary sodium loops, which are activated following a scram signal and are adjusted to modify the flow rates in the respective loops so that a relatively constant temperature is maintained and 2) certain plant protective system functions not previously modeled.

The GRS is interested in making these updates compatible with the latest version of the SSC base program library. There are also additional features which are being considered including: 1) steam generator feedwater and drain flow controllers; 2) reactor power limit controller and 3) reactor temperature limit controller.

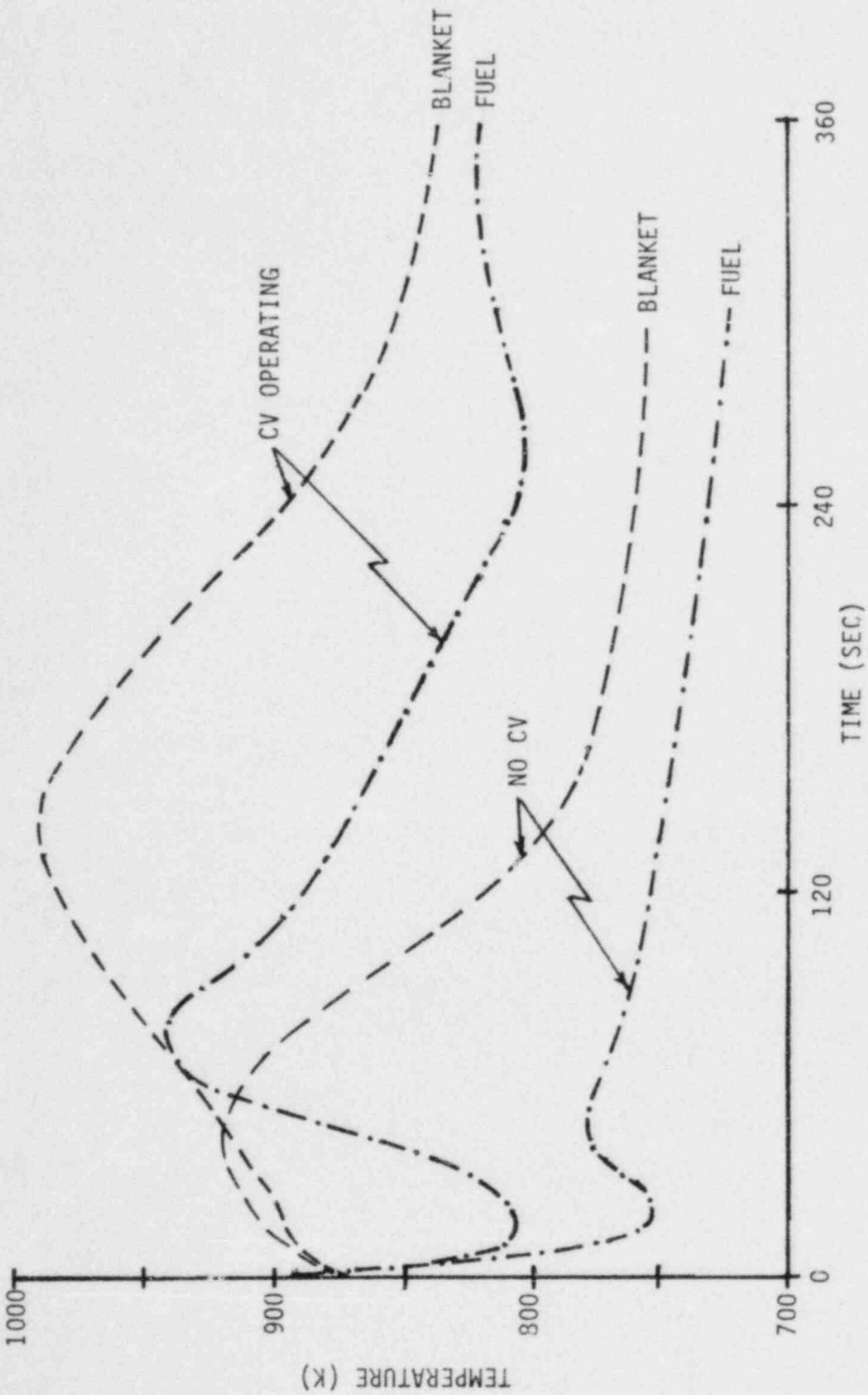

Fig. 2.6 Hot Fuel and Blanket Temperatures Following Normal Scram

The two additional in-vessel plant control systems have been modeled for use in the SSC simulation of the SNR-300 reactor. These two controllers, the Reactor Power Limiter Control (PLC), and the Temperature Limiter Control (TLC), are designed to minimize scrams during slow transients. The PLC and the TLC block control rod action and adjust the reactor power output using the trim rods. After completion of the controller action, the control rods are allowed to move either manually or automatically.

The controller models have been tested in a stand-alone computer code for a number of different transient inputs. Incorporation of these models into SSC will be done as soon as additional modeling details are obtained. Final testing on a series of appropriate transients will be done at that time.

In order to improve the user interactive output options of SSC, a standardized set of graphics symbols for use in SSC plant representations is being developed. These standardized symbols will be used to represent the values of the various plant parameters at steady state and during the transient.

2.2 SSC-P Code (E.G. Cazzoli)

2.2.1 Code Maintenance (E.G. Cazzoli)

The pool version of SSC is under review and is being modified in the latest cycle of the program library, in order to take advantage of recent improvements in SSC-L. In order to check that the updated version of SSC-P incorporating the revisions is correct, previously simulated plant transients performed for Phenix will be repeated and comparisons made for consistency.

2.2.2 Modeling Considerations to Represent the EBR-II Primary System (I.K. Madni, W.C. Horak, J.G. Guppy)

The Experimental Breeder Reactor II (EBR-II) is an LMFBR power plant of pool design, located in Idaho, rated to produce 62.5 MW thermal power (20 MWe). The mission of EBR-II has evolved to the point where, together with serving as an irradiation facility for fuels and materials, it is being extensively used to provide experimental in-plant test data on the thermal, hydraulic, and neutronic response of the core and plant to normal and abnormal operation. These tests have, and will continue to provide very useful information for the future design, operation and safety analysis of LMFBR plants. For example, the test data can form the basis for validation or further development of models intended to predict plant behavior during a variety of operational conditions.

In support of the SSC application efforts to provide predictions of EBR-II overall plant behavior, models are required to represent the EBR-II primary system. These modifications are required due to some special design features in EBR-II, which lie outside the models already present in SSC (Guppy, et al., 1983b). The immediate application for these models, as part of SSC, is to simulate the current series of whole-plant type transients, including natural circulation, that are being planned for the EBR-II plant beginning in 1984. The comparisons thus obtained will also contribute towards the validation of SSC as a plant simulation tool.

EBR-II is a pool reactor in which all the primary components including reactor, pumps, intermediate heat exchanger, piping, as well as shutdown coolers, and other support systems are submerged in a large pool of sodium, contained within the primary tank. The space between the sodium free surface and primary tank is filled with argon gas. The primary tank is of double-wall construction (tank within a tank), the space between the inner and outer tanks being filled with inert gas. The outer tank is heavily insulated to minimize heat loss from the primary system.

The reactor is centrally located at the bottom of the primary tank, with the pumps and heat exchanger arranged radially around the reactor and elevated somewhat above it. The reactor consists of a hexagonal shaped central core, containing enriched uranium, surrounded by radial and axial blankets, containing either depleted uranium, or stainless steel. The subassemblies are contained in and supported by a stainless steel reactor vessel, comprised of a grid plenum assembly, reactor vessel shell, and reactor vessel cover, and surrounded by a radial neutron shield. The vessel top cover, which also contains neutron shielding, is removable to permit fuel handling. It contains penetrations for entry of control rod drive shafts, special in-core test facilities, etc. During power operation, a small amount of leakage occurs through various openings in the cover. This leakage flow is employed as a part of the neutron shield cooling system in this region.

Forced flow to the reactor is provided by two main sodium pumps, which are vertically mounted, single-stage, centrifugal units, operating in parallel, each rated at a maximum of approximately 0.35 m^3/s at 61 m head. Each impeller is submerged in primary sodium; however, the motor units are located outside the primary tank. Primary system flow is varied by manually adjusting the pump speeds.

An auxiliary electromagnetic pump of small capacity and low head operates in series with the large primary pumps. During normal operation, the auxiliary pump has no appreciable effect on the primary coolant flow. The main purpose of this pump is to augment thermal convection under certain conditions of reactor shutdown. The reactor outlet piping (whose linear run is shaped like a Z) carries hot sodium through the environment of the cold pool, at substantially lower temperature. It is therefore provided with an insulating steel sleeve, surrounding the pipe, to minimize heat losses. The space between pipe wall and sleeve is filled with stagnant sodium from the pool.

The IHX transfers essentially all of the heat generated in the reactor to the secondary system. It is a single-pass counter flow heat exchanger. Primary sodium (radioactive) enters the exchanger via piping, flows downward around the tubes on the shell side, and returns to the primary tank through a cylindrical opening near the bottom. The secondary sodium (non-radioactive) flows upward through the tubes. To minimize pressure drop in the unit, axial flow is maintained as much as possible. The IHX primary outlet is located above the reactor centerline to provide natural convection shutdown cooling.

The coolant flow path is as follows: sodium from the primary tank enters the pumps through sump-type inlets, and exits into a main pipe where it is divided into high and low pressure streams. High pressure sodium is piped from

each pump outlet directly to the high-pressure inlets of the reactor grid-plenum assembly and flows upward through the core and inner blanket assemblies (inner core region). The control and safety rods, located in the inner core region are also cooled by the high pressure coolant. Low pressure coolant is routed via a smaller line through a throttle valve, to the low-pressure inlets of the grid-plenum assembly, and flows upward through the outer blanket assemblies. Both streams mix in the reactor outlet plenum. The mixed coolant exits the reactor vessel through a simple outlet nozzle, flows via piping, through the auxiliary EM pump and into the shell side of the IHX where it is cooled and returns to the primary tank at nearly the bulk pool sodium temperature. Leakages occur at several points along the coolant flow path.

2.3 SSC-S Code (B.C. Chan)

2.3.1 Improved Upper Plenum Modeling (B.C. Chan)

The FFTF upper plenum was simulated using the upper plenum stand-alone code. A configuration, considered to be representative of the FFTF upper plenum, utilizing a 15 x 13 variable cell spacing mesh was utilized. The inlet temperature and velocity profiles used in this transient calculation were supplied from the results of the SSC four channel core model simulation. A 200 second transient case has been simulated. Results are being analyzed.

2.3.2 Effect of Piping Insulation on Long Term Loss-of-Heat Sink Accidents (W. C. Horak)

An input deck is being assembled to determine the effect of rock wool pipe insulation on a loss-of-heat sink accident. Information has been obtained on some of the material properties and the remainder is expected to be obtained shortly. Selection of the specific reactor type for the simulation has not been finalized.

2.4 Code Validation (W.C. Horak)

2.4.1. FFTF Long Term Simulations (W.C. Horak, R.J. Kennett)

The 100%, 75% and 5% power long term transients were run with the loop indexing corrected. As expected, the simulation results did not change much due to the symmetry of the transients.

As part of the testing of the IHX plena thermal mass model, an FFTF 100% power scram to natural circulation test was simulated for a total of 1800(s). Initial analysis indicates good agreement with the experimental data, especially in the primary cold leg temperature. A more detailed comparison to all the loop data is in progress.

With the completion of the FFTF post-test simulations, a standard test problem for future cycle validation is being developed based on the 35% power FFTF scram to natural circulation test. This deck is based on the four channel, two loop deck used for the long term simulations. Since this test was asymmetric in the secondary heat transport loops, it should prove a useful addition to the current set of standard test problems.

REFERENCES

ENGEL, F. C., et al., "Characterization of Heat Transfer and Temperature Distribution in an Electrically-Heated Model of an LMFBR Blanket Assembly," Nucl. Eng. Design, 62, 335 (1980).

ENGEL, F. C., et al., "Loss-of-Flow Transient Heat Transfer Tests of a Full Size LMFBR Blanket Model," ASME Paper No. 82-WA/HT-35 (1982).

GUPPY, J. G., et al., (1983a), "SSC Development, Validation and Application," Safety Research Programs Sponsored by Office of Nuclear Regulatory Research Quarterly Progress Report, July 1 - Sept. 30, 1983, Brookhaven National Laboratory Report to be published.

GUPPY, J. G., et al., (1983b), "Super System Code (SSC, Rev. 2), An Advanced Thermohydraulic Simulation Code for Transients in LMFBRs," Brookhaven National Laboratory, BNL-NUREG-51650, April 1983.

HORNBECK, R. W., Numerical Marching Techniques for Fluid Flows With Heat Transfer, National Aeronautics and Space Administration, NASA-SP-297, Washington, D. C. (1973).

JUNEAU, J., and KHAN, E., "Analysis of Steady State Combined Forced and Free Convection Data in Rod Bundles," Argonne National Laboratory, FRA-TM-116 (1979).

KHAN, E., "LMFBR In-Core Thermal-Hydraulics: The State of the Art and U.S. Research and Development Needs," PNL-3337/UC-32, Battelle-Pacific Northwest Laboratory (1980).

KHATIB-RAHBAR, M., and CADY, K. B., "Dynamical Models and Numerical Simulation of System-Wide Transients in Loop-type LMFBR," Nucl. Eng. Design, 64, 259 (1981).

KHATIB-RAHBAR and CAZZOLI, E. G., "Intra-Assembly Flow Redistribution in LMFBRs: A Simple Computational Approach," Trans. Am. Nucl. Soc., 45, 816, (1983), also see First Proceeding of Nuclear Thermal Hydraulics, 13 (1983).

KHATIB-RAHBAR, M. and CAZZOLI, E. G., "Two-Dimensional Modeling of Intra-Subassembly Heat Transfer and Buoyancy-Induced Flow Redistribution in LMFBRs," Brookhaven National Laboratory Report, NUREG/CR-3498, BNL-NUREG-51713, (1984).

PATANKAR, S. V., Numerical Heat Transfer and Fluid Flow, Hemisphere Publishing Co., McGraw -Hill, New York (1980).

PUBLICATIONS

CHAN, B. C., "A Buoyancy-Dominated Model for LMFBR Upper Plenum Flows," Brookhaven National Laboratory, BNL report to be published, 1984.

CHAN, B. C., KENNETT, R. J., GUPPY, J. G., "A Numerical Investigation of Buoyancy-Induced Flow Stratification in the LMFBR Upper Plenum," Brookhaven National Laboratory, BNL report to be published, 1984.

GUPPY, J. G., HORAK, W. C., VAN TUYLE, G. J., "Independent Assessment of the Natural Circulation Capability of the Heterogeneous Core CRBR," Trans. Am. Nucl. Soc. 45, 416, (1983).

HORAK, W. C., et al., "Short Term Post Test Analysis of the FFTF Scram to Natural Circulation Transients Using SSC," Brookhaven National Laboratory, BNL report to be published, 1984.

HORAK, W. C., KENNETT, R. J., GUPPY, J. G., "Long Term Post-Test Simulation of the FFTF Natural Circulation Tests," Brookhaven National Laboratory, BNL report to be published, 1984.

KHATIB-RAHBAR, M., CAZZOLI, E. G., "Two-Dimensional Modeling of Intra-Subassembly Heat Transfer and Buoyancy-Induced Flow Redistribution in LMFBRs," Brookhaven National Laboratory, NUREG/CR-3498, BNL-NUREG-51713, 1983.

KHATIB-RAHBAR, M., "Core Coolability Following Loss-of-Heat Sink Accidents," Trans. Am. Nucl. Soc. 45, 365, (1983).

KHATIB-RAHBAR, M., "Intra-Assembly Flow Redistribution in LMFBRs: A Simple Computational Approach," Trans. Am. Nucl. Soc. 45, 816, (1983) also see 1st Proc. of the T&H Division, 13-20 (1983).

3. Balance of Plant Modeling (J.G. Guppy)

The Balance of Plant (BOP) Modeling Program deals with the development of safety analysis tools for system simulation of nuclear power plants. It provides for the development and validation of models to represent and link together BOP components (e.g., steam generator components, feedwater heaters, turbine/generator, condensers) that are generic to all types of nuclear power plants. This system transient analysis package is designated MINET to reflect the generality of the models and methods, which are based on a momentum integral network method. The code is to be fast-running and capable of operating as a self-standing code or to be easily interfaced to other system codes. Reference is made to the previous quarterly progress report (Guppy, 1983) for a summary of accomplishments prior to the start of the current period.

3.1. Balance of Plant Models (G. J. Van Tuyle)

The turbine stage model recently incorporated in MINET is functioning as planned. In tests conducted thus far, the model is very stable and passes all consistency tests.

With the increased usage of modules with very large pressure gradients, the MINET steady state network pressure and flow solver began to have difficulty in converging. As a result, special logic was introduced to deal with such a module when it is in a segment by itself. With the revision, the pressure change across an isolated pump, valve, or turbine stage is recalculated during each internal iteration of the pressure and flow solver. Additionally, choking across a valve is now factored into the steady state calculation. Thus, the user can now introduce modules with very large pressure gradients, as long as they are isolated in a segment.

With Version 1 of MINET complete, at least in terms of modeling, further model development will be incorporated into Version 2, which will include a generic control system model. Several control functions are currently under development, partially in support of an effort to represent the SNR-300 control system.

3.2. MINET Code Improvements (G.J. Van Tuyle, T.C. Nepsee)

The version of MINET ("Version 0") being utilized with CY-41 of SSC has not been altered during the last year. The current development effort remains focused on the stand-alone version, now designated Version 1. With most of the features of Version 1 now in place and working, the effort will focus on testing and adding new features when needed. In the recent period, a Thom two-phase friction multiplier was incorporated and a viscosity function was revised to improve its efficiency.

Testing of the heat exchanger module, using several different input decks, has revealed a few additional areas for improvement in the steady state iterative schemes. These gaps were closed, and no significant problems have since appeared in any of the test runs.

The critical flow models in MINET have been revised in order to reduce storage requirements and provide a more comprehensive representation. With the new package, Extended Henry-Fauske is used for subcooled flow, Moody is used for two phase choking, and an isentropic representation is used for superheated flow. The code interpolates between Extended Henry-Fauske and Moody near the boiling boundary so as to reduce problems with discontinuities. As the previous Moody function contained a great deal of tabular data, a substantial reduction in storage requirements was attained.

Because the MINET steady state solver is highly generalized, it is quite likely the user may underconstrain the problem, in which case, user guesses may effectively become boundary conditions. This is not, in itself, a problem. However, MINET must choose which of the user's guesses to consider fixed and which ones are to be used to bring the system to equilibrium. Recently, this process has been optimized so as to guarantee not only a solution for the underconstrained problem, but also the best solution, i.e., one with the minimum adjustment of user estimated conditions. While this whole area is very subtle, the achievement is significant and resolves a very tricky problem.

Print interval control, transaction file generation and context save functions have been completed and tested. Appropriate revisions have been made to the input data file definition to allow full user control of the above functions.

An updated version of MINET (Version 1.6) has been constructed incorporating revisions to the input processor and computational code.

Interfaces for boundary module data have been designed and partly implemented. Two new interface subroutines were introduced and some minor computational code modifications were made as part of the implementation.

An enhancement to the input processor code has been made to allow correct processing of networks with fluid connections between heat exchanger shell and tube sides.

Several modifications have been made to the input processor to minimize peak storage size in order to accommodate data sets for test cases requiring large numbers of system nodes. A case requiring storage for approximately five hundred nodes has been successfully run without the need to use CDC Large Core Memory. A one-thousand node case is now being developed.

3.3. MINET Standard Input Deck (G.J. Van Tuyle)

For Version 0 of MINET (SSC, CY-41), input deck E1 continues to be the standard for EBR-II. Two new standard decks have been documented, S3 for the German SNR-300 plant, and K1 for the German KNK-II facility.

For Version 1, deck E1, for the EBR-II system, is being utilized repeatedly to check out the impact of various code modifications, such as the recent revision of the critical flow package. Deck X2, a generalized balance of plant configuration, is being tested as a precursor to a first BWR balance of

plant deck, to be used in the RAMONA application. Deck H1 was used in a validation study using helical coil steam generator transient test data obtained from PNC of Japan. Decks X1 (example) and P2 (PWR) are supplemental test decks.

3.4. MINET Applications (G.J. Van Tuyle)

Results of several test cases indicate that Version 1 of MINET is functioning as planned, at least as far as can be determined at this stage. A validation study using EBR-II transient data yielded excellent results, with the simulation producing nearly identical results to those obtained using Version 0 of MINET (SSC, CY-41).

The 20% reduction in feedwater transient for the PNC (Japan) helical coil heat exchanger was re-run using the new version of MINET. In the previous application, using Version 0, we did not account for the structure, yielding MINET results that lead (in time) the experimental temperatures at the sodium outlet. In the recent run, we accounted for the structure, and noted a significant improvement in the calculated sodium outlet temperature prediction. The simulation was performed using MINET deck H1, which is shown schematically in Figure 3.1. Sodium and water inlet temperatures were held constant, and calculated and measured outlet temperatures were as shown in Figure 3.2.

In testing example deck X2, which is a generic balance of plant configuration, a number of time step sizes and nodalizations were used. We found that a relatively large time step may be possible, although more realistic component sizings and conditions will have to be considered before this can be stated with any certainty. In the nodalization studies, the basic X2 deck was simulated for 100 seconds of null (steady-state) transient using from 42 to 500 nodes. Using a 5 second time step (which gave very stable results), the 42 node run required about 1.3 seconds of CDC 7600 CPU time, and the 500 node run needed just over 8 seconds. The fact that the run time increases roughly with the number of nodes, and that these runs could be and were made using CDC 7600 small core memory, supports our contention that MINET can accommodate the enormity of balance of plant systems without suffering undue execution penalties.

The capabilities built into the stand-alone MINET (Version 1) far exceed those in Version 0, which is currently working with SSC. Therefore, after further validation of Version 1, we will interface Version 1 with SSC to obtain a far more extensive representation of LMFBR systems.

Preparations are currently being made to interface MINET with the RAMONA-3B code, for BWR plant transient analysis, in support of the Severe Accident Sequence Analysis (SASA) Program. The initial objective will be to provide improved feedwater/ECCS flow and temperature boundary conditions for ATWS events, such as main steam isolation valve (MSIV) closure without scram. Prior to this planned application, a validation study of the combined RAMONA-3B/MINET representation, using startup test transient data from the Browns Ferry (BWR) plant, will be conducted.

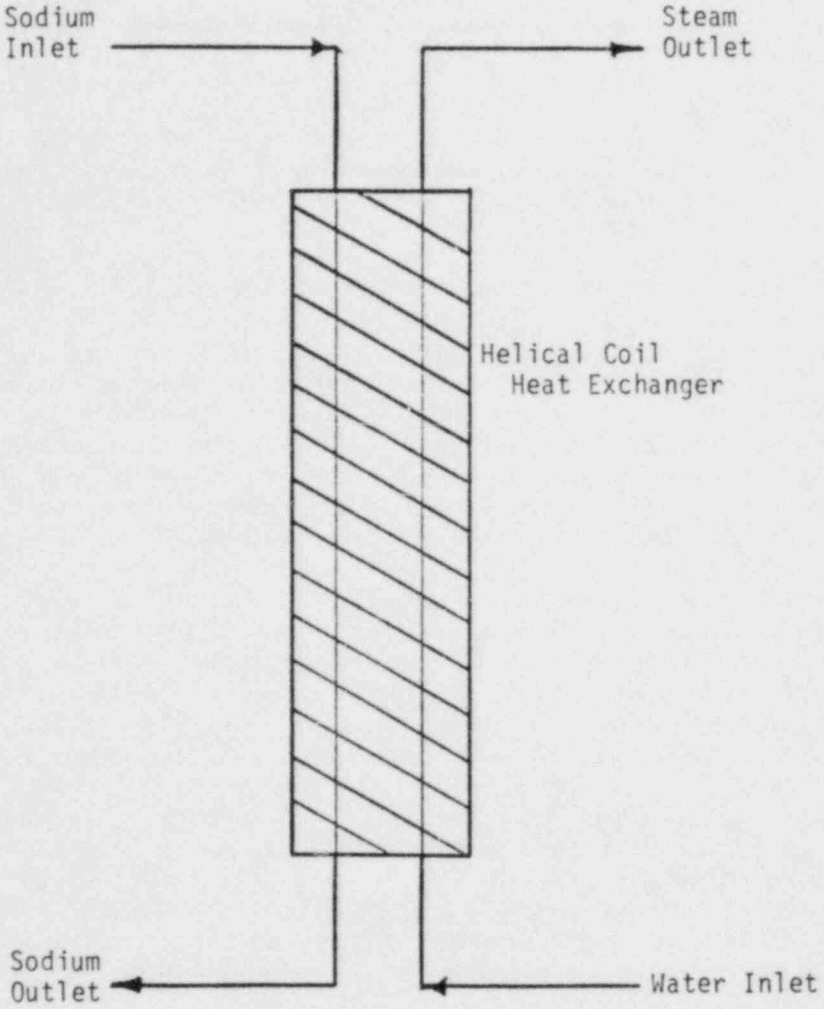

Fig. 3.1 MINET Standard Deck H1. Helical Coil Steam Generator Test Rig

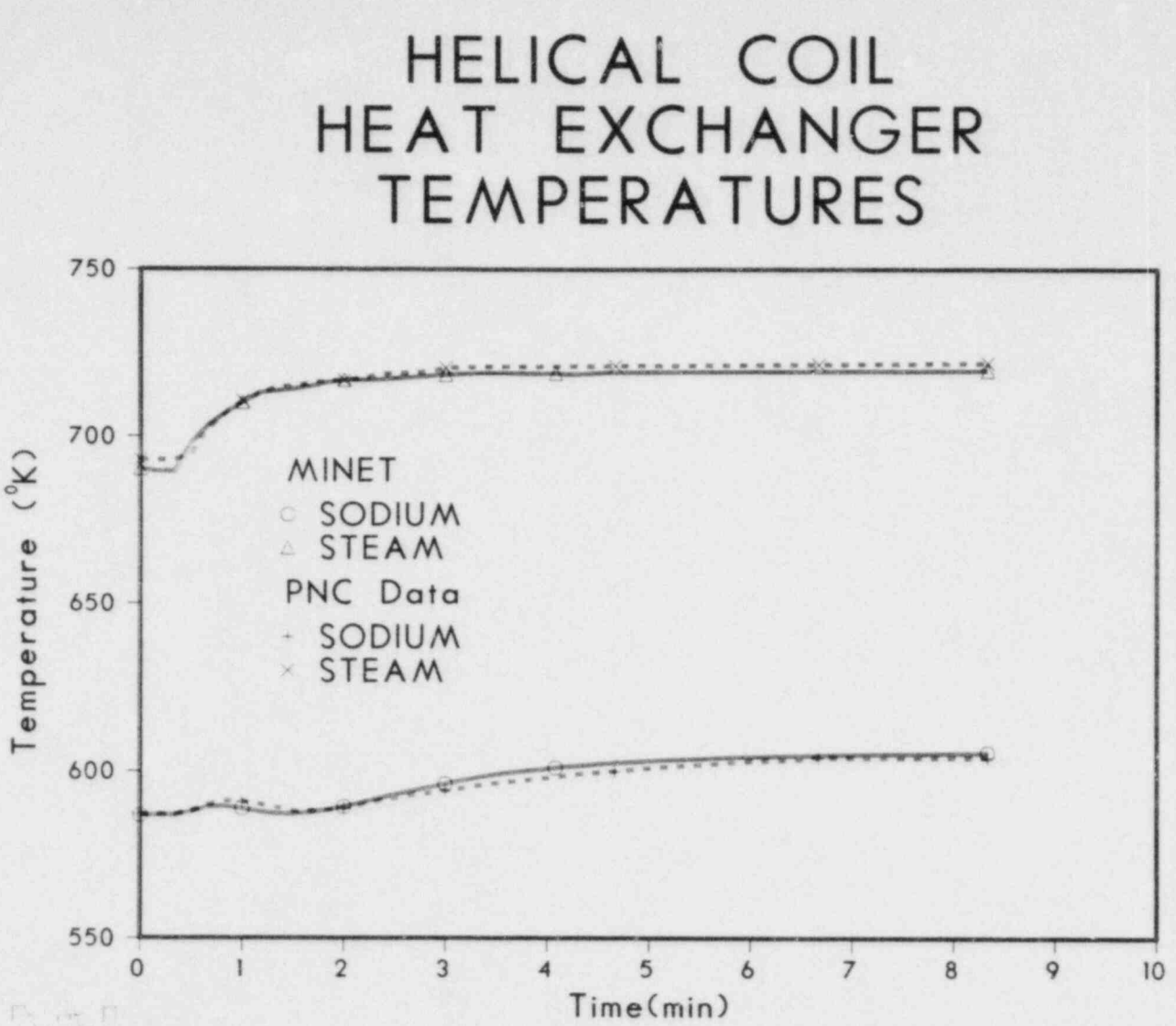

Fig. 3.2 HX Outlet Temperatures, Revised to Include Structural Heat Capacitance

Among the various options for running transients using RAMONA are the possibilities of specifying flow rate and temperature vs time tables for the feedwater, reactor core isolation cooling (RCIC) system, and high pressure injection (HPI) system contributions. The current plan is to specify these options, but to have MINET write the entries into the RAMONA tables. With a similar approach already planned for the MINET boundary condition tables, this means each code would be unaware of the other, which we consider to be the ideal case.

3.5. User Support (G.J. Van Tuyle)

Recent efforts have been focused on developing a control system model for the SNR-300 steam generator system, including feedwater and drain valve controllers. As this model is for Version 0 of MINET, which is not slated for further development, the control actions are being programmed specifically for the SNR-300 facility. However, several controller functions planned for use in Version 1, are being used in this SNR-300 effort.

The process of documenting Version 1 of MINET continues. An input description, a simple example deck (X1), and a four part "Code Documentation" report are currently in progress.

REFERENCE

GUPPY, J. G., et al., (1983) "Balance of Plant Modeling," Safety Research Programs Sponsored by Office of Nuclear Regulatory Research Quarterly Progress Report, July 1 - Sept. 30, 1983, Brookhaven National Laboratory Report to be published.

PUBLICATIONS

VAN TUYLE, G. J., "MINET, Validation Study Using EBR-II Test Data," Brookhaven National Laboratory, BNL report to be published.

VAN TUYLE, G. J., NEPSEE, T. C., GUPPY, J. G., "MINET Code Documentation," Brookhaven National Laboratory, NUREG/CR-3668, BNL-NUREG-51742, February 1984.

VAN TUYLE, G. J., "Simulation of a Helical Coil Sodium/Water Steam Generator, Including Structural Effects," Brookhaven National Laboratory, BNL report to be published.

VAN TUYLE, G. J., "Implementation of SNR-300 Steam Generator System Controller Models Into SSC/MINET," Brookhaven National Laboratory, BNL report to be published.

4. Thermal Hydraulic Reactor Safety Experiments

4.1 Core Debris Thermal Hydraulic Phenomenology: Ex-Vessel Debris Quenching

(T. Ginsberg, J. Klein, J. Klages, and C. E. Schwarz)

This task is directed towards development and experimental evaluation of analytical models for prediction of the rate of steam generation during quenching of core debris under postulated LWR core meltdown accident conditions. This program is designed to support development of LWR containment codes.

4.1.1 Experimental Results and Analysis

Experimental results have been previously presented (Ginsberg, 1983a) which suggest that superheated debris beds, which are cooled by overlying pools of water, quench in a bi-frontal cooling process. An initial cooling front propagates down the column and removes a fraction of the stored energy in the bed. The remaining energy is removed during passage of the upward-directed front during which time the bed is finally quenched. A model has been presented to characterize the quench process (Ginsberg, 1983b).

The results summarized above, and the model based upon the results, were deduced from experiments with small particles (1-3 mm). Somewhat different behavior has been observed with the larger particles used in more recent experiments. These results are described below.

The previous work indicated that the speed of the downward-propagating front could be computed from the frontal energy balance equation

$$v_d f_d (\rho c)_{eff} (1-\varepsilon)(T_p - T_{sat}) = -q''_d \qquad (4.1)$$

where v_d is the frontal speed, f_d is the fraction of bed energy removed during passage of the downward front, $(\rho c)_{eff}$ is the effective heat capacity of the bed including the walls, ε is the bed porosity, T_p and T_{sat} are the initial particle and water saturation temperatures, and q''_d is the bed heat flux based upon the bed cross-sectional area.

The position, z_d, of the downward front is given by

$$\frac{dz_d}{dt} = -v_d \qquad (4.2)$$

where d/dt is the time derivative. With v_d assumed constant and with water assumed to contact the top of a bed of height H at time $t=t_o$, Eq. (4.2) is integrated to give

$$\frac{z_d}{H} = 1 - \frac{v_d(t-t_o)}{H} \qquad (4.3)$$

Equation (4.3) is written in dimensionless form

$$z^* = 1 - T^* \qquad (4.4)$$

where $z^* = z_d/H$ and $T^* = v_d(t-t_o)/H$. The position of the downward front, calculated using Eqs. (4.1) and (4.4), should be independent of particle diameter when plotted in the dimensionless form of Eq. (4.4).

The experimental results are shown in Figure 4.1 for the four particle sizes tested in the bed quench program. The results suggest that the quench model described above well-characterizes the data for the 0.89 and 3.18 mm particle beds. The data for the 6.35 mm particles suggest that water initially penetrates the bed more rapidly than is computed using Eq. (4.1). The downward penetration does not proceed in the linear pattern observed for the beds of smaller particles. The initially large penetration rate decreases as the front progresses into the bed until the front reaches the bottom of the bed.

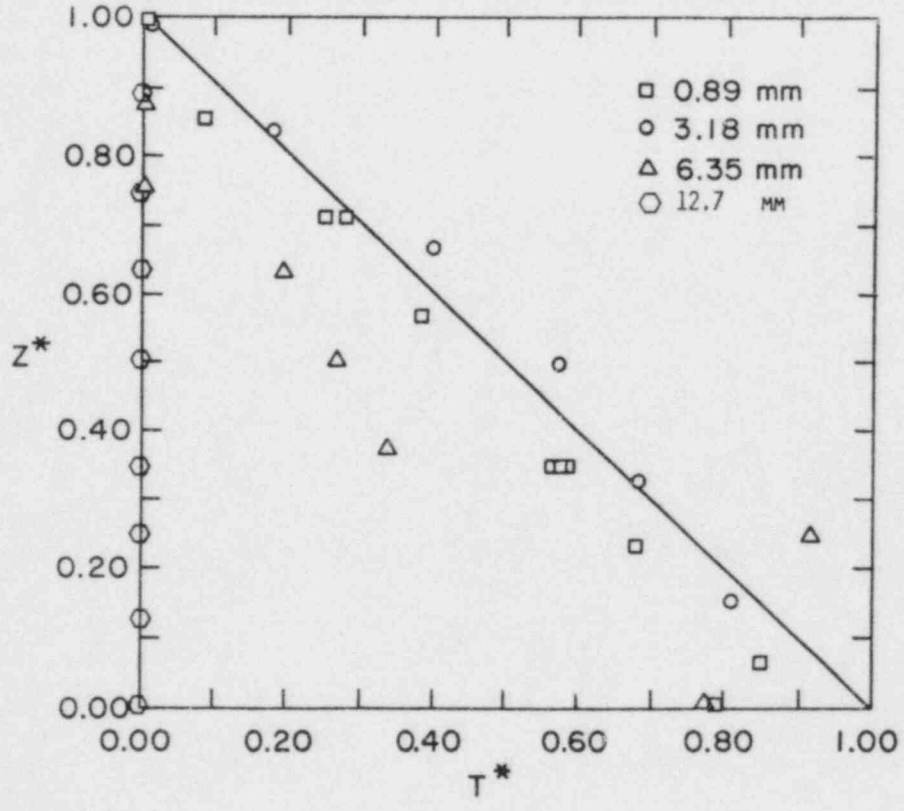

Figure 4.1 Dimensionless Downward Frontal Position as Function of Dimensionless Time.

The data for the 12.7 mm particles clearly show a markedly different behavior. The bed thermocouple traces suggest that immediately upon introduction of water to the bed each of the thermocouples was exposed to cooling. In some cases the cooling was rapid, indicating water cooling, while in other cases slower steam cooling was indicated. The initial cooling is represented in Figure 4.1 by the data points at $T^* = 0$. The initial penetration of water leads to immediate arrival of water to the base of the bed. No downward frontal cooling behavior is observed at all. The quench process proceeds as the bed refills from the bottom of the bed upwards. The upward quench pattern is not shown in Figure 4.1. More complete assessment of the large particle data is under way and analytical modeling is also proceeding.

4.2 Core Debris Thermal Hydraulic Phenomenology: In-Vessel Debris Quenching

(N. K. Tutu, T. Ginsberg, J. Klein, J. Klages and C. E. Schwarz)

The purpose of this task is to develop an understanding of the transient quenching of in-vessel debris beds (formed in the reactor core region) when the coolant is injected from below. The experimental results would, in addition, generate a data base for verifying the transient thermal-hydraulic models for the quenching process.

4.2.1 Model Development

A quasi steady 1-D model for debris bed quenching developed earlier (Tutu et al., 1983) for the case where the coolant is injected from below at a constant rate has now been extended to include steam cooling and fluid momentum equations. The model assumes the existence of a "heat transfer layer" traveling up the bed at a constant speed. Predictions include the distribution of solid temperature, vapor temperature, local steam generation rate and the void fraction within the heat transfer layer.

Figure 4.2 shows the predictions for solid temperature, vapor temperature, and the void fraction for a typical case. Here, x is the vertical distance above the liquid/quench front in a coordinate system moving with the quench front, T_s^∞ is the initial debris bed temperature, J_L^o is the liquid injection superficial velocity at the bottom of the bed, and α is the void fraction. The liquid is assumed to enter at saturation temperature T_{sat} for this calculation, and the heat transfer layer thickness L has arbitrarily been defined to be the distance between the 5% and 95% values of the dimensionless solid temperature profile $\Delta T_s/\Delta T_s^\infty$. The sharp jump in the solid temperature and void fraction profiles near the quench front ($x/L \approx 0$) is due to the high heat transfer rates in the nucleate and transition boiling regimes. As expected, the vapor temperature lags the solid temperature.

If $\dot{q}''$ is the heat lost by the debris bed per unit time per unit total bed area, the model prediction in terms of the liquid injection rate and the initial debris bed temperature is:

$$\frac{\dot{q}''}{J_L^o \Delta T_s^\infty} = \frac{\rho_L \mathcal{L}^*}{\Delta T_s^\infty + \varepsilon \rho_L \mathcal{L}^* / \{\rho_s c_s (1-\varepsilon)\}} \qquad (4.5)$$

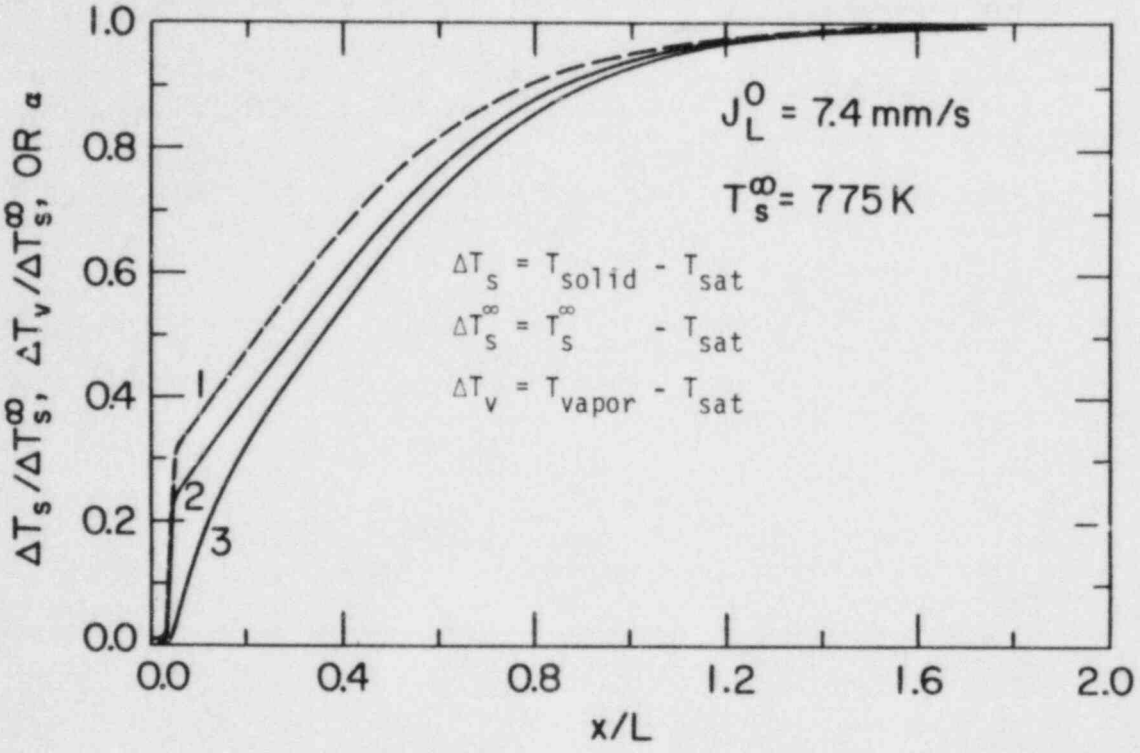

Figure 4.2 Average heat flux measurements and prediction.
□: J_L^0=1.01 mm/s; ◇: J_L^0= 1.98 mm/s;
Δ: J_L^0= 4.42 mm/s; ▽: J_L^0 =7.4 mm/s.

where $\mathcal{L}^* = \lambda + c_p^v \Delta T_s^\infty$, ρ_L is the density of the liquid phase, ρ_s is the density of the solid, c_s the specific heat of solid, c_p^v is the specific heat of vapor at constant pressure, ϵ is the bed porosity, and λ is the latent heat of vaporization. This prediction of the steady-state heat flux, together with the values of the average heat flux measured during our experiments, is shown in Figure 4.3. Considering the scatter in the data, the agreement is reasonable.

An initial topical report which includes details of the model development and experimental results performed to date is in progress.

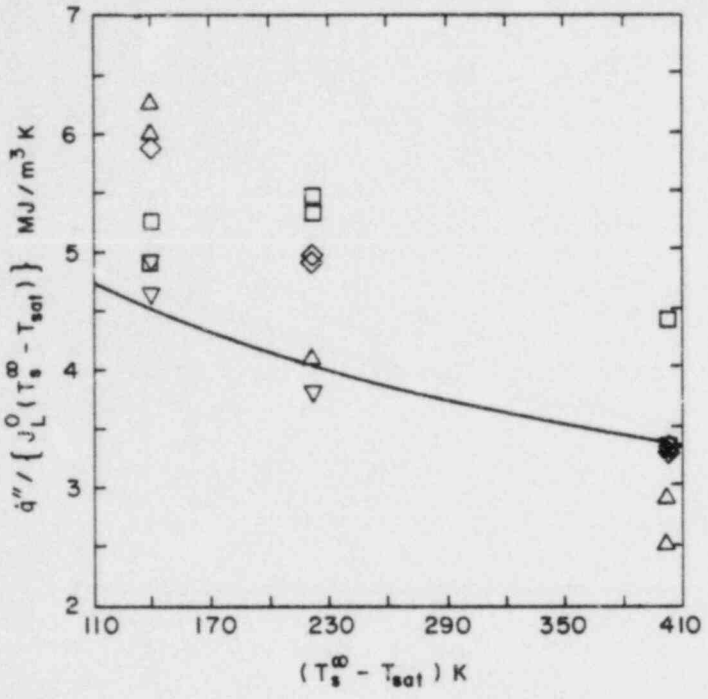

Figure 4.3 Prediction for Solid Temperature, Vapor Temperature, and Void Fraction within the Heat Transfer Layer. 1: Void Fraction, 2: Solid Temperature, 3: Vapor Temperature.

4.3 Core-Concrete Heat Transfer Studies: Coolant Layer Heat Transfer (G. A. Greene and T. F. Irvine (SUSB))

The purpose of this task is to study the mechanisms of liquid-liquid boiling heat transfer and its effect on the ex-vessel attack of molten core debris on concrete. This effort is in support of the CORCON development program at Sandia National Laboratories.

4.3.1 Previous Experimental Results

In the previous quarterly progress report, results were presented for two series of liquid-liquid film boiling experiments. One of these was the R-11/liquid metal boiling series which exhibited a stable boiling mode and compared well to the Berenson flat-plate film boiling model previously described. This series established a base line for comparison to other data. The second series of data was the H_2O/liquid metal boiling mode, characterized by splashing of the coolant out of the test section and spiking of the melt through the boiling interface into the water pool (as inferred from thermocouple data). These data were found to exceed the Berenson flat-plate film boiling model by

as much as a factor of four or more. In some cases, these unstable liquid-liquid film boiling tests were observed to transition into pool-geometry steam explosions.

Neither of these coolant layer test series, R11/liquid metal or H_2O/liquid metal, included the effect of noncondensable gas blowing through the liquid-liquid interface to simulate the release of gases from concrete during a core-concrete interaction. A third series of tests was begun this quarter to investigate the effect of a transverse, nonreactive, noncondensable gas flux through the liquid-liquid interface on the magnitude of the liquid-liquid film boiling heat flux. Freon 11 (R11) was chosen as the coolant in this series of tests in order to avoid steam explosions and to take advantage of the well-established zero gas flux base line, represented by the Berenson film boiling model and the first series of R11/liquid metal boiling data.

4.3.2 Bubbling-Enhanced Film Boiling Apparatus

In order to perform the liquid-liquid film boiling tests with transverse noncondensable gas flux, a bubbling device was constructed to insert into the stainless steel test vessel. The bubbler is a spiral coil of 0.25 inch stainless steel tubing with twenty bubbling ports, each 0.033 inch diameter. The bubbler is inserted into the molten pool and fixed to the test section side so that it rests horizontally on the pool bottom. Gas is fed into the bubbler through two inlets in a countercurrent flow to minimize the pressure gradient in the coil, ensuring a uniform bubbling configuration at each of the holes. Hydrodynamic tests in a water pool verified the uniformity of the bubbling rate. At the inlet to the gas generator, argon gas is injected at constant pressure and flow rate through a 0.50 inch pipe heater, to preheat the noncondensble, nonreactive gas to the temperature of the molten pool of metal. The power to the pipe heater is continually reduced or terminated during the experiment to maintain the gas temperature as close as possible to the constantly decreasing temperature of the liquid metal.

4.3.3 Experimental Results: R11/Liquid Metal Film Boiling with Gas Bubbling

Four tests have been performed with R11/liquid metal film boiling with transverse gas flux, tests 201-204. In these tests, the initial superficial gas flux through the boiling interface was in the approximate range 0.6 to 1.0 cm/s for the duration of the tests. These numbers are approximate and subject to revision pending final analysis of the data. The measurements of superficial gas flux were complicated by a reducing flow rate during the tests due to solidification of the melt around the bubbling ports. This has been corrected and future experiments will not suffer from this problem.

A composite of the measured boiling heat flux vs. superheat for these tests is shown in Figure 4.4. The high range data were measured with a molten lead pool, the lower range data were measured with a molten Wood's metal pool. Future tests will also include a bismuth pool, as well as nonmetallic pools. Included on this figure is the Berenson film boiling model, which was found to predict the R11/liquid metal heat flux in the absence of transverse gas flux

accurately. It is immediately clear that the heat flux measured is considerably enhanced over the nonbubbling data, on the average by as much as a factor of three to five, even at low superficial gas velocity in the range 0.6 to 1.0 cm/s. Further tests are planned to quantify this enhancement to the film boiling heat flux with gas bubbling with additional melt materials, coolant materials, and at higher gas superficial velocity.

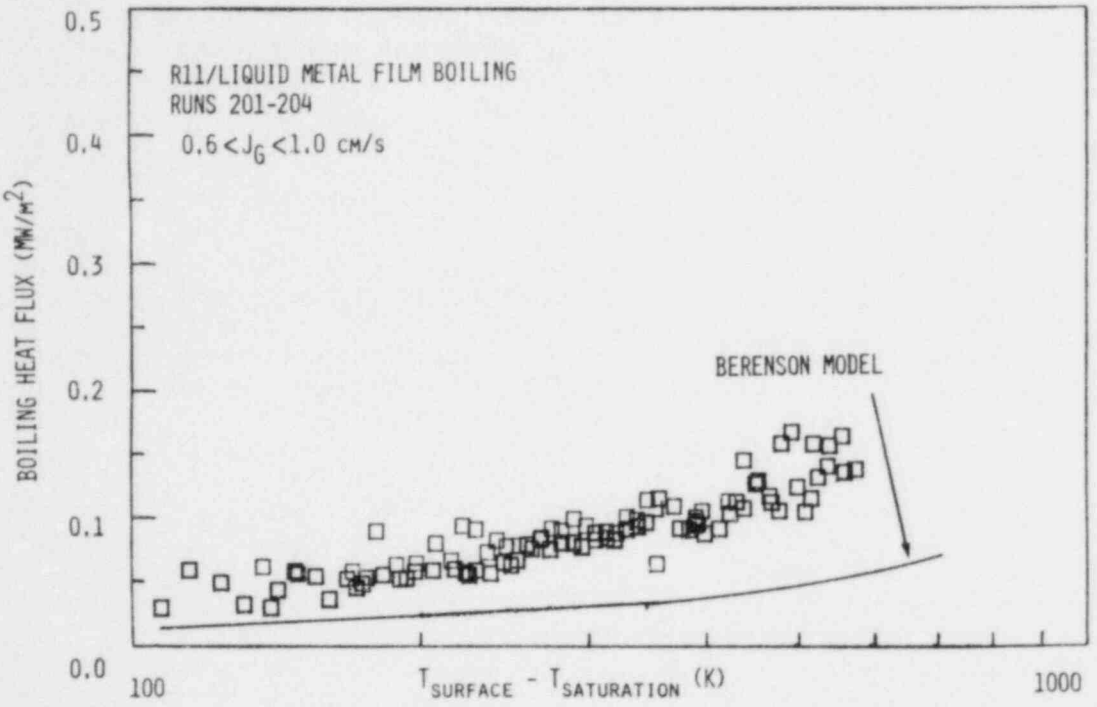

Figure 4.4 Liquid-Liquid Film Boiling of Freon-11 Over Pools of Molten Wood's Metal and Lead with Transverse Non-condensable Gas Flux.

REFERENCES

GINSBERG, T., (1983a), "Core Debris Thermal-Hydraulic Phenomenology," Ch. 4 in Safety Research Programs Sponsored by Office of Nuclear Regulatory Research, Quarterly Progress Report, January 1 - March 31, 1983; compiled by Allen J. Weiss, NUREG/CR-2331, BNL-NUREG-51454, Vol. 3, No. 1, 1983a.

GINSBERG, T., (1983b), "A Model for Superheated Debris Bed Quench for Severe Accident Containment Calculations," First Proceedings of Nuclear Thermal Hydraulics, American Nuclear Society, 1983b.

TUTU, N. K. et al., (1983), Ch. 4 in Safety Research Programs Sponsored by Office of Nuclear Regulatory Research, Quarterly Progress Report, April 1 - June 30, 1983; compiled by Allen J. Weiss, NUREG/CR-2331, BNL-NUREG-51454, Vol. 3, No. 2, 1983.

5. Development of Plant Analyzer
(W. Wulff)

5.1 Introduction

This program is being conducted to develop an engineering plant analyzer, capable of performing accurate, real-time and faster than real-time simulations of plant transients and Small-Break Loss of Coolant Accidents (SBLOCAs) in LWR power plants. The engineering plant analyzer is being developed by utilizing a modern, interactive, high-speed, special-purpose peripheral processor, which is designed for time-critical systems simulations. The engineering plant analyzer supports primarily safety analyses, but it serves also as the basis of technology development for nuclear power plant monitoring, for on-line accident diagnosis and mitigation, and for upgrading operator training programs and existing training simulators.

There were three activities related to the LWR Plant Analyzer Development Program; namely, (1) the assessment of the capabilities and limitations in existing simulators for nuclear power plants, (2) the selection and acquisition of a special-purpose, high-speed peripheral processor suitable for real-time and faster than real-time simulation of power plant transients, and (3) the development of the software for this peripheral processor.

(1) One each of operating PWR and BWR power plants and their simulators had been selected to establish the status of current real-time simulations with respect to modeling fidelity for the thermohydraulics in the Nuclear Steam Supply System (NSSS). The assessment consisted of establishing the modeling assumptions in the process descriptions for the NSSS, and of comparing NSSS-related simulator results with results from RETRAN calculations. The evaluation was performed to determine the current simulator capabilities and limitations of providing engineering predictions for operational transients and for transients caused by loss of coolant injection, by a loss of feedwater or feedwater heaters, by a loss of heat sink (steam generator failure), or by a mismatch between fission power and cooling rate.

(2) The AD10 of Applied Dynamics International (ADI) of Ann Arbor, Michigan, had been selected earlier as the special-purpose, high-speed peripheral processor on the basis of its capacity to execute faster and more efficiently the operations which are currently being performed in training simulators by general-purpose computers. Specifically, the special-purpose processor was selected for efficient, high-speed integration of ordinary differential equations and for direct, on-line interactions with the user, with instrumentation, with both digital and analog signals from other computers and with graphic devices for continuous, on-line display of a large number of computed parameters.

(3) The software development for the new peripheral processor is carried out in two phases. One phase was the implementation of an existing thermohydraulics model for a BWR system to simulate operational transients on the new processor. This phase served to compare the computing speed and accuracy of

the AD10 processor with those of the CDC-7600 mainframe computer, and thereby to demonstrate in principle the feasibility of computing realistic transients at faster than real-time computing speeds. The second phase is the modeling of the primary loop outside of the vessel and its controls, neutron kinetics and thermal conduction for the complete BWR simulation and the formulation and implementation of a thermohydraulic model for the faster than real-time analysis of operational and SBLOCA transients in PWR power plants. This is supplemented by implementation of multicolor graphics displays.

Below is a brief summary of previously obtained results and a detailed summary of achievements during the current reporting period.

5.2 Assessment of Existing Simulators (W. Wulff and H. S. Cheng)

The assessment of these current simulator capabilities consisted of evaluating qualitatively the thermohydraulic modeling assumptions in the simulator and of comparing quantitatively the predictions from the simulator with results from the detailed systems code RETRAN.

The results of the assessment have been published earlier in three reports (Wulff, 1980; Wulff, 1981a; Cheng and Wulff, 1981). It had been found that the reviewed training simulators were limited to the simulation of steady-state conditions and quasi-steady transients within the parameter range of normal operations. Most PWR simulators delivered before 1980 cannot simulate two-phase flow conditions in the primary reactor coolant loops, nor the motion of the two-phase mixture level beyond the narrow controls range in the steam generator secondary side. Most BWR simulators delivered before 1980 cannot simulate two-phase flow conditions in the recirculation loops or in the downcomer and lower plenum, nor can they simulate coolant level motions in the steam dome, the lower regions of the downcomer (below the separators), or in the riser and core regions. These limitations arise from the lack of thermohydraulic models for phase separation and mixture level tracking (Wulff, 1980; 1981a).

The comparison between PWR simulator and corresponding RETRAN results, carried out for a reactor scram from full power, showed significant discrepancies for primary and secondary system pressures and for mean coolant temperatures of the primary side. The discrepancies were found even after the elimination of differences in fission power, feedwater flow and rate of vapor discharge from the steam dome. Good agreement was obtained between simulator and RETRAN calculations for only the early part (narrow control range) of the water level motion in the steam generator. The differences between simulator and RETRAN calculations have been explained in terms of modeling differences (Cheng and Wulff, 1981).

5.3 Acquisition of Special-Purpose Peripheral Processor (A. N. Mallen and R. J. Cerbone)

The AD10 had been selected earlier as the special-purpose peripheral processor for high-speed, interactive systems simulation. A brief description of

the processor has been published in a previous Quarterly Progress Report (Wulff, 1981b). A PDP-11/34 DEC computer serves as the host computer.

Two AD10 units, coupled directly to each other by a bus-to-bus interface and equipped with a total of one megaword of memory, have been installed with the PDP-11/34 host computer, two 67 megabyte disc drives, a tape drive and a line printer. On-line access is facilitated by a model 4012 Tektronix oscilloscope terminal and a 28-channel signal generator. The system is accessed remotely via four ADDS CRT terminals and two DEC Writer terminals, one also equipped with a line printer. An IBM Personal Computer is also used to access the PDP-11/34 host computer but primarily to generate labelled, multicolored graphs from AD10 results. An advanced multicolor graphics terminal is needed, however, for extensive on-line display of simulated parameters generated by the AD10 at real-time or faster computing speeds.

5.4 Software Implementation on AD10 Processor

A four-equation model for nonhomogeneous, nonequilibrium two-phase flow had been formulated and supplemented by constitutive relations from an existing BWR reference code, then scaled and adapted to the AD10 processor to simulate the Peach Bottom-2 BWR power plant (Wulff, 1982a). The resulting High-Speed Interactive Plant Analyzer code (HIPA-PB2) has been programmed in the high-level language MPS-10 (Modular Programming System) of the AD10. After implementing the thermohydraulics of HIPA-PB2 on the AD10, we compared the computed results and the computing speed of the AD10 with the results and the computing speed of the CDC-7600 mainframe computer, to demonstrate the feasibility of achieving engineering accuracy at high simulation speeds with the low-cost AD10 minicomputer (Wulff, 1982b).

It has been demonstrated (Wulff, 1982b) that (i) the high-level, state equation-oriented systems simulation language MPS-10 compressed 9,950 active FORTRAN statements into 1,555 calling statements to MPS-10 modules, (ii) the hydraulics simulation occupies one-fourth of available program memory, (iii) the difference between AD10 and CDC-7600 results is only approximately $\pm$ 5% of total parameter variations during the simulation of a severe licensing base transient, (iv) the AD10 is 110 times faster than the CDC-7600 for the same transient, and (v) the AD10 simulates the BWR hydraulics transients ten times faster than they progress in real-time. It has been demonstrated now that even after the inclusion of models for neutron kinetics, conduction, balance of plant dynamics and controls, the AD10 still achieves ten times real-time simulation speed for all transients reported earlier (Wulff, 1983c).

The HIPA-PB2 hydraulics program used earlier for the feasibility demonstration is now being expanded to simulate neutron kinetics (point kinetics), thermal conduction in fuel elements and the thermohydraulics of the components shown in Figure 5.1.

The stand-alone program modules for neutron kinetics with feedback simulation and scram control, for thermal conduction in fuel elements, for compressible flows in the steam line and for the control logic for operating the

safety and relief valves tested earlier (Wulff, 1982c; 1983a) have been implemented in HIPA-PB2. Models have been formulated and tested separately for the control systems and the plant components forming the loop through turbines, condensers and the feedwater trains during the previous reporting period.

Specific accomplishments of the current reporting period are described below.

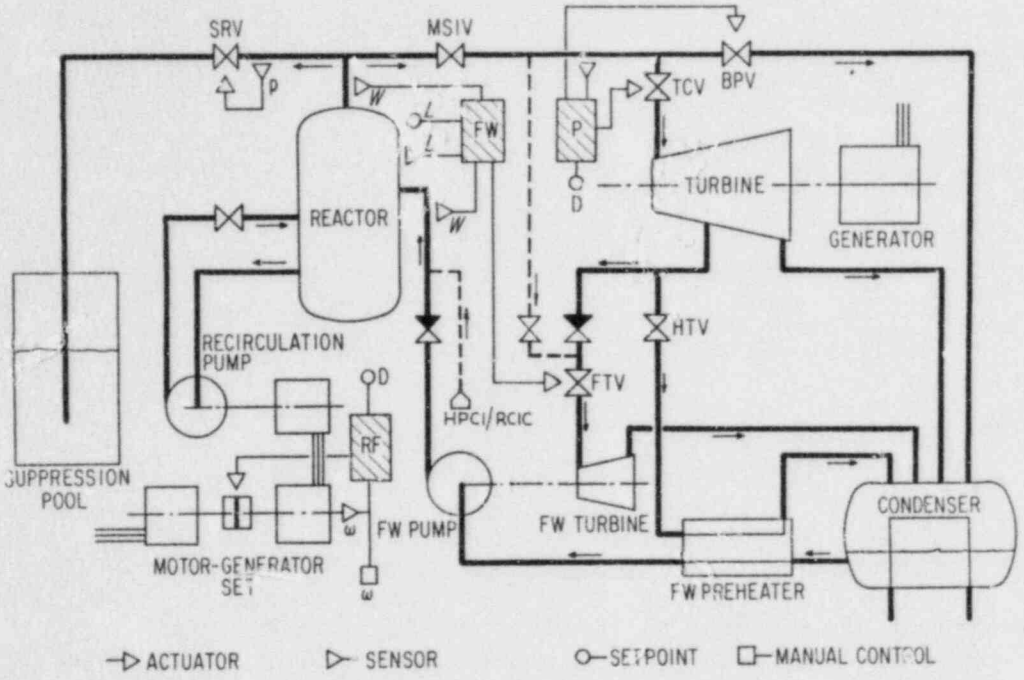

Figure 5.1 Flow Schematic and Control Blocks for BWR Simulation; FW - Feedwater Controller, P - Pressure Controller, RF - Recirculation Flow Controller.

5.4.1 Program Assembly and Assessment (H.S. Cheng, A.N. Mallen and W. Wulff)

During the current reporting period, the plant analyzer began to execute HIPA-PB2 for the completed plant model, as shown in Figure 5.1. Most of the work performed during the current reporting period is, therefore, a combination of preliminary developmental code assessment and of program modifications prompted by the assessment.

The control panel used for the on-line interactive change of input parameters is energized by a standard adjustable dc power supply, which furnishes +10V and -10V to each of the 32 analog input channels. It has been observed that the power supply had a peak noise level of 20 mV. The site preparation manual requires a noise level below 1.2 mV for full accuracy of the 12-bit

analog to digital converter. The 20 mV-random noise produced physically impossible parameters (negative values for cross-sections, Second Law violations, etc.).

A better power supply was installed with a peak-to-peak noise level of approximately 5 mV. To remove this remaining noise, a software correction was made for all input channels, consisting of a division and a subsequent multiplication by 64 of the 16-bit representation for each analog input variable. This double shift effected the replacement of the last two noisy bits of the 12-bit input value by zeros. It produced exact values for -1, 0, and +1 as needed for logic operations, but it diminished the accuracy from $\pm$0.00049 to $\pm$0.00195 in the fractional representation ($\pm$1) of the analog input signals. The reduced accuracy is still as good as the dial readout from the ten-turn resistors used for adjusting the analog signals. Also, the accuracy of $\pm$0.2% is better than instrumentation accuracy and therefore adequate.

By comparing plant analyzer results with GE results (NEDO-24222, 1981) it was observed that on-off and spring-loaded valve characteristics of relief and safety valves, respectively, had been inadvertently reversed. For an ATWS induced by MSIV, the plant analyzer showed smooth, nearly constant discharge through the relief valves, while GE results showed on-off periodic flows. After reversal of the valve characteristics in the plant analyzer, it showed also on-off discharge through the relief valves.

The logic for two additional safety trips has been added, one to open the bypass when the turbine stop valve closes to 1/10 of full opening, following a turbine trip; the other to trip the feedwater pump when the recirculation flow controller fails in maximum demand position.

Reactivity feedback has been added for Alternate Rod Insertion (ARI) and for boron in the core. A boron transport model has been formulated but not yet implemented.

Work has been initiated to produce a steady state automatically from the output of the AD10. This capability is part of the scheme for applying HIPA to other BWR power plants. It is also needed for developmental assessment of HIPA-PB2. Instead of seeking the steady state through iterative methods in the host computer, which would require a FORTRAN code for steady-state calculations, we have chosen to simulate the steady state for fixed operating parameters in the AD10 and to save and store the output for a number of desirable conditions.

A neutral computational instability has been observed for the first time in the mass flow rate integrators of the steam line, under conditions of no flow after MSIV closure. It has been determined that as the flow oscillations decrease below ~0.1% of full scale, the friction and form losses become zero. Frictional losses decrease with the second power of the velocity. Once they are less than one least significant bit (0.00003), the dissipative friction terms are recognized in the AD10 as zeros. The loss of dissipation reduces the magnitudes of the negative real parts of the integrator eigenvalues. This can cause instability. The loss of dissipation is obviously due to the limited dynamic range of the 16-bit word in the AD10.

To avoid the instability, we have developed a method to increase the dynamic range by three decades through dynamic rescaling. At a carefully chosen value $\bar{w}_b$ of the velocity $\bar{w}$, the argument in the function generator for friction $\bar{f}$, we divide the scale factor C by 1,000 and replace the product $C \cdot \bar{f}$ by $(C/1000) \cdot (1000\bar{f})$. The break point $\bar{w}_b$ is chosen such that $1000 \cdot \bar{f}(\bar{w}_b)$ is slightly less than full scale. The new scaling coefficient (C/1000) is represented at full accuracy by the 48-bit floating point format in the NIP processor. For all $\bar{w} > \bar{w}_b$ we use the previous formulation $C \cdot \bar{f}$. This technique will be implemented during the next reporting period. We plan also to move the integrator for the overall system pressure of the pressure vessel into the fast integrating (i.e., multi-stepping) loop of the steam line dynamics simulation, thereby reducing the time step for system pressure integration.

Work will be continued on the developmental assessment.

5.4.2 Model Development (W. Wulff)

A simple boron transport model has been developed by integrating in closed form the differential equations of boron conservation. Instead of integrating the boron conservation equation for the mass fraction c_B in the liquid phase, we integrate the equation to obtain the volumetric density $(1-\alpha) \cdot c_B \equiv C_B$ as needed directly for the boron reactivity calculation. Here, α is the vapor void fraction.

By neglecting the (unimportant) compressibility of liquid, one arrives at

$$\frac{\partial C_B}{\partial \tau} + \nabla \cdot (\vec{v}_\ell C_B) = 0 \qquad (5.1)$$

for the equation of boron concentration,* where τ and v_ℓ designate time and the liquid velocity as obtained from the hydraulics calculations. Notice that Eq. 5.1 not only yields the boron concentration in the most convenient form for fission calculations, but it is also independent of void fraction and of vapor generation rate which are needed to compute the boron concentration c_B in the liquid. Equation 5.1 is used to model first the three-dimensional mixing process in the injection volume (lower plenum for Peach Bottom plant), based on a lumped-parameter model, and then to model the one-dimensional boron transport, using the one-dimensional form of Eq. 5.1.

For perfect mixing in the time-invariant volume V of the lower plenum, Eq. 5.1 yields the volume-average and exit concentration $\langle C_B \rangle$ of V:

$$\left.\begin{aligned} \frac{d\langle C_B \rangle}{d\tau} &= \frac{1}{V}\left[(A\, v_\ell C_B)_{inj} + (A\, v_\ell C_B)_{dc} - \langle C_B \rangle\, (A\, v_\ell)_{cr}\right] \\ \langle C_B \rangle &= 0 \quad \text{for } \tau \leq 0 \,. \end{aligned}\right\} \qquad (5.2)$$

*Neglecting also diffusion.

Here, $(A\ v_\ell)$ represents the volumetric flow rate of the liquid with velocity v_ℓ, passing through cross-section A. The subscripts inj, dc and cr designate locations at boron injection ports, downcomer exit and core entrance. Since $(A\ v_\ell)_{inj}/(A\ v_\ell)_{cr} \approx 10^{-3}$ one can approximate $(A\ v_\ell)_{dc}$ by $(A\ v_\ell)_{cr}$ and introduce

the characteristic time of mixing $$\tau_m \triangleq \frac{V}{(A\ v_\ell)_{cr}}\ , \tag{5.3.}$$

and the characteristic time for injection $$\tau_{inj} \triangleq \frac{V}{(A\ v_\ell)_{inj}}\ . \tag{5.4}$$

where the symbol $\triangleq$ means "defined as." Here τ_m depends on time τ if the core flow varies, but τ_{inj} is fixed for time-invariant injection rates. With Eqs. 5.3 and 5.4, Eq. 5.2 simplifies to

$$\left.\begin{aligned} \frac{d\langle C_B\rangle}{d\tau} + \frac{\langle C_B\rangle}{\tau_m} &= -\frac{(C_B)_{inj}}{\tau_{inj}} - \frac{(C_B)_{dc}}{\tau_m} \\ \langle C_B\rangle &= 0 \quad \text{for } \tau \leq 0 \end{aligned}\right\} \tag{5.5}$$

which yields the volumetric boron concentration at the core entrance

$$F(\tau) \triangleq \langle C_B\rangle = e^{-\int_0^\tau \frac{d\tilde{\tau}}{\tau_m}} \int_0^\tau \left[\frac{(C_B)_{inj}}{\tau_{inj}} + \frac{(C_B)_{dc}}{\tau_m}\right] e^{\int_0^{\tilde{\tau}} \frac{d\xi}{\tau_m(\xi)}}\, d\tilde{\tau}\ . \tag{5.6}$$

If the core flow is nearly steady after boron injection and has only small oscillations induced from relief valve actions, then τ_m is constant ($\approx$2.6 seconds at full flow) and Eq. 5.6 yields

$$F(\tau) \triangleq \langle C_B\rangle \approx \frac{\bar{\tau}_m}{\tau_{inj}} (C_B)_{inj}\left(1 - e^{-\frac{\tau}{\bar{\tau}_m}}\right) + \int_0^{\tau/\bar{\tau}_m} (C_B)_{dc}\, e^{-\frac{\tau-\tilde{\tau}}{\bar{\tau}_m}}\, d\left(\frac{\tilde{\tau}}{\bar{\tau}_m}\right)\ . \tag{5.7}$$

The second term is zero until the boron has circulated once through the core and downcomer which takes the time τ_{cy} of approximately 20 seconds. Thus

$$F(\tau) \triangleq \langle C_B \rangle = \frac{\bar{\tau}_m}{\tau_{inj}} (C_B)_{inj} \left(1 - e^{-\frac{\tau}{\bar{\tau}_m}} \right)$$

$$\text{for } 0 \leq \tau < \tau_{cy} . \qquad (5.8)$$

Equation 5.8 is valid in spite of the assumptions that τ_m and v_ℓ can be replaced by cycle mean values because τ_m is very small when compared with the time required for reactor shutdown by boron injection. For times $\tau < \tau_{cy}$, $\langle C_B \rangle$ is obtained by periodic superposition.

For the boron propagation through the reactor vessel we used Eq. 5.1 in its one-dimensional form and obtained

$$\left.\begin{aligned} \frac{\partial C_B}{\partial \tau} + v_\ell \frac{\partial C_B}{\partial z} &= - \frac{\partial v_\ell}{\partial z} C_B \\ C_B(0,z) &= f(z) \\ C_B(\tau,0) &= F(\tau) . \end{aligned}\right\} \qquad (5.9)$$

Equation 5.9 can be integrated, since $v_\ell(\tau,z)$ is known from hydraulics calculations. The general solution is found by obtaining time τ and position z of any characteristic curve with parameter s from

$$d\tau = \frac{dz}{v_\ell} = ds$$

and then by integrating

$$- \frac{1}{\frac{\partial v_\ell}{\partial z}} \cdot \frac{dC_B}{C_B} = ds$$

along the characteristic curve, utilizing the initial and boundary conditions of Eq. 5.9. Instead of this integration, we approximate v_ℓ as before, and the velocity gradient by

$$\left.\begin{aligned} v_\ell &= \bar{v}_\ell \\ \frac{\partial v_\ell}{\partial z} &= \frac{1}{\bar{\tau}_z} \end{aligned}\right\} \qquad (5.10)$$

and keep $\bar{v}_\ell$ and $\bar{\tau}_z$ fixed for $0 \leq \tau \leq \tau_{cy}$. Substituting Eq. 5.10 into 5.9 we obtain

$$\left.\begin{aligned} &\frac{\partial C_B}{\partial \tau} + \bar{v}_\ell \frac{\partial C_B}{\partial \tau} + \frac{1}{\bar{\tau}_z} C_B = 0 \\ &C_B(0,z) = f(z) \\ &C_B(\tau,0) = F(\tau). \end{aligned}\right\} \tag{5.11}$$

Taking the Laplace transform of Eq. 5.11 and integrating with respect to z, one finds the transform C_B^* of C_B:

$$C_B^* = e^{-\frac{z}{\bar{v}_\ell \tau_z}} \left(e^{-\frac{z}{\bar{v}_\ell} s} F^*(s) \right) + \frac{1}{\bar{v}_\ell} \int_0^z f(x)\, e^{-\frac{s+\tau_z^{-1}}{\bar{v}_\ell}(z-x)}\, dx . \tag{5.12}$$

Here $F^*(s)$ is the transform of Eq. 5.8, $f(x)$ is the initial boron concentration, i.e.,

$$f(x) \equiv 0 \quad \text{for} \quad 0 \leq \tau \leq \tau_{cy} , \tag{5.13}$$

and afterwards it is obtained from periodic superposition. The inverse transform of C_B^* in Eq. 5.12, with Eq. 5.8 and 5.13

$$\begin{aligned} C_B &= F\left(\tau - \frac{z}{\bar{v}_\ell}\right) \cdot u\left(\tau - \frac{z}{\bar{v}_\ell}\right) \cdot e^{-\frac{z}{\bar{v}_\ell \tau_z}} \\ &= \frac{\tau_m}{\tau_{inj}} \cdot (C_B)_{inj} \cdot \left[1 - e^{-\frac{\tau - z/\bar{v}_\ell}{\tau_m}}\right] \cdot u\left(\tau - \frac{z}{\bar{v}_\ell}\right) \cdot e^{-\frac{z}{\bar{v}_\ell \cdot \tau_z}} \end{aligned} \tag{5.14}$$

where

$$\left.\begin{aligned} u(x) &= 0 \quad \text{for} \quad x < 0 \\ &= 1 \quad \text{for} \quad x \geq 0 \end{aligned}\right\} \tag{5.15}$$
$$0 \leq \tau \leq \tau_{cy},\ 0 \leq z \leq L_c .$$

For times $\tau > \tau_{cy}$ the solution for C_B is obtained by periodic superposition from Eq. 5.14. Notice $\bar{v}_\ell$ in Eq. 5.14 is the mean liquid velocity in the core during the time $0 \leq \tau \leq \tau_{cy}$.

For point kinetics, C_B of Eq. 5.14 must be averaged over the core from z=0 to z=L_c:

$$\langle C_B \rangle_{core} = \frac{1}{L_c} \int_0^{L_c} C_B \, dz$$

$$= \frac{1}{L_c} \int_0^{\mathrm{Min}\{L_c, \bar{v}_\ell \cdot \tau\}} \left[1 - e^{-\frac{\tau \bar{v}_\ell - z}{\bar{v}_\ell \tau_m}} \right] e^{-\frac{z}{\bar{v}_\ell \tau_z}} \, dz \cdot \frac{\bar{\tau}_m}{\tau_{inj}} \cdot (C_B)_{inj} \tag{5.16}$$

For $\tau < L_c/\bar{v}_\ell$ the result is:

$$\frac{\langle C_B \rangle_{core}}{\frac{\tau_m}{\tau_{inj}} (C_B)_{inj}} = \frac{1}{\kappa} \left\{ \frac{1}{\xi} (1 - e^{-\xi\hat{\tau}}) - \frac{1}{1-\xi} (e^{-\xi\hat{\tau}} - e^{-\hat{\tau}}) \right\} . \tag{5.17}$$

For $L_c/\bar{v}_\ell \leq \tau < \tau_{cy}$, the result is:

$$\frac{\langle C_B \rangle_{core}}{\frac{\tau_m}{\tau_{inj}} (C_B)_{inj}} = \frac{1}{\kappa} \left\{ \frac{1}{\xi} (1 - e^{-\xi\kappa}) + \frac{e^{-\hat{\tau}}}{1-\xi} (1 - e^{\kappa(1-\xi)}) \right\} . \tag{5.18}$$

The right-hand sides depend only on three ratios, namely $\kappa \triangleq L_c/(\bar{v}_\ell \tau_m)$, $\xi \triangleq \tau_m/\tau_z$ and the time ratio $\hat{\tau} \triangleq \tau/\tau_m$, which greatly facilitates the implementation of this model in HIPA-PB2.

5.4.3 Graphics Display (S. V. Lekach)

As reported previously, an IBM Personal Computer had been programmed to accept simultaneously and on-line eight selected AD10 output parameters and time to display the parameters in labelled diagrams as functions of time.

The library of blank curves with a selected set of time scales between five and thousand seconds and with suitable parameter scales as listed in Table 5.1 has been completed. The number of parameters that can be stored simultaneously in the IBM Personal Computer memory has now been increased from eight to fifteen, the present limit of available output converters.

The graphics software package is being translated from IBM BASIC to the universally utilized C-Language. Thus, the package becomes transportable and it accommodates users who access the AD10 with other minicomputers or graphics terminals.

Table 5.1

Currently Available Graphics Blank for AD10 Output Display

Parameter	Dimension	Range
Pressure	N/m	40×10^5 - 100×10^5
Mixture Mass Flow at Core Entrance	kg/s	0 - 16,000
Vapor Mass Flow at Core Exit	kg/s	0 - 4,000
Mixture Mass Flow at Core Exit	kg/s	0 - 16,000
Liquid Mass Flow at Riser Exit	kg/s	0 - 16,000
Mass Flow at Steam Line Entrance	kg/s	-2,000 - 4,000
Feedwater Flow at Pump	kg/s	0 - 16,000
Bypass Flow Rate	kg/s	0 - 500
Fuel Centerline Temperature	C	200 - 1,500
Cladding Superheat Temperature	C	-15 - 15
Core Mean Void Fraction	-	0 - 1
Fission Power	GW	0 - 100
Total Reactivity	$	-45 - 45
Recirculation Pump Speed	rpm	0 - 1,800
Feedwater Turbine Speed	rpm	0 - 6,000

5.5 Plant Analyzer Demonstrations (D. Humphrey, Photography and Plant Analyzer Group)

A 16-mm silent color movie of approximately five minutes-duration has been produced to show how the plant analyzer is operated through keyboard commands and through manipulations on the control panel. The movie also shows the instant response to the user commands, the AD10's high simulation speed and the instant replay of the results from the IBM Personal Computer.

The AD10 output has been photographed directly from the screens of the Tektronix storage oscilloscope (on-line display) and of the IBM monitor. The movie contains three transients, a feedwater heater failure, a turbine generator load rejection and a turbine trip without bypass.

Nine presentations and demonstrations of the plant analyzer have been made for 22 visitors from China (Peoples' Repuplic of China), France, Germany, Italy, Japan, Sweden, Taiwan and the United Kingdom.

5.6 Future Work

Work will be continued on the developmental assessment of the plant analyzer. Work has been started and will continue on the interim report, documenting the plant analyzer.

REFERENCES

CHENG, H. S. and WULFF, W., (1981), "A PWR Training Simulator Comparison with RETRAN for a Reactor Trip from Full Power," Informal Report, BNL-NUREG-30602, Brookhaven National Laboratory, September 1981.

GE, NEDO-24222 (1981), Assessment of BWR Mitigation of ATWS, Vol. II, NUREG-0460, Alternate No. 3.

WULFF, W., (1980), "PWR Training Simulator, An Evaluation of the Thermohydraulic Models for its Main Steam Supply System," Informal Report, BNL-NUREG-28955, September 1980.

WULFF, W., (1981a), "BWR Training Simulator, An Evaluation of the Thermohydraulic Models for its Main Steam Supply System," Informal Report, BNL-NUREG-29815, Brookhaven National Laboratory, July 1981.

WULFF, W., (1981b), "LWR Plant Analyzer Development Program," Ch. 6 in Safety Research Programs Sponsored by the Office of Nuclear Regulatory Research, Quarterly Progress Report, April 1-June 30, 1981; A. J. Romano, Editor, NUREG/CR-2231, BNL-NUREG-51454, Vol. 1, No. 1-2, 1980.

WULFF, W., (1982a), "LWR Plant Analyzer Development Program," Ch. 5 in Safety Research Programs Sponsored by the Office of Nuclear Regulatory Research, Quarterly Progress Report, January 1-March 31, 1982; A. J. Romano, Editor, NUREG/CR-2331, BNL-NUREG-51454, Vol. 2, No. 1, 1982.

WULFF, W., (1982b), "LWR Plant Analyzer Development Program," Ch. 5 in Safety Research Programs Sponsored by the Office of Nuclear Regulatory Research, Quarterly Progress Report, July 1-September 30, 1982; compiled by Allen J. Weiss, NUREG/CR-2331, BNL-NUREG-51454, Vol. 2, No. 3, 1982.

WULFF, W. (1982c), "LWR Plant Analyzer Development Program," Ch. 5 in Safety Research Programs Sponsored by the Office of Nuclear Regulatory Research, Quarterly Progress Report, October 1-December 31, 1982; compiled by Allen J. Weiss, NUREG/CR-2331, BNL-NUREG-51454, Vol. 2, No. 4, 1982.

WULFF, W., (1983a), "LWR Plant Analyzer Development Program," Ch. 5 in Safety Research Programs Sponsored by the Office of Nuclear Regulatory Research, Quarterly Progress Report, January 1-March 31, 1983; compiled by Allen J. Weiss, NUREG/CR-2331, BNL-NUREG-51454, Vol. 3, No. 1, 1983.

WULFF, W., (1983b),"LWR Plant Analyzer Development Program," Ch. 5 in Safety Research Programs Sponsored by the Office of Nuclear Regulatory Research, Quarterly Progress Report, July-September 30, 1983; compiled by Allen J. Weiss, NUREG/CR-2331, BNL-NUREG-51414, Vol. 3, No. 3, 1983.

WULFF, W. (1983c), "NRC Plant Analyzer Development," Proc. Eleventh Water Reactor Safety Research Information Meeting, held at National Bureau of Standards, Gaithersburg, MD, Oct. 24-28, 1983, U.S. Nuclear Regulatory Commission. To be published.

6. Code Assessment and Application (Transient and LOCA Analyses)

(P. Saha, U. S. Rohatgi, C. J. Hsu, L. Neymotin,
H. R. Connell, and C. Yuelys-Miksis)

This project includes the independent assessment of the latest released versions of LWR safety codes such as TRAC, RELAP5, and RAMONA-3B, and the application of these codes to the simulation of plant accidents and/or transients. Two major code application tasks namely, the RESAR-3S large break LOCA study and the BWR/4 MSIV closure ATWS analysis, are in the final stages of completion. Also, the code assessment activity will resume after the implementation of TRAC-BD1/MOD1 code on the BNL computer.

The details of the progress achieved during the reporting period of October to December 1983 are described below.

6.1 Code Assessment

No code assessment task was undertaken during this reporting period. However, the latest version of TRAC-BWR code, i.e., TRAC-BD1/MOD1, has been received at BNL in December 1983, and will soon be implemented on the BNL computer.

6.2 Code Application

6.2.1 LOCA Analysis of Westinghouse RESAR-3S Plants (U. S. Rohatgi and C. Yuelys-Miksis)

The BNL best-estimate calculation for the 200% cold leg break in a Westinghouse 4-loop RESAR-3S plant has been completed using the TRAC-PD2/MOD1 code with the BNL deck (Rohatgi, 1983). This calculation was run up to 64.6 seconds of transient and required thirty-nine (39) CPU hours on the BNL CDC-7600 computer. As mentioned in the previous quarterly report (Rohatgi, 1983), the peak clad temperature of 800.5°K (981°F) occurred in the blowdown phase. This is slightly lower than the LANL prediction of the peak clad temperature of 811°K (1000°F) with TRAC-PF1. The peak clad temperature occurred at around 2.5 seconds and the subsequent maximum clad temperatures for the hot pins were always lower than this first peak. The final rod cooldown began when the core entered the reflood phase at 29.9 seconds. During the reflood phase the maximum clad temperature was less than 550°K. At approximately 55 seconds, the calculation stopped due to an "overflow" condition in the pressurizer. It was found that the code had a division by the pressurizer liquid inventory which created this overflow condition when the pressurizer was completely dry. This problem was resolved and the calculation was continued up to 64.6 seconds. At this time, the core region was essentially quenched as the void fraction in the inner ring reduced to about 0.2 and all the fuel clad temperatures cooled down to less than 412°K.

The second calculation used the evaluation type initial and boundary conditions as described in the previous quarterly report (Rohatgi 1983). This calculation has been run up to 200 seconds of problem time and has required sixty-seven (67) CPU hours on the BNL CDC-7600 computer. The peak clad temperature of 1072°K (1470°F) occurred during the reflood phase of the transient at 65 seconds. The clad temperatures oscillated during the transient but did not exceed 1072°K.

This calculation also experienced several difficulties during the 200 second transient. It first stopped at 28.57 seconds due to large oscillations in the cold legs when the cold water mixed with steam. This problem was resolved by combining three cold leg cells near the vessel into one large cell. This damped the oscillations and the calculation successfully proceeded to 47.13 seconds, at which time the pressurizer became completely dry creating an "overflow" condition. The problem was resolved through the same update as was done for the previous best-estimate calculation. At 86.41 seconds, an error in the zircaloy thermal expansion table was corrected based on information supplied by the LANL staff. The error did not affect our previous calculation since the clad temperatures were below 1073°K.

Throughout the reflood phase, the above calculation showed oscillations in the clad temperature, break flow and vessel liquid inventory. The second cell of the active core periodically emptied. There was no sustained refilling of the core. The best-estimate calculation also exhibited oscillations. However, in that calculation the ECCS flow rates were about three times larger than that in the second calculation and hence, there was early refilling and quenching of the core. In the second calculation, the core was being cooled by the steam after the peak clad temperature had occurred. From preliminary investigations it seems that more energy is being lost through the break than being introduced through the decay heat and ECCS flow. This ensures that the core will continue to cool.

At 200 seconds, the bottom two levels of the core region were quenched and the void fraction at the second level decreased to approximately 0.2. The void fraction in the third level which is the middle of the core and where the peak clad temperature occurred, also started to decrease. However, quenching did not yet start at this level. Because of high computing cost, the calculation will be terminated at approximately 250 seconds and it is most likely that the clad temperature will not exceed the peak value of 1072°K (1470°F) which occurred at 65 seconds.

Both the best-estimate and the evaluation type calculations are being analyzed in detail, and the results will be documented in a separate topical report. A comparison of these calculations with the Westinghouse licensing or Appendix K calculation as shown in Figure 6.1, indicates an overall safety margin of approximately 1200°F, of which approximately 700°F is due to the conservative physical models and approximately 500°F is due to the conservative initial and boundary conditions.

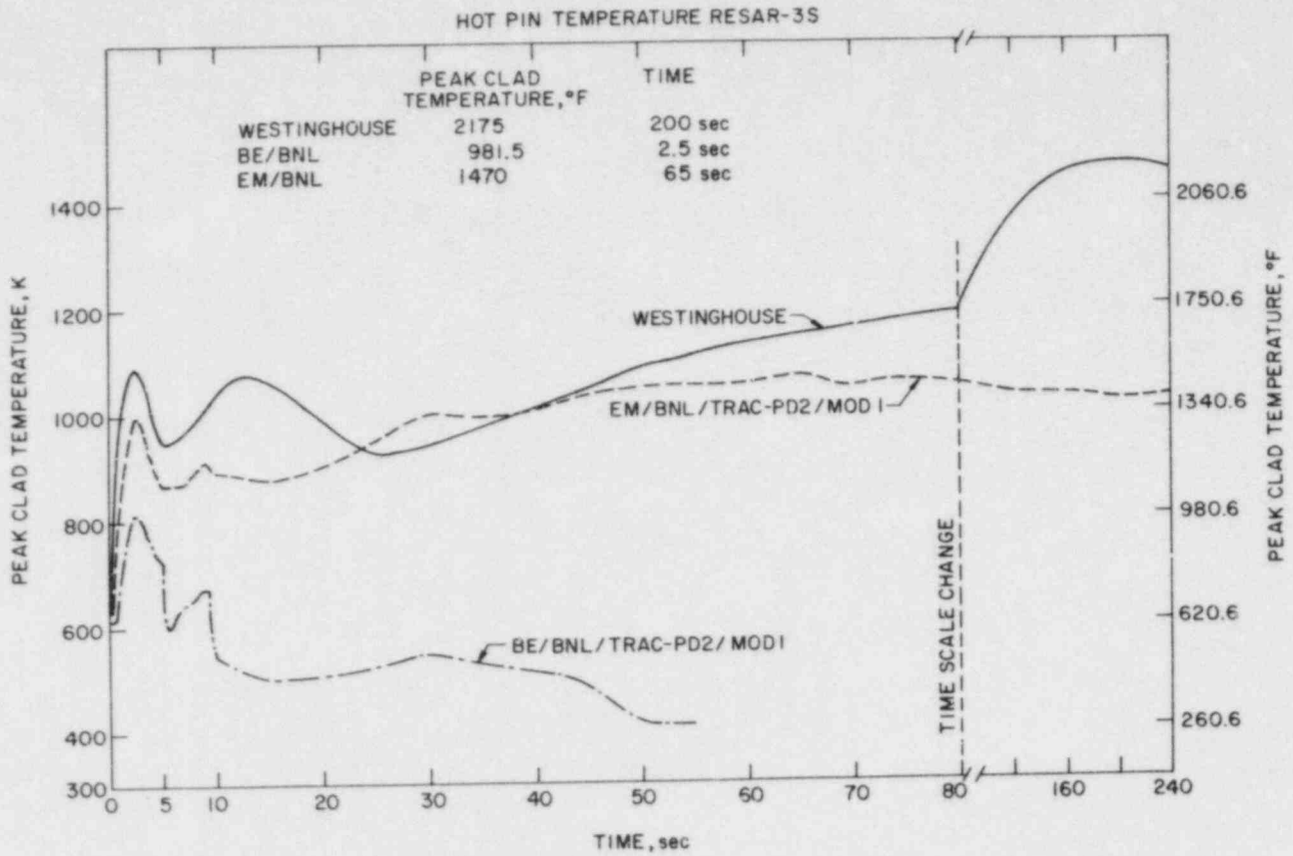

Figure 6.1 Comparison Between the BNL TRAC-PD2/MOD1 Calculations and the Westinghouse Licensing Calculation for the 200% Cold Leg Break in a Westinghouse RESAR-3S Plant. (BNL Neg. No. 2-692-84)

6.2.2 BWR/4 ATWS Calculations Using TRAC-BD1 and RAMONA-3B Codes (C. J. Hsu, L. Neymotin, and H. R. Connell)

During this reporting quarter, the TRAC-BD1 calculation for a typical BWR/4 MSIV closure ATWS has been completed. The RAMONA-3B calculation for the same transient has also been performed up to 560 seconds of real time. Another TRAC-BD1 calculation with the RAMONA-calculated core power has also been performed for the first 150 seconds of the transient for comparison of only the thermohydraulic results of these two codes. For ease of understanding, we will first discuss the short-term (0 - 150 sec) results, followed by the long-term (0 - 1200 sec) results.

Short Term (0 - 150 sec) Results

The initial part of the transient following the MSIV closure, but before boron injection, as calculated by both RAMONA-3B and TRAC-BD1 is discussed first. Selected results for the first 150 seconds as depicted in Figures 6.2 through 6.8 and compared in Table 6.1 show overall good agreement between the RAMONA-3B and TRAC-BD1 predictions. These are discussed below with emphasis on the system parameters considered to be the most important from the plant safety viewpoint.

As expected, immediately after the MSIV closure initiation, the reactor vessel pressure experienced a rapid increase (Figure 6.2) which, in turn, caused void collapse in the core (Figure 6.3) introducing a positive reactivity insertion. As a result, total core power (Figure 6.4) increased significantly during the first 4 seconds of the transient. Differences in the peak power predictions (230% in RAMONA-3B vs. 520% in TRAC-BD1) as well as in the core power up to approximately 30 seconds can be partly explained in terms of void fraction predictions (through void reactivity effects). Another cause is the three-dimensional neutronics modeling in RAMONA-3B vs. point kinetics in TRAC-BD1. Since TRAC-BD1 had generated more power, opening of three banks of relief valves could not arrest the pressure rise (as it occurred in the RAMONA-3B calculation), so that even the fourth bank i.e., the safety valves, had to open (Figure 6.5). At approximately 30 seconds, the S/RV actions together with the recirculation pump trip brought the power, pressure, and other system parameters to a quasi-steady-state condition with good agreement between the two calculations. Beyond this point, the reactor was cooled by natural circulation with a core flow of approximately 20% of the steady state value (Figure 6.6). No critical heat flux (CHF) condition was experienced in either calculation.

As seen in Figure 6.4, the core power started to increase slightly after 100 seconds. This turnaround in power is due to the positive reactivity insertion when the cold HPCI and RCIC water enters the core. The cold water injection was activated by a low water level signal at slightly different times in these two calculations (Figure 6.7) in accordance with the water level predictions as shown in Figure 6.8. In the TRAC-BD1 calculation the collapsed water level dropped to the set point elevation earlier than in RAMONA-3B. This is consistent with the slightly higher core power prediction in TRAC-BD1 as shown in Figure 6.4.

One of the major reasons for the differences observed in the detailed results produced by the RAMONA-3B and TRAC-BD1 codes, can be attributed to the differences in the neutronics and power calculations. The TRAC-BD1 calculation was performed with point kinetics using the same axial power distribution as the RAMONA-3B steady-state distribution. The power distribution was kept invariant in the TRAC-BD1 calculation throughout the transient, whereas RAMONA-3B used a three-dimensional time dependent neutron kinetics. The effect of this difference can be seen in Figure 6.9 where the RAMONA-3B axial core power distributions at different times are presented. The corresponding axial void fraction profiles are shown in Figure 6.10. It is seen that a slight variation in axial void profile can indeed produce a large change in the axial power distribution which a point kinetics code like TRAC-BD1 cannot predict.

Another area of concern is the difference in the void predictions. A large difference in the core average void fraction (including bypass) can be seen between the RAMONA-3B and TRAC-BD1 calculations (Figure 6.3). RAMONA-3B uses a slip correlation to calculate the void fraction for a given quality. Since TRAC-BD1 solves two phasic momentum equations to calculate the individual phase velocities, some difference in void prediction is expected. Further investigations are in progress in order to explain the differences seen in Figure 6.3.

Since close coupling between the neutronics and thermohydraulics in a BWR makes interpretation of the code predictions a very complex task, an additional TRAC-BD1 calculation was performed for the first 150 seconds with the RAMONA-3B core power history as a boundary condition. The RAMONA-3B power was imposed because of its detailed treatment of the neutronics part of the calculation. Spatial power variation as a function of time, however, could not be imposed on TRAC-BD1 code; therefore, only the total core power was used. Results of this calculation answer the questions concerning the differences in the thermohydraulic modeling only, and their impact on the code predictions.

A few selected results from this calculation are compared with the RAMONA-3B results in Figures 6.11 through 6.13. It is seen that the system pressures (Figure 6.11) are now in much better agreement and the existing differences are clearer to explain. In the TRAC-BD1 calculation, the system pressure increases at a slower rate because considerably more steam was released through the MSIV during its closure than in the RAMONA-3B calculation. As a result, the S/RV opening was delayed in the TRAC-BD1 calculation (Figure 6.12), and the system pressure after an abrupt closure of MSIV rises more rapidly than in the RAMONA-3B calculation. However, the TRAC-BD1 core average fuel temperature prediction exhibits excellent agreement with the RAMONA-3B results as shown in Figure 6.13.

Based on comparisons between the TRAC-BD1 "power imposed" calculation and the RAMONA-3B results, it can be said that the thermohydraulic models of both RAMONA-3B and TRAC-BD1 provide adequate representation of an ATWS event

in a BWR. However, for the reactor power calculation, RAMONA-3B with three-dimensional neutron kinetics is by far a superior tool to the TRAC-BD1 with point kinetics. Also, the computer running time for RAMONA-3B is much lower (a factor of $\sim$ 4) than TRAC-BD1. Therefore, it is recommended that RAMONA-3B be extensively used for the analysis of ATWS type events in BWRs.

Long Term (0 - 1200 sec) Results

During the final stage of the ATWS calculation using the TRAC-BD1 code, it was discovered that the code was not conserving the boron mass, which led to an early hot shutdown of the reactor at approximately 420 seconds. The output from this calculation was sent to the INEL staff for their comments. After performing some test calculations of their own, the INEL staff agreed that there were errors in the code which would result in non-conservation of boron mass if leakage flow from the active core to the bypass region was allowed to exist. They suggested that the core leakage flow area be completely sealed off, allowing all the core bypass flow to enter the core bypass region directly from the lower plenum. Following their suggestion, a new steady-state calculation was performed by completely closing the core leakage flow area, thus preventing any direct thermohydraulic communication between the core and the bypass region.

Based on this new model, the ATWS calculation was repeated, and after the boron activation at t = 165 sec, test calculations were done to ascertain that the boron mass was indeed conserved. Highly concentrated borated water at 43 gpm with boron concentration of 23800 ppm was injected into the lower plenum. The entire ATWS calculation was successfully carried out to t = 1200 sec, and the reactor was brought to hot shutdown condition (with about 2% of steady state power) at approximately t = 1100 sec. The RAMONA-3B calculation was also continued after the initiation of boron injection at t = 165 sec. Figure 6.14 shows the core average boron concentration histories predicted by both the codes. It can be seen that after 300 seconds the increase in boron concentration, as predicted by TRAC-BD1, slows down whereas RAMONA-3B predicts almost a linear increase during the first 400 seconds. Note that in the TRAC-BD1 calculation the bypass boron is included in the core-average value. This is believed to be the major reason for the discrepancy seen in Figure 6.14. Another reason is due to the differences in the vessel water inventory histories predicted by the two codes. It is found that due to a lower power prediction in the TRAC-BD1 calculation, the liquid inventory in TRAC-BD1 was larger than in the RAMONA-3B calculation.

As mentioned before, TRAC-BD1 predicted the reactor power to drop to $\sim$ 2 percent of the steady state power at $\sim$ 1100 seconds. The core average (including bypass) boron concentration at this time was $\sim$ 330 ppm. Some of the TRAC-BD1 long term results are shown in Figures 6.15 through 6.17, depicting the transient behavior of the normalized reactor power, steam dome pressure, and the downcomer water level, respectively. For the time period prior to the boron injection, i.e., for t = 0 to 165 sec, the transient

results agreed quite closely with those obtained previously with the core-to-bypass leakage, except for slight differences (approximately 485% vs. 520%) in the first power peak.

After 600 seconds, the combination of HPCI and RCIC flows, which was initiated at about t = 75 sec due to low downcomer water level (Level 2), contributed to a gradual increase of the core water inventory when the relief valve flow diminished. At t = 950 sec, the downcomer water level reached Level 8 (approximately 2.4 m higher than Level 2), which is the shut-off point for the HPCI and RCIC flows. From Figure 6.17, it can be observed that the water level started to fall after the termination of the HPCI and RCIC flows. This reduction of water mass into the reactor vessel led to a rapid increase in the boron concentration in the core region, and the reactor power decreased from about 18% to 2% of steady state value.

Finally, a stand-alone program was used to calculate the suppression pool water temperature and mass based on the relief and safety valve flow rates obtained in the ATWS calculations. The initial pool water volume and temperature were assumed to be 136000 ft^3 and 90°F, respectively. The results for both TRAC-BD1 and RAMONA-3B are shown in Figure 6.18. It is seen that in spite of some differences in the predictions of other variables, such as core average void fraction, both RAMONA-3B and TRAC-BD1 predictions for the pool water temperature are very close. This indicates that the total energy produced in the core and eventually released through the S/RVs is within a few percent in both calculations. This is not very surprising since the point kinetics feedback parameters used in the TRAC-BD1 calculation and the three-dimensional cross sections used in the RAMONA-3B calculation were both developed for the Peach Bottom 2 End-of-Cycle 2 condition.

The RAMONA-3B calculation will be continued until the reactor hot shutdown condition is achieved, and the results of this task will be documented in a separate topical report.

REFERENCES

ROHATGI, U. S., and YUELYS-MIKSIS, C., (1983) "LOCA Analysis of Westinghouse RESAR-3S Plants," in Safety Research Program Sponsored by Office of Nuclear Regulatory Research, Quarterly Progress Report, July 1 -September 30, 1983, NUREG/CR-2331, BNL-NUREG-51454, Vol. 3, No. 3, Section 6.2.1.

Table 6.1 Sequence of Events for the BWR/4 MSIV Closure ATWS Calculation

EVENT	RAMONA-3B	TRAC-BD1
MSIV closure starts, sec.	0.0	0.0
S/RV starts to open, sec.	2.62	3.47
Recirculation pump trips, sec.	3.7	3.95
MSIV is completely closed, sec.	4.0	4.0
Maximum core averaged fuel temperature is reached, sec.	4.5 (773°C)	5.7 (835°C)
Maximum system pressure reached, sec.	8.5 (8.56 MPa)	11 (9.3 MPa)
HPCI and RCIC injection begin, sec.	86.6	75.8
Boron injection begins, sec.	165.0	165.0

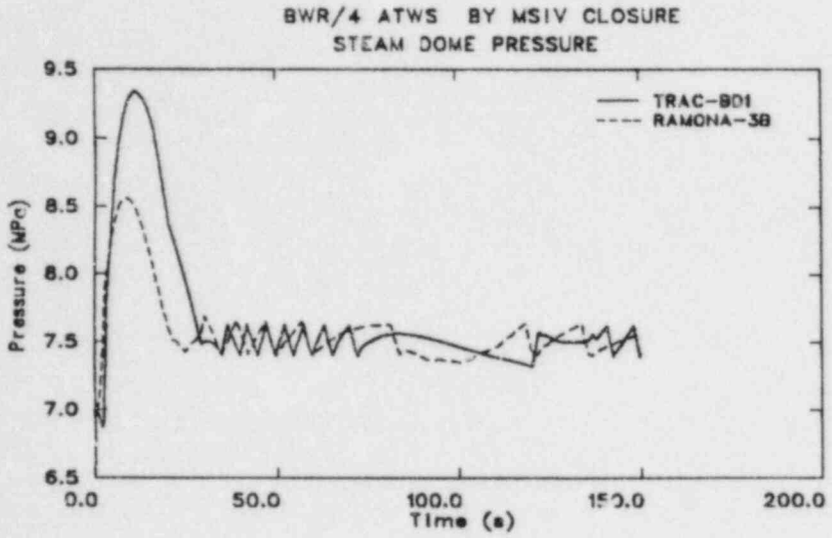

Figure 6.2 Comparison Between the RAMONA-3B and TRAC-BD1 Steam Dome Pressures. (BNL Neg. No. 1-1169-84)

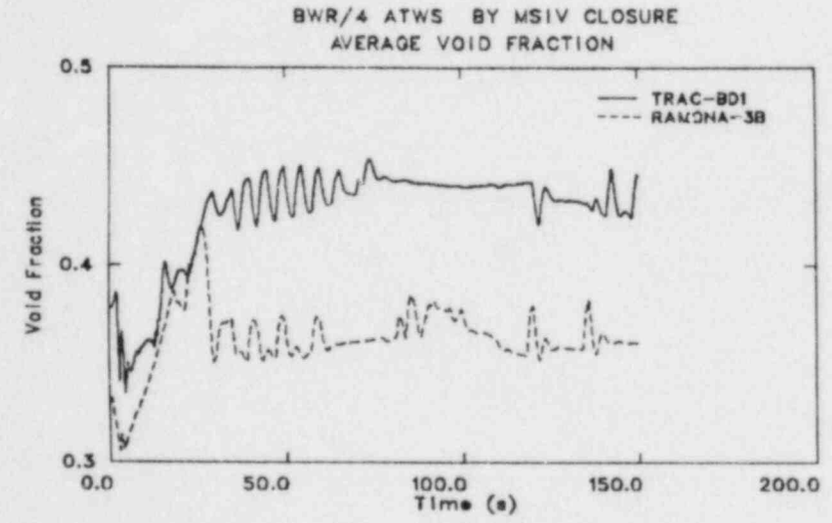

Figure 6.3 Comparison Between the RAMONA-3B and TRAC-BD1 Core Average Void Fractions Including Bypass. (BNL Neg. No. 1-1159-84)

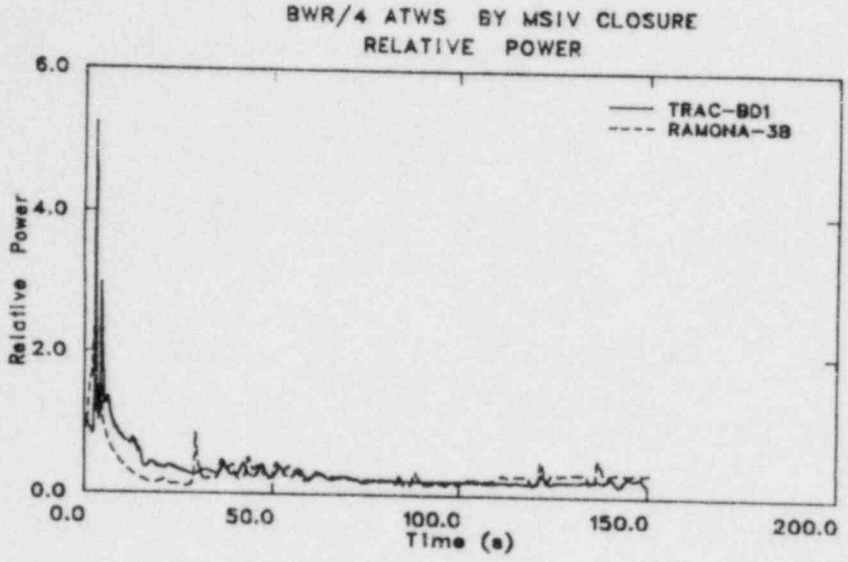

Figure 6.4 Comparison Between the RAMONA-3B and TRAC-BD1 Reactor Powers (Relative to Steady State). (BNL Neg. No. 1-1170-84)

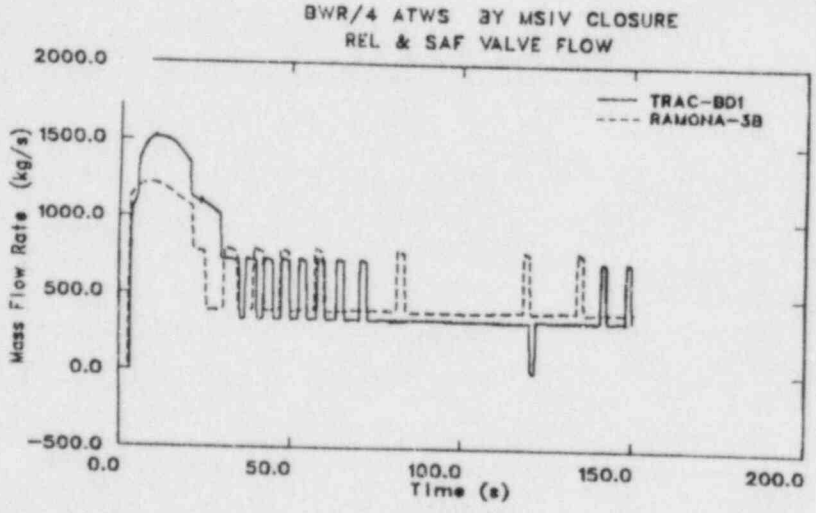

Figure 6.5 Comparison Between the RAMONA-3B and TRAC-BD1 Relief and Safety Valve Flow Rates. (BNL Neg. No. 1-1167-84)

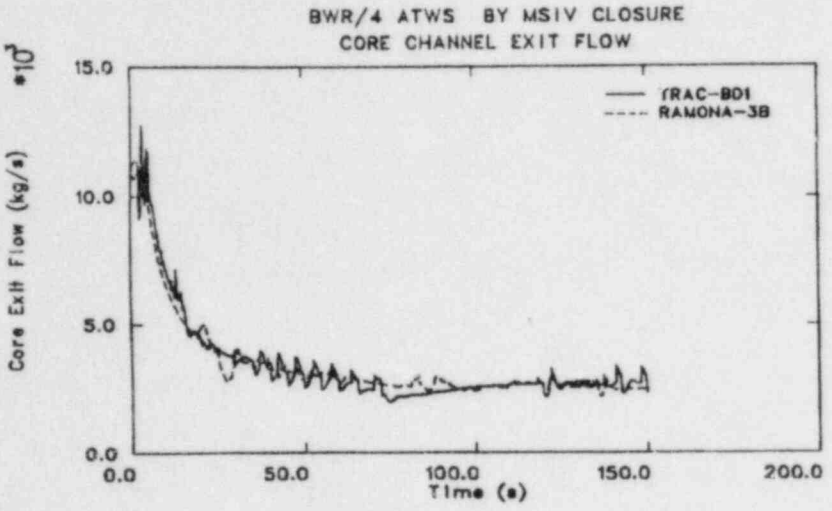

Figure 6.6 Comparison Between the RAMONA-3B and TRAC-BD1 Core Exit Flow Rates. (BNL Neg. No. 1-1168-84)

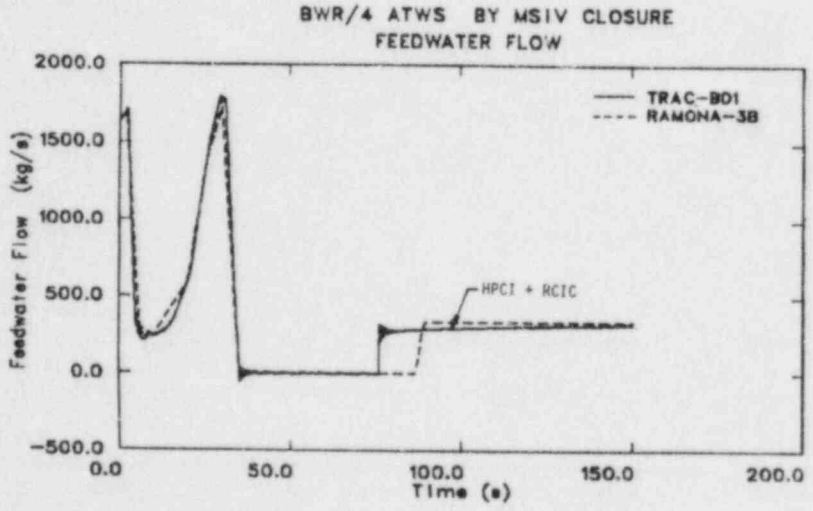

Figure 6.7 Comparison Between the RAMONA-3B and TRAC-BD1 Feedwater Sparger Flow Rates Including HPCI and RCIC. (BNL Neg. No. 1-1161-84)

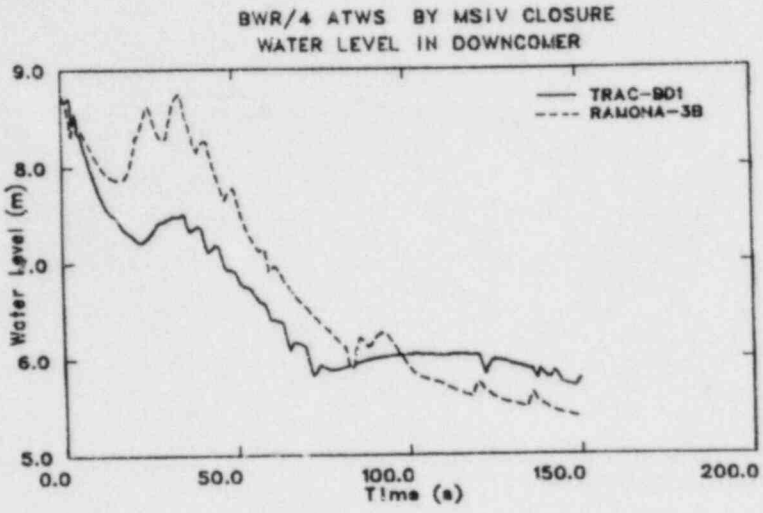

Figure 6.8 Comparison Between the RAMONA-3B and TRAC-BD1 Downcomer Collapsed Water Levels.
(BNL Neg. No. 1-1164-84)

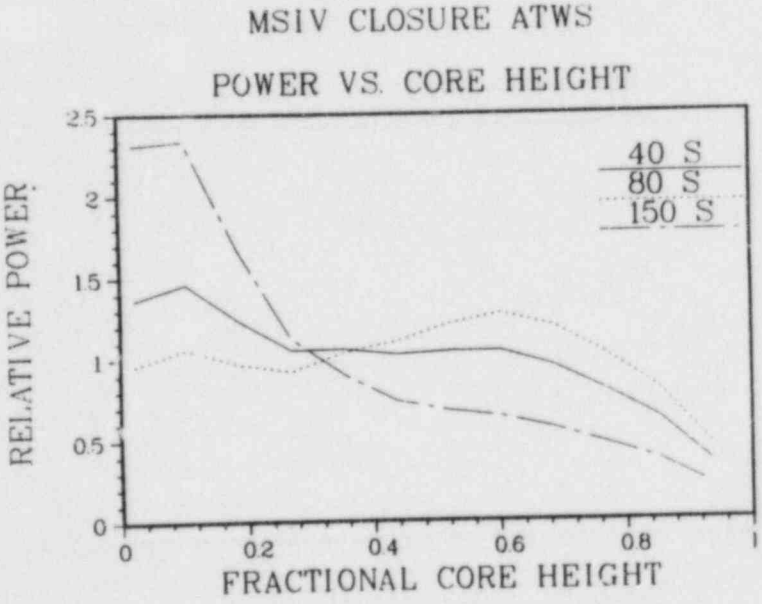

Figure 6.9 Comparison of RAMONA-3B Axial Power Distribution at Various Times During the ATWS Event.
(BNL Neg. No. 1-1162-84)

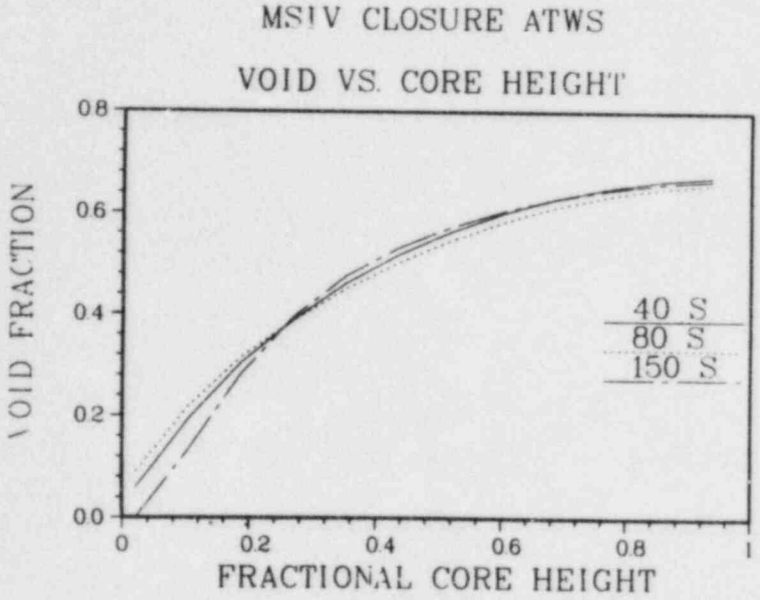

Figure 6.10 Comparison of RAMONA-3B Axial Void Distribution at Various Times During the ATWS Event. (BNL Neg. No. 1-1163-84)

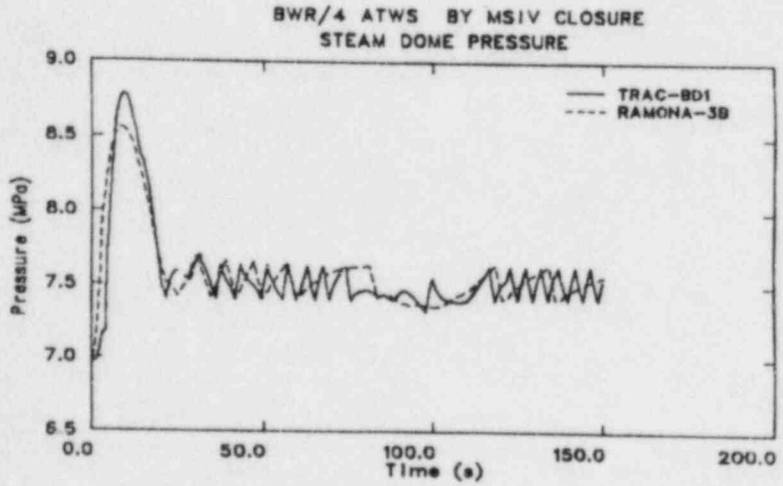

Figure 6.11 Comparison of Steam Dome Pressures as Calculated by TRAC-BD1 with RAMONA-3B Core Power. (BNL Neg. No. 1-1165-84)

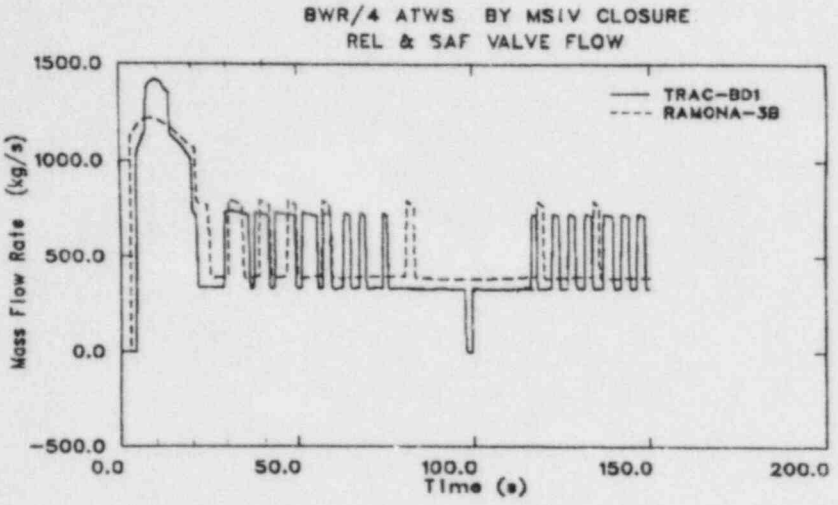

Figure 6.12 Comparison of Steam Discharge Rates Through Relief and Safety Valves as Calculated by RAMONA-3B and TRAC-BD1 With RAMONA-3B Core Power. (BNL Neg. No. 1-1158-84)

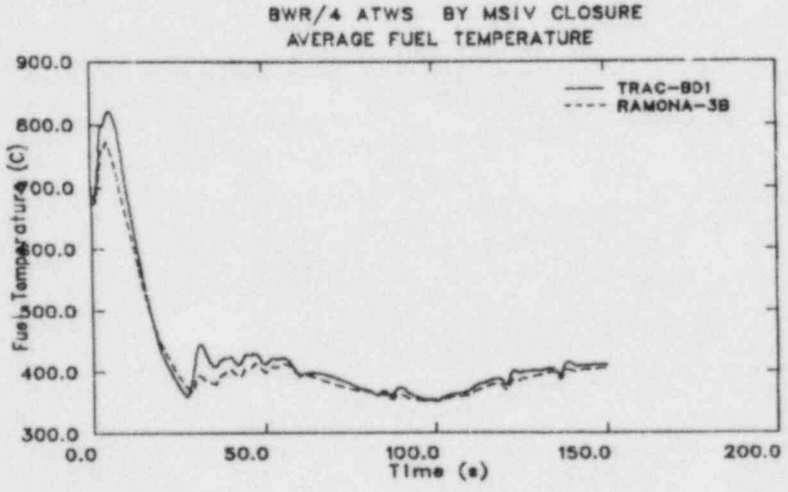

Figure 6.13 Comparison of Average Fuel Temperatures as Calculated by RAMONA-3B and TRAC-BD1 With RAMONA-3B Core Power. (BNL Neg. No. 1-1166-84)

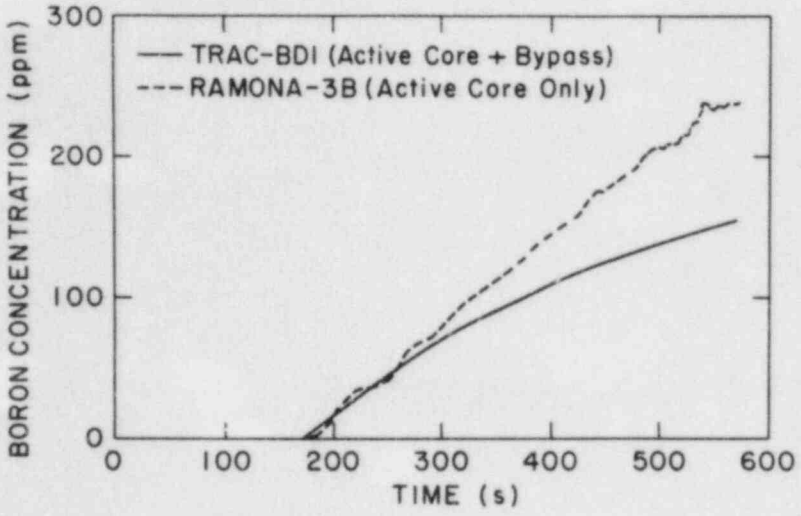

Figure 6.14 Comparison Between the RAMONA-3B and TRAC-BD1 Core Average Boron Concentration. (Note that the TRAC-BD1 result includes the bypass whereas the RAMONA-3B result does not.) (BNL Neg. No. 2-598-84)

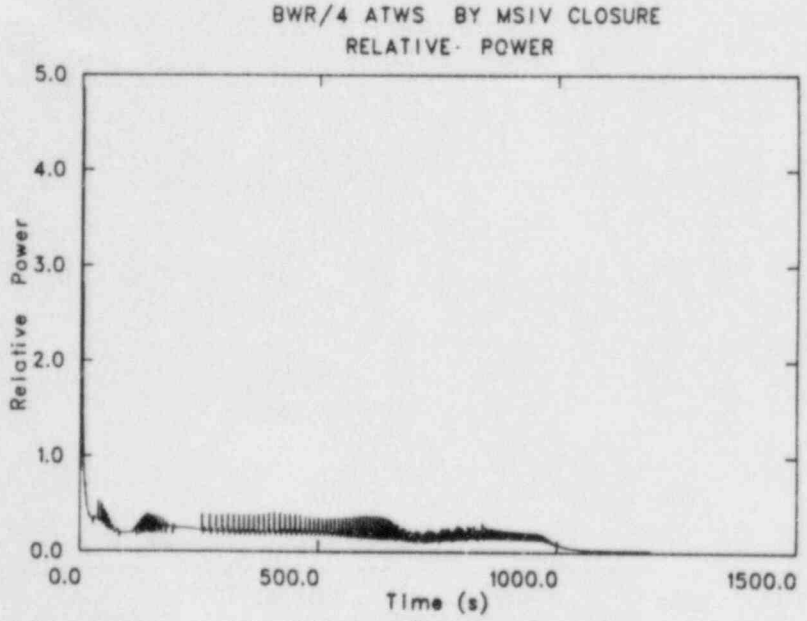

Figure 6.15 Long Term TRAC-BD1 Result for the Reactor Power (Relative to Steady State). (BNL Neg. No. 1-1160-84)

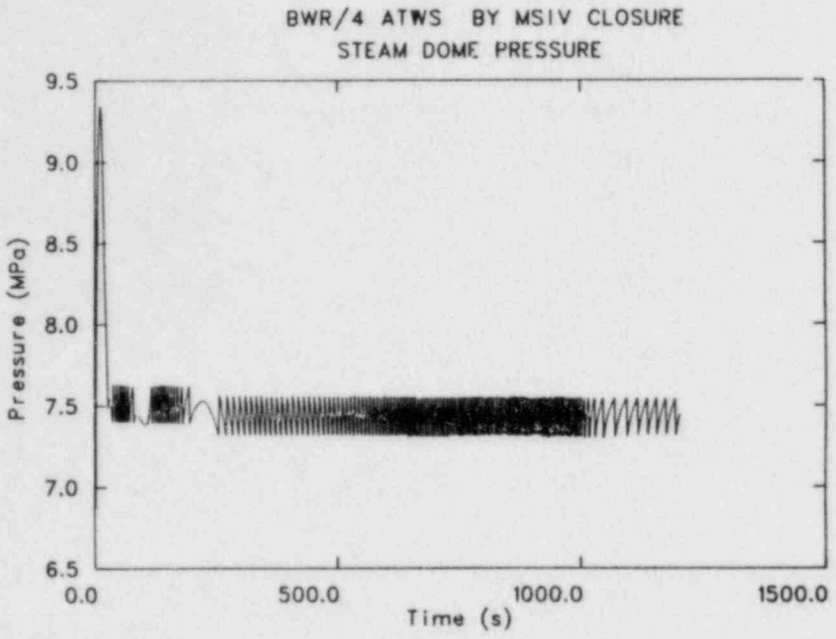

Figure 6 16 Long Term TRAC-BD1 Result for the Steam Dome Pressure. (BNL Neg. No. 1-1157-84)

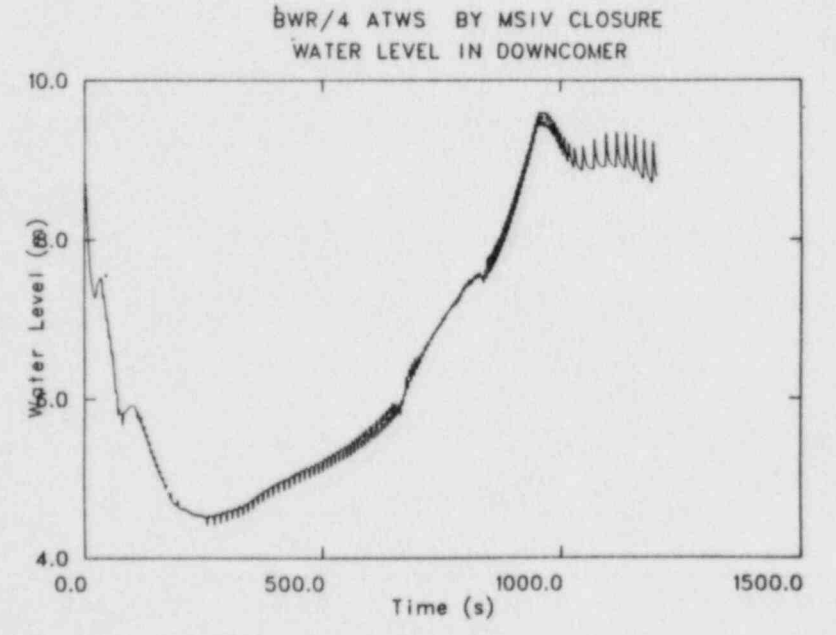

Figure 6.17 Long Term TRAC-BD1 Result for the Downcomer Collapsed Water Level. (BNL Neg. No. 1-1172-84)

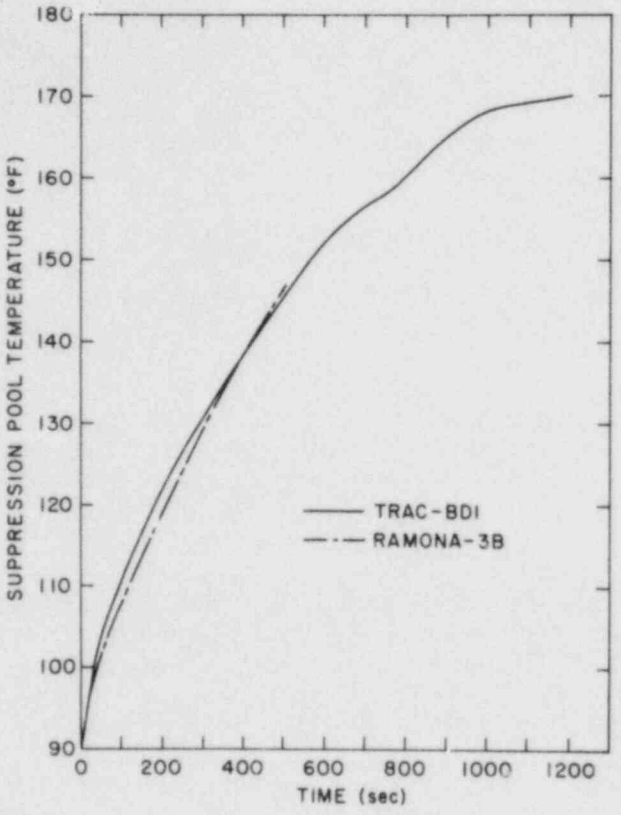

Figure 6.18 Comparison Between the RAMONA-3B and TRAC-BD1 Suppression Pool Water Temperatures. (BNL Neg. No. 2-597-84)

7. Thermal Reactor Code Development (RAMONA-3B)

(P. Saha, L. Neymotin, G. Slovik and H. R. Connell)

This project includes the modifications, improvements and preliminary (or developmental) assessment of the BWR transient analysis code called RAMONA-3B. This is the only BWR systems transient code with three-dimensional neutron kinetics, and it is now available, at no cost, to U. S. organizations for the analysis of U. S. reactors.

During this reporting period of October to December 1983, several corrections and improvements have been made to both the hydraulic and neutronic parts of RAMONA-3B. Some of these tasks were performed in the course of providing support for a typical BWR/4 MSIV closure ATWS calculation. The details of the progress achieved are described below.

7.1 Support for the BWR/4 MSIV Closure ATWS Calculation (L. Neymotin)

As reported in the October 1983 monthly highlight letter (Saha, 1983), a preliminary BWR/4 MSIV closure ATWS calculation was run up to 1000 seconds of the transient. Although the results looked physically reasonable, a detailed analysis indicated that the boron mass injected into the reactor vessel was not conserved. The reason for this anomaly was found in an erroneous treatment of coupling between the one-dimensional lower plenum and multi-channel core region. After correction, another calculation was run up to 560 seconds of transient and conservation of boron mass has been achieved.

A few corrections have also been made in the recirculation loop modeling, particularly in the recirculation flow momentum equation. Before these corrections were made, the flow through the recirculation pump had remained at approximately 7 % of the steady-state value long after the recirculation pump was tripped. In the latest calculation, the recirculation loop flow becomes essentially zero in 80 seconds after the pump trip which is more reasonable.

A comparison between the RAMONA-3B and TRAC-BD1 results for the initial stage of the same ATWS event (0 - 150 sec.) is presented in Section 6.2.2 of this report.

7.2 Corrections/Improvements in the Neutronics Area (G. Slovik)

During this reporting quarter several corrections were made in the neutronics area of the code. These areas were:

a) The eigenvalue (i.e., k_{eff}) determined from the static calculation was not normalizing the fission source term properly at the initiation of a dynamic calculation. The correct data pointers were realigned to balance the neutron source term at time equal to zero.

b) The decay heat model was corrected so that the prompt and delayed heat would be properly accounted for during a transient calculation.

c) The energy per fission was built into the code to be 200 MeV/fission. This is not general enough because this value can vary from 185 to 207 MeV/fission depending on exposure. Hence, the code was modified to accept this number as an input option.

7.3 Implementation of RAMONA-3B Improvement Tasks Performed by Scandpower (G. Slovik and H. R. Connell)

7.3.1 Collapsing of 3-D Cross Sections to 1-D Data

The stand-alone code, FRAM, which performs the actual collapsing of the 3-D cross sections to 1-D data has been compiled on the BNL computer. Work has begun in verifying the collapsing procedure at BNL using the acceptance test problem specified to Scandpower.

7.3.2 Reactivity Edits

The reactivity edits including the total and partial reactivities as developed by Scandpower have been successfully implemented at BNL. However, there are two technical issues that are being resolved between the BNL and Scandpower staff. These are:

a) The total reactivity calculated from the perturbation theory does not match with the sum of the partials. This could be caused by some coding errors or an improper method of calculating the leakage terms. It is worth mentioning that the perturbation theory has been successfully used in two BNL codes, namely BNL-TWIGL (Diamond, 1976) and MEKIN-B (Aronson, 1980) for the reactivity calculations.

b) Only linear terms have been used by Scandpower for the cross section perturbations, although it is well known that the void feedback and scram reactivity terms follow a quadratic law.

As mentioned before, both of these items will be resolved in the near future.

REFERENCES

ARONSON, A. L., CHENG, H.S., DIAMOND, D. J. and LU, M.S., (1980), "MEKIN-B: The BNL Version of the Core Dynamics Code, MEKIN", BNL-NUREG-28071, Brookhaven National Laboratory.

DIAMOND, D. J., ed., (1976), BNL-TWIGL, A Program for Calculating Rapid LWR Core Transients", BNL-NUREG-21925, Brookhaven National Laboratory.

SAHA, P., (1983), "Monthly Highlights for October 1983," BNL Monthly Letter on Thermal Reactor Code (RAMONA-3B) Development to USNRC, October 1983.

8. Calculational Quality Assurance in Support of PTS

(P. Saha, J. H. Jo, U. S. Rohatgi and H. R. Connell)

The objective of this project is to provide a peer review of the thermal-hydraulic calculations that are being performed at LANL (using the TRAC-PWR code) and INEL (using the RELAP5 code) for the NRC Pressurized Thermal Shock (PTS) study. Specifically, this includes a review of the plant decks and the calculations, and an assessment of the reasonableness of the results. The major activities performed during October to December 1983 are noted below.

8.1 Review of TRAC Calvert Cliffs Calculations (J. H. Jo)

Review of the TRAC input decks and steady state results for the Calvert Cliffs plant has been completed. Results of the review have been documented in a BNL memorandum (Jo, 1984) and distributed to the cognizant NRC, LANL and ORNL staff. In general, both the input decks and the steady states have been found to be acceptable. However, as pointed out in the aforementioned memorandum, there are a few items which, in our judgment, should be further investigated and/or explained by the LANL staff.

A BNL staff member (J. H. Jo) attended the working meeting held at LANL on December 13, 1983, to discuss the Calvert Cliffs transient calculations performed by LANL. Based on the information received at that meeting, a quick review of all the eleven transients has been made and an interim report is being written. Work will continue for a more detailed in-depth review of a few selected transients.

8.2 A Simple Procedure for Quantitative Review and Extrapolation of TRAC or RELAP5 Calculations (U. S. Rohatgi and J. H. Jo)

A set of procedures based on different degrees of complexity have been developed using the overall mass and energy balances. The primary side pressure is determined from two limiting models for the pressurizer. A simplified version of this procedure has been used to check some of the TRAC Calvert Cliffs transient results by hand calculations. A report is being written on the details of the procedure.

8.3 Review of H. B. Robinson-2 Calculations (U. S. Rohatgi)

A BNL staff member (U. S. Rohatgi) attended a working meeting at INEL on November 3, 1983 to discuss the last five transient calculations performed by INEL using the RELAP5 code. All the eleven transient calculations assigned to INEL have been completed. The input listings for the full power and hot standby cases along with some transient results have been received. These are currently being reviewed.

8.4 Implementation of TRAC-PF1/MOD1 Code (H. R. Connell)

Implementation of the TRAC-PF1/MOD1 code on the BNL computer has been completed. All four sample problems have been run satisfactorily.

An UPDATE file from LANL was taken from the LANL VAX computer and implemented in TRAC-PF1/MOD1 at BNL. These updates plus another acquired during the TRAC-PF1/MOD1 workshop at LANL have made the code operational at BNL for full-scale plant problems.

Two BNL staff members (H. R. Connell and C. Yuelys-Miksis) attended the TRAC-PF1/MOD1 workshop on December 6-7, 1983 at Los Alamos National Laboratory.

REFERENCES

JO, J. H., (1984), "BNL Review of PTS Input and Steady State Calculations Performed by LANL for Calvert Cliffs Nuclear Plant," BNL Memorandum to P. Saha, January 12, 1984.

II. DIVISION OF ENGINEERING TECHNOLOGY

SUMMARY

Stress Corrosion Cracking of PWR Steam Generator Tubing

The experimental program on stress corrosion cracking (SCC) at Brookhaven National Laboatory (BNL) is aimed at the development of a quantitative model for predicting the behavior of Inconel 600 tubing in high temperature aqueous media.

Laboratory tests involve U-bends, constant extension rate tests (CERT), and constant load. Plots are made of failure time and crack velocity vs. temperature, and also of SCC time vs. stress, using mainly pure water, and some tests with environments related to the ingredients of primary or secondary water. Cold work of Alloy 600 is also included.

SCC was earlier found in four U-bends of production tubing exposed in deaerated, pure water at 315°C, and provided a continuous Arrhenius plot from 365°C to 315°C. No further examination was made during this quarter. CERT with 0.01% carbon material was started in secondary water ingredients. Tests at constant load are consistent with a log-log relationship between the applied stress and the time to fracture at 365°C for low carbon Alloy 600, but stresses appreciably below the yield point have not yet given any failures. Computer programs are continued for handling the proposed model used for predictive purposes for Inconel steam generator tubing.

A proposed standard test procedure for ASTM balloting is in final modified form, dealing with Electrochemical Potentiokinetic Reactivation (EPR) tests used in detecting sensitization of stainless steels. The first ballot produced two negative votes, which were resolved by the present outlined procedures, and fresh balloting is due this spring in the G-1 ASTM committee.

Model verification with tubing from the Surry steam generator at Pacific Northwest Laboratories is still strongly advocated, together with some tests in constant extension.

Bolting Failure Analysis

An increase in the number of bolting failures attributed to lubricant coolant interaction at nuclear power plants has caused a great deal of concern regarding the more judicious use of lubricants by the nuclear power industry. An investigation performed on eleven commonly used lubricants by the nuclear power industry was completed during this quarter. The investigation included EDS analysis of the lubricants, notched tensile CERT of bolting materials with the lubricants, frictional testing of the lubricants, and weight loss testing of a bonded solid film lubricant. The work generally showed that there is a

vast amount of variance in the mechanical properties of common bolting materials, that MoS_2 can hydrolize to form H_2S at 100°C and cause SCC of common bolting materials, and that the use of copper-containing lubricants can also be potentially detrimental to high strength steels in an aqueous environment.

Probability Based Load Combinations for Design of Category I Structures

A procedure for developing probability-based load combination criteria for design of Category I structures has been established. This procedure is utilized in developing load factors for concrete containments. The proposed load combination is in load and resistance factor design (LRFD) format and follows the Turkstra combination rule. Four sample containments are constructed using the generalized Latin hypercube sampling technique. Furthermore, an objective function is defined and a minimization scheme is being developed to find the optimum load factors. Work on deviation of load factors for various load combinations is being carried out.

In order to evaluate the reliability level implied in current design criteria, a reliability assessment of the Clinton and Zion containment structures has been carried out. The geometries and dimensions of the containment are obtained from the FSAR and drawings. The cylinder and dome reinforcements are also established. Various loads are considered in the analysis. The flexural limit state is defined based on the ultimate strength of reinforced concrete. Then, the limit state probability for various load combinations is computed.

Mechanical Piping Benchmark Problems

The study of multiple supported piping systems was intensified to achieve a completion of the computations in time to permit a reporting of the salient results to the PVRC Steering Committee for Piping at their January 24 meeting. Additionally, the evaluation of a new physical benchmark, the NRC/EPRI Main Pipe Line 1, was initiated.

Identification of Age-Related Failure Modes

The objective of this program is to determine which aging and service wear effects are likely to impair plant safety, and which methods of inspection and surveillance will be effective in detecting significant aging effects.

The first two categories of components to be addressed are small motors in mild environments and battery chargers/inverters.

The program for each component will proceed through three phases: a research phase, an experimental phase, and an evaluation and conclusion phase. At the end of this quarter, the motor research phase is partially completed. The experimental phase will be conducted in the next quarter.

9. Stress Corrosion Cracking of PWR Steam Generator Tubing

(D. van Rooyen)

The objective of this program is to develop quantitative data to serve as a predictive basis for determining the useful life of Alloy 600 tubing in service. For this purpose, tests are being run on production tubing of Inconel 600 at different carbon levels to examine the various factors that influence the cracking of tubing. Verification was planned with tubing to be obtained from a decommissioned steam generator, but this will not be possible due to a reduction in funding level for 1984, but is still strongly recommended.

The present experimental program addresses two specific conditions, i.e., 1) residual stress conditions where deformation occurs but is no longer active, such as when denting is stopped and 2) where plastic deformation of the metal continues, as would occur during denting. Laboratory media consist of pure water as well as solutions to simulate environments that would apply in service; tubing from actual production is used in carrying out these tests. The environments include both normal and "off" chemistries for primary and secondary water. Material condition also includes various degrees of cold work. At this time, tests are aimed at AVT at 345°C.

9.1 Constant Load

For the case where denting or active deformation is no longer occurring, it is necessary to obtain data that relate failure times to stress, i.e., the load on the tube. In service these stresses can consist of residual plus operational stress, and may be complex. Tensile specimens under applied load have given good data for 0.01% carbon Inconel, but not for 0.03 and 0.05% carbon heats, and the latter appear to need a different stress pattern. This information should be developed.

The effect of temperature was shown in the previous report, together with the data from various environments. Cold work effects are not effectively sorted out by the constant load test, and were discontinued. The long term, low stress test with as received material at 365°C continues, but no cracks have yet occurred. This may indicate a deviation from the formula developed above the yield point, but this is too early to be a definite conclusion.

9.2 CERT

CERT data on SCC require a better distinction between the initiation and propagation stages that can be achieved by our present extrapolation technique. Corrections are needed to improve the quantitative determination of SCC induction times, which are used for calculating crack propagation rates and used for predicting strain levels at which SCC will become a problem. An activation energy of 33 Kcal/mole continues to be the best value available for crack growth, pending the introduction of a better correction in the calculation, but the spread between various curves could be caused by crack

initiation variations, and more work may lead to a simplification of the predictive formula.

No complete sets of data are yet available for CERT in AVT, although this work is continuing.

We have discontinued plans for the new test that would permit simulation of an active dent.

9.3 U-Bends

Split tube type U-bends cracked in earlier tests at 325°C-365°C and suggested a possibility that the carbon level of the Inconel influences the crack initiation/temperature relationship, i.e., activation energy seemed to increase with increasing carbon content. A larger number of replicate samples have been exposed in water at 290°C and 315°C since 1981. These U-bends have not shown cracking for 0.02 and 0.03% carbon, but the 0.01% material showed cracks in four samples in the previous quarter. No further cracks have been seen because no inspection was due in this report period.

Testing continues with tubes at 365°C in pure H_2O to correlate a static "dent" size with susceptibility to SCC of 0.01% carbon Alloy 600. The "dents" were made by pressing semicylindrical pieces of metal onto the outside surface while the tube is in a test jig, and range from 5 to 40 mils.

9.4 Future Work

Future work will be the continuation of long-term tests, and exposures in AVT. However, it is strongly recommended that work on the model, especially in crack propagation rates, be re-started to complete the quantitative relationships. These may be simplified by limited further work, and without the effort the work to data may lose much of its potential application.

10. Bolting Failure Analysis

(J. R. Weeks and C. J. Czajkowski)

All work on the Bolting Failure Analysis Program was completed during this quarter, and a final report drafted. The following are the conclusions from this work.

10.1 The appearance of potentially detrimental elements in the chemical analysis (EDS scans) of the various lubricants clearly shows a marked difference in composition between supposedly similar (e.g. MoS_2 based) lubricants. For this reason, an independent chemical analysis of lubricants used on critical nuclear components prior to their application is advisable.

10.2 The steaming tests of the chemically pure MoS_2 show that in the presence of steam (100°C), MoS_2 will hydrolize to form detrimental gaseous sulfides (H_2S).

10.3 Carbon disulfide was shown to remove previously applied MoS_2 from a carbon steel fastener producing a simplified cleaning procedure. The potential for carbon disulfide to cause SCC of these steels should be investigated before the cleaning procedure is used in field applications.

10.4 The wide variation of measured coefficients of friction for similar lubricants shows that generalizations of this value for "same type" (e.g. MoS_2 based, graphite-based, copper-based or nickel-based) should not be made and that the coefficient of friction should be determined (or obtained) for the specific lubricant used.

10.5 The notched tensile tests of the bolting materials showed that both A540 B24 Class 2 and A193 B7 materials are susceptible to a SCC failure in steam at 280°C. The use of MoS_2 or a copper + graphite lubricant appear to enhance the susceptibility to SCC. The use of a solid bonded film lubricant does not significantly improve the bolting material's performance with either steam or MoS_2. There may be some benefit in using the bonded film lubricant with copper bearing lubricants.

10.6 The variation in notched tensile strengths with no discernible difference on the fracture faces of the A540 B24 Class 2 material shows that bolts cut from the same rod may exhibit different mechanical properties.

10.7 The weight loss experiments, using previously coated solid bonded film lubricant specimens, show a marked decrease in metal loss at 100°C and 178°C when compared to previously reported bare metal data. This protection disappears at 600°F (315°C), when the results differ little between previously coated and bare metal specimens.

11. Probability Based Load Combinations for Design of Category I Structures

(H. Hwang, M. Reich, J. Pires, P.C. Wang,
M. Shinozuka, B. Ellingwood and S. Kao)

11.1 Load Combination Criteria for Design of Concrete Containments

A procedure for developing probability-based load combination criteria for design of category I structures has been established. The major steps of this procedure are as follows:

1. Select an appropriate load combination format.
2. Establish N sample structures.
3. Determine a target limit state probability.
4. Design each sample structure.
5. Estimate limit state probability associated with each sample structure.
6. Compute an objective function.
7. Determine a set of load factors along the direction of maximum descent with respect to the objective function.
8. Repeat steps 4 to 7 until a set of load factors that minimize the objective function is found.

This procedure is specifically utilized in deriving load combination design criteria for concrete containments. The proposed load combination is in Load and Resistance Factor Design (LRFD) format and follows the Turkstra combination rules. The ranges of design parameters such as geometries, material strengths and loadings are examined and representative values of each parameter are recommended. Then, four sample containments, as shown in Table 11.1, are constructed using the generalized Latin hypercube sampling technique.

The objective function adopted in this study is shown as follows:

$$\Omega(\gamma,\phi) = \sum_{i=1}^{N} w_i \left(\log P_{f,i} - \log P_{f,T}\right)^2$$

where γ and ϕ are load factor and resistance factor respectively. $P_{f,i}$ is the limit state probability computed from the i-th sample containment and $P_{f,T}$ is the specified target limit state probability. w_i represents a weight factor for i-th sample containment. A minimization scheme is being developed so that the optimum load factors can be found in a few iterations. Some of the load factors may be preset to a specific value in order to reduce the number of variables in the minimization. For example, dead load factor is preset to be 1.2 or 0.9, depending on whether the dead load has a stabilizing effect.

A computer program for design of reinforced concrete containments has been developed to expedite the design process. Work on derivation of load factors for various load combinations is being carried out and is going to continue in this FY year.

11.2 Reliability Assessment of Containment Structures

As mentioned in the previous quarterly reports, a reliability assessment of the Indian Point Unit 3 containment structure has been carried out in order to evaluate the reliability level implied in the existing design criteria.

In addition to the Indian Point Unit 3 containment, the reliability assessment of Clinton and Zion containments under various loads has also been carried out in this reporting quarter. The geometries and dimensions of the containment are obtained from the FSAR and drawings. The cylinder and dome reinforcements are also established. Various loads are considered in the analysis. The flexural limit state is defined based on the ultimate strength of reinforced concrete. Then, the limit state probability for various load combinations are computed.

11.3 Reliability Analysis of Shear Walls

For shear wall structures the previous developed reliability analysis is being refined. The resistance capacity of the shear wall will be simplified. A report on reliability analysis of shear wall is being written.

Publications

Ellingwood, B., "Probability Based Safety Checking of Nuclear Plant Structures", BNL-NUREG-51737, NUREG/CR-3628, December 1983.

Table 11.1 PWR Reinforced Concrete Containment Samples

Design parameters	Sample 1	Sample 2	Sample 3	Sample 4
Inside radius	70'-0"	60'-0"	60'-0"	70'-0"
Dome rise ratio	1.0	1.0	1.0	1.0
Cylindrical height	150'-0"	150'-0"	150'-0"	150'-0"
Cylindrical wall thickness	4'-6"	3'-6"	4'-6"	3'-6"
Dome wall thickness	3'-6"	2'-6"	3'-6"	2'-6"
Concrete compressive strength (psi)	4000	4000	5000	5000
Steel yield strength (psi)	60,000	60,000	60,000	60,000
Dead load (lb/ft^3)	150	150	150	150
Accidental pressure (psi)	47	42	52	57
Safe shutdown earthquake (g)	0.17	0.32	0.50	0.25

12. Mechanical Piping Benchmark Problems

(P. Bezler, M. Subudhi, and S. Shteyngart)

12.1 Physical Benchmark Development

The draft report describing the blind predictions for the extended Z bend test was reviewed by the NRC technical monitor. An updated draft was submitted for printing.

A new physical benchmark evaluation was initiated during the period. A sketch of the system is shown in Figure 12.1. The pipe line consists of 6" and 8" SCH 40 pipe supported and excited by four hydraulic actuated sleds (S1-S4, Figure 12.1). The system was constructed and tested by ANCO Engineers Inc. at their facility in Culver City, CA. The tests were conducted under a program jointly sponsored by the NRC and EPRI. The system is designated the NRC/EPRI Main Pipe Line 1 and represents the first of a series of progressively more complex systems to be tested under the program.

In preparation for the benchmark evaluation a preliminary finite element model of the system was developed. Figure 12.2 shows a computer graphics display of this model. It consists of some 55 points located to define the system geometry and to correspond to instrumentation locations.

Using the model, natural frequency determinations were made for the system. In these calculations the system was considered fixed at the four sled locations, filled with water and pressurized to 1000 psi. The results of these calculations and some test results are summarized in Table 12.1. The first column of this table lists the analytical mode number, the second column the predicted natural frequency, the third column corresponding mode shape information and the last column lists the natural frequencies measured during hammer tests.

As can be seen by comparing columns 2 and 4 there is approximate agreement between the predicted and measured system natural frequencies. Before the benchmark evaluation is performed some refinement of the model will be made to improve the degree of agreement.

12.2 Multiple Supported Piping System

During this perod a concentrated effort was directed towards completing all the scheduled calculations in the Multiple Supported Piping study by mid-January. This target date was selected to permit a presentation of key results to the PVRC Steering Committee for Piping at their January 24th meeting in Ft. Lauderdale, FL.

Specifically, the computation of dynamic and pseudo-static response for the last BNL model was completed. Additionally, the computation of total response, the combination of the dynamic and pseudo-static response components, was initiated for all models. With the completion of these efforts the results will be organized in both the table format presented in the previous quarterly report and in a figure format to be developed.

Some comments concerning the prediction of total response is appropriate. As has been stated in previous quarterly reports, fourteen dynamic response predictions and five pseudo-static response predictions are being developed for each response parameter, per seismic event, per problem. To compute the total response for each parameter for all possible combinations and permutations of the dynamic and pseudo-static responses would be difficult and not particularly informative. Instead the time history estimate of the pseudo-static response component was accepted as representing the lower bound estimate for this component (only a technique which provided a conservative estimate of the pseudo-static component would be adopted for use). Next this estimate of the pseudo-static response is combined with the fourteen estimates for dynamic response considering both SRSS and absolute summation. This procedure results in 28 estimates of total response for each parameter/seismic event/problem. Each of these is then compared to the time history estimates of total response to quantify the degree of exceedance for each computational option. As mentioned above these computations are underway.

An additional effort during the period was the preparation of an abstract describing some of the work under this study for the 5th ASCE-EMD conference. At the end of the period notification was received that the abstract was accepted and the preparation of a paper was initiated.

Table 12.1

NRC/EPRI Main Line 1

	Predicted		
Mode No.	Frequency (Hz)	Direction of Max Component of Eigenvector	Measured Frequency (Hz)
1	4.09	Y	4.62
2	6.88	Y	7.11
3	8.54	X	9.16
4	10.75	Z	11.66
5	13.0	X	13.54
6	17.0	X	17.71
7	17.85	Y	18.53
8	19.0	Z	23.94
9	23.94	Z	25.87
10	25.3	X	28.06

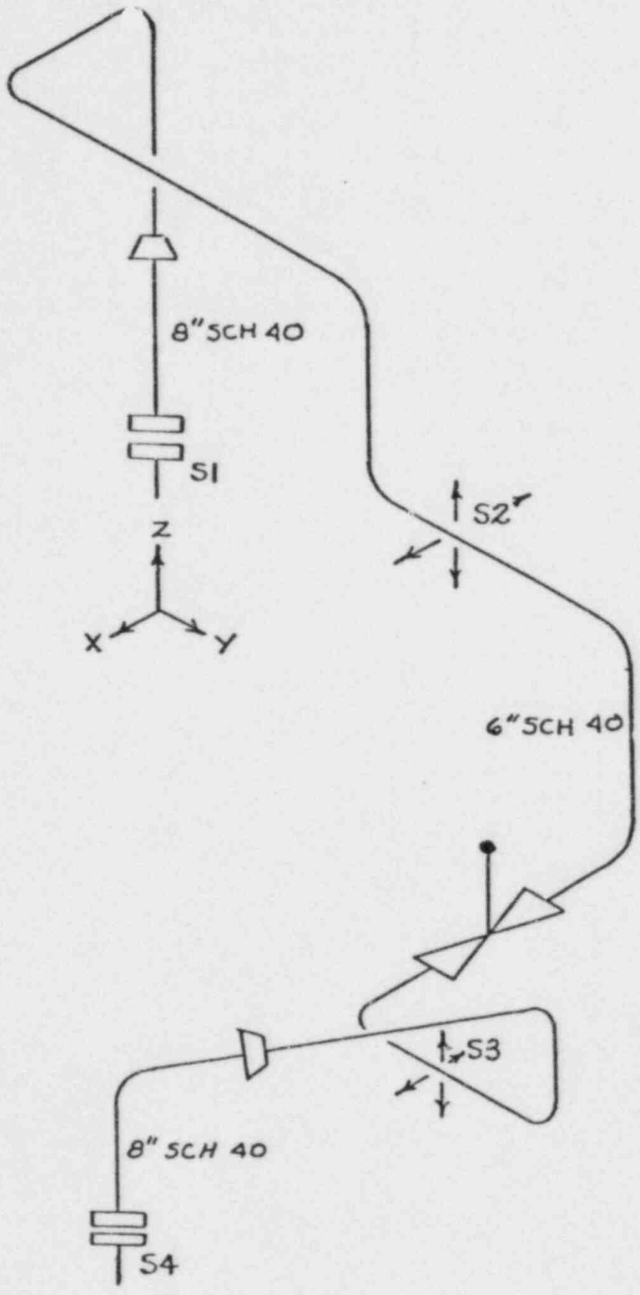

Fig. 12.1 NRC/EPRI Main Pipe Line 1.

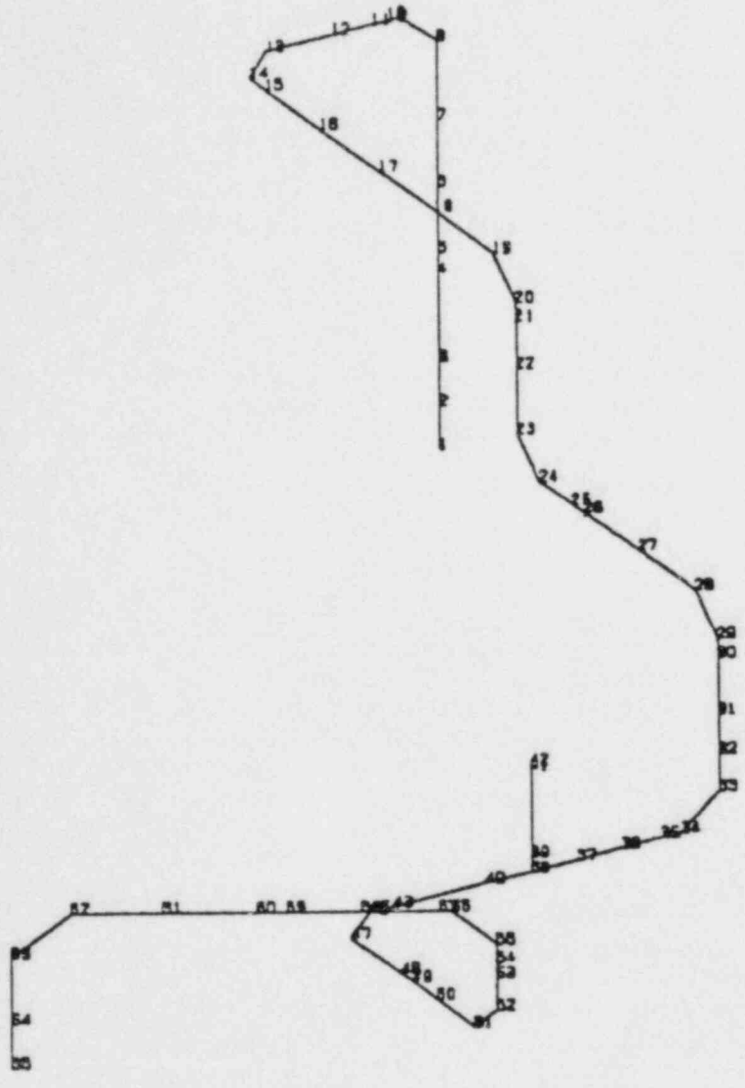

Fig. 12.2 Finite Element Model NRC/EPRI Main Pipe Line 1.

13. Identification of Age Related Failure Modes
(J.H. Taylor)

The objectives of this program are twofold: 1) to determine what aging and service wear effects are likely to impair plant safety, and 2) to determine what methods of inspection and surveillance will be effective in detecting significant aging effects prior to the loss of safety function so that proper maintenance and timely repair or replacement can be implemented.

The objectives mentioned above will be obtained by addressing components used in nuclear power plants on an individual basis. The selection of components to be studied will be made by using risk analysis, failure histories, special NRC interests, and expert judgement. The first two categories of components to be addresed are small motors in mild environments, and battery chargers/inverters.

The program will proceed through three phases for each component: a research phase, an experimental phase, and an evaluation and conclusion phase. As of the end of the first quarter of FY 1984, significant progress has been made on the motors, which is detailed below. Work on the battery chargers and inverters is scheduled for the next quarter.

13.1 Research Phase - Motors (J. Higgins)

The acquisition of motors (and other components for future use) is being pursued at operating and decommissioned reactors. Some motors have been identified at a decommissioned plant. They are of an older design and their relevancy to contemporary equipment is under evaluation.

Available sources of information are being researched to provide input to the scope and type of examinations to be conducted and towards defining the functional parameters important for defect characterization, and determination of the aging and service wear effects that are likely to impair plant safety. Typical examples of the sources of information are failure analyses and reports by other national laboratories, licensees, architect engineers, and equipment manufacturers. Preliminary results indicate that aging is not a problem that affects the performance of motors. That is, motor failures are caused not by aging but by improper maintenance or by external stresses, such as failures of the driven equipment.

13.2 Experimental Phase - Motors (J. Higgins and J. Curreri)

A test plan has been prepared, which includes visual examinations, operational tests, and seismic testing according to a generic floor response spectra. This testing will be conducted at BNL, although the seismic portion may be performed at an outside testing facility. The testing will be conducted in the second quarter of FY 1984.

III. DIVISION OF FACILITY OPERATIONS

SUMMARY

Analysis of Human Error Data for Nuclear Power Plant Safety-Related Events

Brookhaven National Laboratory (BNL) has been tasked in this program to develop and apply realistic human performance data and models to help evaluate the human's role in nuclear power plant safety. To meet this objective, the major current efforts are being placed in the following areas of investigation:

- the development of Human Error Probabilities (HEPs);
- the use of Performance Shaping Factors (PSFs) and quantified expert judgment in the evaluation of human reliability - the Success Likelihood Index Method (SLIM);
- the development of the Multiple Sequential Failure (MSF) model.

As a result of these efforts, BNL has developed several documents which report on the findings in the above areas, namely:

- Human Error Probability Estimation Using Licensee Event Reports (NUREG/CR-3519);
- SLIM-MAUD: An Approach to Assessing Human Error Probabilities Using Structured Judgment (NUREG/CR-3529).

Human Factors in Nuclear Power Plant Safeguards

BNL has been tasked in this program to develop a long-term research plan for studying the effects of human factors on the security at nuclear power plants. In the past, relatively little attention has been paid to human factors affecting security personnel, in spite of the high level of attention the Three Mile Island 2 accident brought to human factors affecting operational personnel. In order to remedy this, the NRC is developing a coordinated long-term research plan, and to meet this objective, BNL has developed a planning document to assist NRC in identifying safeguards-related human factors research that can be undertaken over the next 5-7 years. This document is entitled "Long-Term Research Plan for Human Factors Affecting Safeguards at Nuclear Power Plants," (NUREG/CR-3520). In addition, as a result of the BNL identified research needs, the human factors aspects of safety/safeguards interaction issues are being addressed by BNL.

Emergency Action Levels

BNL has been tasked in this program to develop guidance for Emergency Action Levels (EALs) that can be integrated into Emergency Operating Procedure (EOP) guidelines. From this guidance, a method will be developed that can be applied by licensees to verify that the EALs incorporated into their EOPs are usable in the control room under accident conditions. This should result in a reliable and timely basis for declaring emergencies without being too complex or burdensome to those who are trying to safely mitigate the accident. Thus far, a preliminary assessment has been made to integrate EALs and EOPs based on the degradation of the fission product barrier criteria.

Protective Action Decisionmaking

In this new program, BNL is developing a technical basis for the NRC's guidance on protective action decisionmaking based on an evaluation of the consequences of nuclear power plant accidents. These actions include sheltering, evacuation and relocation, but specific recommendations have proven to be difficult to justify because of uncertainties in potential accident sequences. Consequently, BNL will establish strategies appropriate to those sequences for which emergency planning is necessary, emphasizing credible failure modes, links to emergency action levels based on in-plant observables and containment status, and other factors such as weather. A final NUREG report will be written in a manner understandable to laypeople.

14. Analysis of Human Error Data for Nuclear Power Plant Safety Related Events

(W. J. Luckas, Jr.)

Brookhaven National Laboratory (BNL) has been tasked in this program to develop and apply realistic human performance data and models to help quantify and qualify the human's role in nuclear power plant (NPP) safety. To meet this objective, the major current efforts are being placed in the following areas of investigation, namely:

- The prediction of Human Error Probabilities (HEPs) using Licensee Event Report (LER) data and nuclear systems expertise - a utility analysis.

- The use of Performance Shaping Factors (PSFs) and quantified expert judgement in the evaluation of human reliability - the Success Likelihood Index Method (SLIM).

- The development of the Multiple Sequential Failure (MSF) Model.

14.1 Utility Analysis of Using LER Data for HERs Prediction

(K. J. Voska)

The objective of this research has been the development of a methodology which can be used to obtain human error rate (HER) data from an analysis of Licensee Event Reports (LERs). A further objective was to assess the practicality, acceptability, and usefulness of using the HERs obtained to predict human error probabilities (HEPs) for use in Probabilistic Risk Assessment (PRA).

In order to calculate HER, the total number of observed errors must be divided by the total opportunity for error as follows:

$$\text{HER} = \frac{\text{total number of a particular type of human errors}}{\text{total number of opportunities for those errors}}$$

A method for the calculation of HERs was originally presented in NUREG/CR-1880 and -2417. This method has undergone several revisions to provide a more structured set of procedures for the identification, classification, and quantification of human errors reported in LERs. It is intended that the procedures be "stand-alone" in the sense that consistent and reproducible results can be obtained by different users with minimal support.

During the first quarter of FY 1984, work continued on the refinement of the method and the drafting of a final report. The most recent revisions to the method include efforts to integrate the structure of the data classification scheme with the structure of a human reliability data bank presently being developed (see NUREG/CR-2744). The final report NUREG/CR-3519 has been given a new title: "Human Error Probability Estimation Using Licensee Event Reports.

14.2 Success Likelihood Index Method (SLIM) Development
(E. A. Rosa)

The use of Performance Shaping Factors (PSFs) and quantified expert judgment using SLIM is important in the evaluation of human reliability. It should be noted that the amount of authentic quantitative human reliability data that exists is small (and is likely to remain small for the foreseeable future). It is therefore likely that subjective judgment and extrapolation will continue to play an important part. Nevertheless, present extrapolation techniques are covert, unsystematic, and rely on the knowledge of a limited number of judges. They do not systematically take into account the ways in which PSFs combine together to affect the probability of success in particular situations. Moreover, certain tasks cannot effectively be quantified using reductionist approaches. For these tasks, involving diagnosis, decision making and other cognitive activities, a holistic technique will probably be necessary.

Quantified subjective judgment has emerged from the previous analysis as being of critical importance for human reliability evaluation. SLIM is a quantified subjective judgment approach which uses PSFs as comprising any or all of the factors which combine to produce the observed likelihood of success. The basic premise of the approach is that when an expert judge (or judges) evaluate(s) the likelihood that a particular task will succeed, he or she is essentially considering the utility of the combination of PSFs in the situation of interest in either enhancing or degrading reliability. SLIM has the means of positioning a task on a subjective scale of likelihood of success, which is subsequently transformed to a probability scale. This positioning is derived by considering the judges' perceptions of the effects of the PSF in determining task reliability. NUREG/CR-2986 documents the initial appraisal of SLIM.

During the first quarter of FY 1984, efforts were devoted to completing the draft of NUREG/CR-3518 entitled "SLIM-MAUD: An Approach to Assessing Human Error Probabilities Using Structured Judgment." The addition of Multi-Attribute Utility Decomposition (MAUD) to the basic SLIM procedure represents the incorporation of an interactive microcomputer based program into the elicitation procedures so that assessors may generate their own PSFs. The assessor generated PSFs are evaluated for theoretical consistency by the program and then converted to failure probabilities. An assessment of progress on the development of the MAUD addition to SLIM is an essential precursor to the actual field testing of the technique.

14.3 Multiple Sequential Failure Model Development
(P. K. Samanta, J. N. O'Brien)

The dependence of human failure on multiple sequential action is important in the evaluation of human reliability. NUREG/CR-2211 has analyzed the nature of this dependence and has distinguished it from other types of multiple failures. Human error causes selective failure of components depending on

when the failure started. Two models have been initially developed for quantifying the failure probability in a multiple sequential action. The first is very general in nature and does not require any dependent failure data. The failure probability obtained from this model is a conservative one with associated uncertainty. The uncertainty is calculated considering many possible sources such as data, coupling, and modeling. In the second model, details of the process in multiple sequential failures (MSF) are taken into account. The model increments the conditional failure probabilities by a certain amount from their lower bounds (independent failure probability). This approach provides important insights into the influence of dependence of failures on system reliability. The model can be used effectively to choose an optimum system considering the individual failure probability, dependence factor, and the amount of redundancy in a system.

During the first quarter of FY 1984, the small-scale psychological experiment being used to test the model was further developed. Programming of test sequences was initiated and experimental tasks were further refined. Subject training approaches were further developed along with other experimental design considerations. Subjects were being selected and expected to be performing in the experiment during the next two quarters.

References

COMER, M. K., KOZINSKY, E. J., SECKEL, J. S., AND MILLER, D. P. (1983). "Human Reliability Data Bank for Nuclear Power Plant Operations," NUREG/CR-2744.

EMBREY, D. E. (1983). "The Use of Performance Shaping Factors and Quantified Expert Judgement in the Evaluation of Human Reliability: An Initial Appraisal," NUREG/CR-2986.

HALL, R. E., FRAGOLA, J. R., and LUCKAS, W. J., JR., Tech. Eds. (1981). Conference Record for NRC/BNL/IEEE Standards Workshop on Human Factors and Nuclear Safety, NUREG/CP-0035.

HALL, R. E., FRAGOLA, J., and WREATHALL, J. (1982). "Post Event Human Decision Errors; Operator Action Tree/Time Reliability Correlation," NUREG/CR-3010.

LUCKAS, W. J., JR. and HALL, R. E. (1981). "Initial Quantification of Human Errors Associated with Reactor Safety System Components in Licensed Nuclear Power Plants," NUREG/CR-1880.

LUCKAS, W. J., JR., LETTIERI, V., and HALL, R. E. (1982). "Initial Quantification of Human Error Associated with Specific Instrumentation and Control system Components in Licensed Nuclear Power Plants," NUREG/CR-2416.

SAMANTA, P. K. and MITRA, S. P. (1981). "Modeling of Multiple Sequential Failures During Testing, Maintenance, and Calibration," NUREG/CR-2211.

SAMANTA, P. K., HALL, R. E., and SWOBODA, A. L. (1981). "Sensitivity of Risk Parameters to Human Errors in Reactor Safety Study for a PWR," NUREG/CR-1879.

SCHMALL, T. M., Ed. (1979). Conference Record for NRC/BNL/IEEE Standards Sponsored December 1979 Workshop on Human Factors and Nuclear Safety.

SPEAKER, D. M., THOMPSON, S. R., and LUCKAS, W. J., JR. (1982). "Identification and Analysis of Human Errors Underlying Pump and Valve Related Events Reported by Nuclear Power Plant Licensees," NUREG/CR-2417.

SPEAKER, D. M., VOSKA, K. J., AND LUCKAS, W. J., JR. (1983). "Identification and Analysis of Human Error Underlying Electrical/Electronic Component Related Events Reported by Nuclear Power Plant Licensees," NUREG/CR-2987.

15. Human Factors in Nuclear Power Plant Safeguards

(J. N. O'Brien)

Brookhaven National Laboratory (BNL) was tasked in this program to develop a long-term research plan for studying the effects of human factors on the security at nuclear power plants. In the past, relatively little attention has been paid to human factors affecting security personnel in spite of the high level of attention the Three Mile Island Unit 2 accident brought to human factors affecting operational personnel. In order to remedy this, NRC sought a coordinated, cost effective, long-term research plan. To meet this objective, BNL developed a planning document to assist NRC in identifying safeguards related human factors research that can be usefully undertaken over the next 5-7 years. In addition, as a result of the BNL identified research needs, the human factors aspects of safety/safeguards interaction issues are being addressed by BNL.

15.1 Safeguards Related Human Factors Long-Term Research Plan

The first step employed to develop this research plan was to assess four principal data sources to identify and rank in importance human factors affecting safeguards. These are: (1) a human factors analysis of the Safeguards Summary Event List, (2) a set of comments supplied by over twenty human factors and/or safeguards experts, (3) an extensive literature review, and (4) NRC's own survey and analysis of human factors affecting safeguards (NUREG-0768).

During the first quarter in FY 1984, a third draft interim report was submitted which discussed the results of a literature review on social scientific research design with particular emphasis on how to design research approaches for safeguards human factors problems. This draft was combined with the two interim reports discussed in preceding quarters to form the basis of an overall final report. A briefing was also held at NRC to discuss the final report.

The format of the final report is in two volumes. Volume I is a summary of the overall research effort and a presentation of the final research plan. It contains an overall description of the four major program elements which are: (1) training and performance evaluation, (2) organizational factors, (3) man-machine interface, and (4) trustworthiness and reliability. For each program element, several project descriptive statements are included to specifically describe the optimal sequence of research efforts. Volume II contains all three interim reports condensed as chapters in the volume. Chapter 1 is an introduction; Chapter 2 describes the effort and results of identifying and ranking safeguards human factors issues; Chapter 3 contains an analysis of the feasibility of research on those issues identified in Chapter 2; and Chapter 4 documents the literature review conducted to investigate scientifically valid research approaches applicable to the issues identified.

The entire plan was presented to the NRC staff in a high-level briefing and, after NRC review, expected to be available in published form (NUREG/CR-3520) during the next quarter.

15.2 Human Factors Aspects of Safety/Safeguards Interactions During Routine Operations and Off-Normal Conditions

(J. N. O'Brien)

The first step of this effort is to examine and address human factors issues which arise from consideration of impacts on the ability of personnel at nuclear power plants to effectively perform their duties as documented in NUREG-0992. Of particular interest are situations at plants which may involve conflicts in roles and missions between security measures and the other organizational units which operate the plant. An example of this is the conflict between security measures aimed at restricting access to critical plant system components to thwart sabotage and vandalism and the needs of operational personnel to have ready access to those same components to safely operate the plant. While this type of conflict has not occurred at any plant in such a way as to produce a significant threat to safety, the potential for such a conflict must be examined to assure adequate performance of plant personnel. This program sets out to examine the human factors aspects of these potential problems and, further, to recommend measures to prevent or mitigate any potential adverse impacts on safety.

In order to effectively address potential problems involving conflicts between security requirements and operational practices, potentially troublesome situations and human factors issues relevant to them must be identified. This involves the consideration of a wide range of situations and human factors issues. Once situations have been identified and relevant human factors issues defined, a systematic examination will reveal how potential conflicts can be prevented or mitigated.

After potentially troublesome situations and relevant human factors issues are identified, a matrix will be constructed with situations on one axis and human factors on the other. The cells in the matrix represent the basis of the analysis from which proposals will be developed to prevent or mitigate adverse effects.

The scope of the resultant report will include input from a number of individuals in the fields of operational safety, security, and human factors. However, no site visits will be conducted. Instead, the data contained in the NUREG-0992 is considered to be representative of that which would come from site visits since that is how the committee's data were generated. NUREG-0992 has been extensively analyzed and conclusions are drawn on the basis of that information and subject to review by a panel of experts in the relevant fields. No formal attempt has been made to corroborate or verify the data presented in NUREG-0992.

16. Emergency Action Levels

(W. J. Luckas, Jr.)

Brookhaven National Laboratory (BNL) has been tasked in this program to develop guidance for Emergency Action Levels (EALs) that can be integrated into Emergency Operating Procedure (EOP) guidelines. From this guidance, a method will be developed that can be applied by licensees to verify that the EALs incorporated into their EOPs are usable in the control room under accident conditions. This should result in a reliable and timely basis for declaring emergencies without being too complex or burdensome to those who are trying to safely mitigate the accident.

EALs are plant specific predetermined observable and/or measurable set of indications (such as a particular set of control room instrument readings having reached specific off-normal values) which are used to declare one of the Emergency Classes (Alert, Site Area Emergency, or General Emergency).

After appropriate examination, an attempt will be made to utilize currently available EALs developed by utilities, such as Kansas Gas and Electric Company on their Wolf Creek Generating Station, that use the breach of fission-product barrier approach as a starting point. The EAL guidance will be verified by testing sample EALs against the example initiating conditions listed in Appendix 1 of NUREG-0654.

During the first quarter of FY 1984, a classification system for the emergency classes based on the degradation of fission product barrier was examined and endorsed by BNL.

17. Protective Action Decisionmaking

(W. T. Pratt, A. G. Tingle, H. Ludewig,
W. R. Casey,* and A. P. Hull*)

17.1 Background

NRC regulations require that, in the case of a major nuclear power plant accident, licensees recommend protective actions to reduce radiation dose to the public. When certain emergency action levels are exceeded, the licensee recommends protective actions to State and local officials. The nature of the protective actions recommended is determined by which emergency action levels are exceeded.

In practice drills, decisions on protective action recommendations have proven to be difficult. NUREG-0654 says that if containment failure is imminent, sheltering is recommended for areas that cannot be evacuated before the plume arrives, but evacuation is recommended for other areas. The assumption in NUREG-0654 is that there would be a greater dose savings if the population were sheltered during plume passage rather than evacuated, but this assumption has not been proven. Furthermore, the recommended protective actions must be based on estimated containment failure times, which are difficult to determine.

Alternatively, other NRC publications suggest that the appropriate response would be early evacuation of everyone within a distance of about 2 or 3 miles for all events that could lead to a major release even if containment failure is imminent or a release is underway. Those at greater distances should take shelter. Further, if a release occurs, the appropriate action would be for monitoring teams to find "hot spots" (radiation dose rate exceeding about 1 R/hr) and for people to evacuate these "hot spots."

17.2 Project Objectives

The objectives of the activities to be performed in this project are to:

(1) characterize the family of potential accident sequence for which emergency planning is necessary,

(2) establish strategies appropriate to these sequences, emphasizing credible failure modes,

(3) identify those factors which would influence the implementation of these strategies,

(4) determine how these factors should be incorporated into the decisionmaking process, and

(5) develop a guidance report on the protective actions to be recommended for combinations of these factors.

---

*BNL Safety and Environmental Protection Division

The final NUREG report for the project will be written in a simplified manner that can be readily grasped by people not intimately familar with accident consequence modeling. In addition, the report will also have a clear and concise summary understandable to laypeople.

17.3 Technical Approach

The work being performed is directed toward developing a technical basis for the NRC's guidance on protective action decisionmaking, such as that contained in NUREG-0654, Appendix 1. The approach is based on an evaluation of the consequences of nuclear power plant accidents as they relate to protective action decisionmaking. The evaluation includes a careful review of previous work (e.g., NUREG/CR-2339, NUREG-0654, NUREG/CR-2025, NUREG-0396, and reports and memoranda by the NRC staff) and its applicability to protective action decisionmaking. The evaluation is also based in large part on results obtained from the CRAC2 computer code (Consequence of Reactor Accident Code, Version 2). These results include previous CRAC2 runs supplied by the NRC Division of Risk Analysis and will be supplemented by selected additional runs where further information is needed. For example, changes in release warning time due to revised Emergency Action Levels, and changes in release characterizations due to revised source terms, could lead to reassessments of protective action strategies. Careful attention will be paid to the validity of the input assumptions and the effects of varying the input assumptions. Careful attention will also be paid to the nature of the output (for example, precisely what physical phenomena or evacuation assumptions are leading to the consequences shown in the output).

Among the aspects being assessed in developing the technical basis for protective action decisionmaking are:

(1) In-plant conditions: BNL staff are assessing whether protective actions can be determined based on the status fo the cladding barrier and reactor coolant barrier only, or if the containment barrier must also be considered. Appropriate links to emergency action levels based on in-plant observables and containment status are being determined.

(2) Warning time: BNL staff are evaluating how consequences vary with warning time and time to start evacuation for various size accidents. The "needed" warning time will be determined.

(3) Distance: BNL staff are evaluating to what distances evacuation, sheltering, and relocation should apply for various classes of accidents.

(4) Sheltering: BNL staff are determining appropriate shielding factors and assessing how sensitive the results are to the average shielding, the range of shielding factors, the fraction of the population achieving shielding, and the distances where shielding would be most effective. In addition, BNL staff will determine to what extent local sheltering capabilities should be factored into site specific criteria.

(5) Non-nuclear disasters as initiating events: Earthquakes and hurricanes may interfere with sheltering, evacuation, relocation, and the ability to warn the public. BNL staff will determine what protective action decisions would be appropriate under these conditions.

(6) Duration of "hot spot" exposure: BNL staff will determine how long it would take to find "hot spots" and determine how long it would take people to relocate. In addition, BNL staff will determine how important it is to selectively relocate from the hottest spots first.

(7) Weather: BNL staff will determine how weather conditions affect the protective action decisions and compare high vs. low wind speed and consider atmospheric stability. In addition, BNL staff will consider the effect of rain at time of release and rain intercepting the plume. How these factors can be used in decisionmaking at the time of the event will be determined.

(8) Plume rise: BNL staff will evaluate the differences between hot and cold releases and determine how this can be considered in protective action decisionmaking.

(9) Evacuation speed: BNL staff will evaluate how speed impacts on evacuation effectiveness and determine whether evacuation speed should be considered in the criteria on a site-specific basis. If evacuation speed needs to be considered, we will determine how it can be best-estimated and determine how speed varies with numbers of evacuees and size of areas to be evacuated. In addition, we will determine if there is a critical speed and determine how plausible the generally assumed 10-mph evacuation speed is for the calculations.

(10) Crosswind vs. radial evacuation: BNL staff will evaluate the merits of evacuation crosswind relative to plume direction rather than radially. Consideration of wind shifts will be made to determine how this can be factored into decisionmaking.

(11) Continuous releases: Even if a puff release is realized, there will be a continuous release. BNL staff will determine what impact a continuous release will have on the protective actions recommended and determine how emergency personnel should be trained to handle continuous releases. In addition, BNL staff will determine what should be done for a slowly building series of puffs.

(12) Entrapment scenarios: BNL staff will determine what protective actions would be appropriate if the ability to evacuate the public is impaired, as in earthquakes, snowstorms, and hurricanes.

The technical basis developed for the protective action decisionmaking will also reflect the new fission product source term information under development by the NRC/RES Accident Source Term Program Office (ASTPO).

17.4 Project Status

The project started in September 1983. The initial effort was related to obtaining and reviewing relevant publications and CRAC2 sensitivity calculations supplied by the Division of Risk Analysis. The latest version of the CRAC2 code was obtained from Sandia National Laboratory and implemented on the BNL computing system. Preliminary calculations have been performed to establish procedure for investigating various evacuation and sheltering strategies. These calculations have indicated that computer time requirements for the project will be inexpensive.

BNL staff attended and made presentations at a program review meeting held in Washington in November. The meeting was a very useful round table discussion in which various NRC staff views were expressed regarding protective action decisionmaking. In general, our suggested approach and scope to the project were well received at the meeting. However, a number of important points were made, which will be taken into account in the project. In particular, it was noted that care should be taken when interpreting CRAC2 analysis, particularly with regard to hotspot calculations. It was also emphasized that recent NRC documents on protective action decisionmaking should be considered preliminary and treated accordingly. In addition, the ASTPO staff are also working in this area and close cooperation between the projects was recommended. It was also considered important to consider a wide range of potential core degraded accidents when developing protective action strategies. Finally, we were encouraged to use the new source term information being generated within ASTPO.

In December, a presentation was given to Dr. Minogue, Director of the Office of Nuclear Regulatory Research, on the status of the project. It was emphasized by Dr. Minogue that we should consider a wide range of potential accident sequences and concentrate on up-to-date assessments of containment performance. BNL staff are participating in the SARP Containment Loads Working Group and the Containment Performance Group and we will, therefore, integrate the work of these groups into our development of protective action strategies.

In accordance with the above goals, we have selected the following six facilities to represent the range of potential reactor and containment designs:

Zion: PWR with a large dry containment
Surry: PWR with subatmospheric containment
Sequoyah: PWR with an ice condenser containment
Brown's Ferry: BWR with a Mark I containment
Limerick: BWR with a Mark II containment
Grand Gulf: BWR with a Mark III containment

Although the work on the technical basis for protective action decisionmaking is underway, the BNL staff have developed a preliminary format for the guidance report and have started writing on general topics pertinent to protective actions.

NRC FORM 335 (11 81) U.S. NUCLEAR REGULATORY COMMISSION

BIBLIOGRAPHIC DATA SHEET

1. REPORT NUMBER (Assigned by DDC)
NUREG/CR-2331
BNL-NUREG-51454, Vol. 3, No. 4

4. TITLE AND SUBTITLE (Add Volume No., if appropriate)
Safety Research Programs Sponsored by Office of Nuclear Regulatory Research, Quarterly Progress Report October 1 - December 31, 1983.

2. (Leave blank)

3. RECIPIENT'S ACCESSION NO.

7. AUTHOR(S)
Compiled by Allen J. Weiss

5. DATE REPORT COMPLETED
MONTH: March | YEAR: 1984

9. PERFORMING ORGANIZATION NAME AND MAILING ADDRESS (Include Zip Code)
Brookhaven National Laboratory
Department of Nuclear Energy
Upton, New York 11973

DATE REPORT ISSUED
MONTH: May | YEAR: 1984

6. (Leave blank)

8. (Leave blank)

12. SPONSORING ORGANIZATION NAME AND MAILING ADDRESS (Include Zip Code)
U. S. Nuclear Regulatory Commission
Office of Nuclear Regulatory Research
Washington, D. C. 20555

10. PROJECT/TASK/WORK UNIT NO.

11. FIN NO. A-3011,14,15,16,24,41
A-3208,15,19,25,26,27,
57,60,66,68,70,71

13. TYPE OF REPORT
Quarterly

PERIOD COVERED (Inclusive dates)
October 1 - December 31, 1983

15. SUPPLEMENTARY NOTES

14. (Leave blank)

16. ABSTRACT (200 words or less)

The Advanced and Water Reactor Safety Research Programs Quarterly Progress Reports have been combined and are included in this report entitled, "Safety Research Programs Sponsored by the Office of Nuclear Regulatory Research - Quarterly Progress Report." This progress report will describe current activities and technical progress in the programs at Brookhaven National Laboratory sponsored by the Division of Accident Evaluation, Division of Engineering Technology, and Division of Facility Operations of the U.S. Nuclear Regulatory Commission, Office of Nuclear Regulatory Research.

The projects reported are the following: High Temperature Reactor Research, SSC Development, Validation and Application, CRBR Balance of Plant Modeling, Thermal-Hydraulic Reactor Safety Experiments, Development of Plant Analyzer, Code Assessment and Application (Transient and LOCA Analyses), Thermal Reactor Code Development (RAMONA-3B), Calculational Quality Assurance in Support of PTS; Stress Corrosion Cracking of PWR Steam Generator Tubing, Bolting Failure Analysis, Probability Based Load Combinations for Design of Category I Structures, Mechanical Piping Benchmark Problems, Identification of Age-Related Failure Modes; Analysis of Human Error Data for Nuclear Power Plant Safety-Related Events, Human Factors in Nuclear Power Plant Safeguards, Emergency Action Levels, and Protective Action Decision Making. The previous reports have covered the period October 1, 1976 through September 30, 1983.

17. KEY WORDS AND DOCUMENT ANALYSIS 17a. DESCRIPTORS

High Temperature Graphite Reactor	Plant Analyzer	Bolting Failure
Super System Code	RAMONA-3B	Load Combinations
MINET Code	Pressurized Thermal Shock	Nuclear Plant Aging
Thermal-Hydraulic Reactor Safety	Stress Corrosion Cracking	Human Error
Emergency Action	Protective Action	Human Factors

17b. IDENTIFIERS/OPEN-ENDED TERMS

18. AVAILABILITY STATEMENT
UNLIMITED

19. SECURITY CLASS (This report)
UNCLASSIFIED

21. NO. OF PAGES

20. SECURITY CLASS (This page)
UNCLASSIFIED

22. PRICE
$

NRC FORM 335 (11 81)